CARBON MAP OF DRC

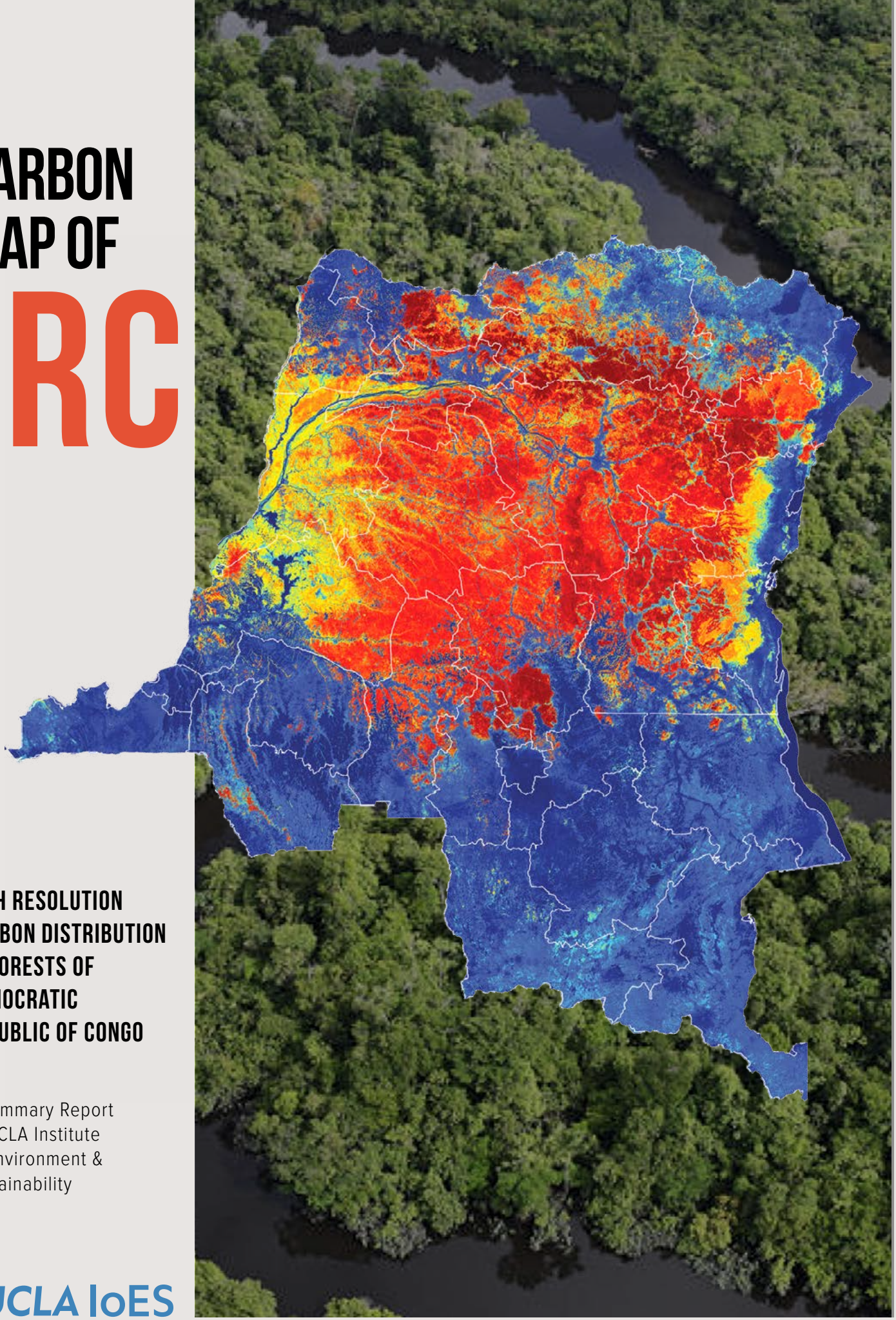

HIGH RESOLUTION CARBON DISTRIBUTION IN FORESTS OF DEMOCRATIC REPUBLIC OF CONGO

A Summary Report of UCLA Institute of Environment & Sustainability

UCLA IoES

CARBON MAP OF DRC

High Resolution Carbon Distribution in Forests of Democratic Republic of Congo

APRIL 2017

A summary report of the Carbon Map and Model Project Performed at the University of California Los Angeles

CONTRIBUTORS

SASSAN SAATCHI[1,2], ALAN XU[2], VICTORIA MEYER[1], ANTONIO FERRAZ[1], YANG YAN[2], AURELIE SHAPIRO[3], LIVIA WITTIGER[3], MINA LEE[4], ELVIS TSHIBASU[4], NORMAN BANKS[5]

[1] Institute of the Environment and Sustainability University of California, Los Angeles

[2] Jet Propulsion Laboratory, California Institute of Technology

[3] World Wide Fund for Nature (WWF), Germany

[4] World Wide Fund for Nature (WWF), DRC

[5] Southern Mapping, South Africa

The project was developed in collaboration with the following agencies in DRC:

- The Ministry of Environment and Sustainable Development
- Direction des Inventaires et Aménagement Forestiers (DIAF)
- Direction du Développement Durable (DDD)
- Observatoire Satellital des Forets d'Afrique Central (OSFAC)

The Carbon Map and Model project is made possible through the support of the International Climate Initiative (IKI) by the German Federal Ministry for the Environment, Nature Conservation, Building and Nuclear Safety (BMUB) and the German Development Bank (KfW).

UCLA IoES

JPL
Jet Propulsion Laboratory
California Institute of Technology

Supported by:
Federal Ministry for the Environment, Nature Conservation, Building and Nuclear Safety
based on a decision of the German Bundestag

KFW

WWF

TABLE OF CONTENTS

EXECUTIVE SUMMARY


© Brent Stirton / Getty Images / WWF-UK

BACKGROUND

Accumulation of carbon in global woody vegetation has become an effective strategy for mitigating climate change. However, the quantification of carbon stored in the vegetation at scales useful for carbon accounting and policy making is lacking. The uncertainty around the carbon stocks in forests, particularly in humid tropics has significant implications for accurately assessing and planning to reduce emissions from deforestation and degradation (REDD+) at national and regional scales.

The Democratic Republic of Congo (DRC) has the second largest area of rainforests in the world, covering a complex system of extensive rivers, humid and dry forests, savanna patches, wetlands, mountain vegetation, and degraded landscapes. The forests of DRC are rich in carbon content and represent one of the most important centers of biological diversity in the world, with over 15,000 plants and animal species. The DRC forests are facing threats from industrial timber extraction, artisanal and illegal logging, slash and burn agriculture, mining, firewood collection and the effects of poaching.

The government of DRC has initiated one of the largest jurisdictional emission reduction programs in Africa and has launched national scale efforts to quantify and monitor changes in carbon stocks of forests. The Carbon Map and Model (CM&M) program is a component of this national effort by developing estimates of carbon stocks through remote sensing technologies. The CM&M project has been developed by World Wide Fund for Nature (WWF) in collaboration with University of California in Los Angeles (UCLA), the Ministry of Environment and Sustainable Development DRC (Potapov et al. 2012), and other national partners with the goal of producing a national forest carbon map using innovative ground, air, and space-borne observations, and building the capacity within the existing institutions in DRC to utilize the carbon map in national forest management, emissions reduction program and sustainable land use planning.

PURPOSE

Here, we report on the development of the first national carbon map of DRC, based on remote sensing techniques, benchmarking the distribution of carbon storage in live aboveground tree biomass of more than 150 million ha of forests in DRC. The report includes a summary of the methodology, the ground and remote sensing data used in developing the map, the regional validation of the carbon stocks, and the overall assessment of the forest carbon distribution. The map has been presented to a diverse group of stakeholders including the Direction des Inventaires et Aménagement Forestiers (DIAF) for further evaluation and validation using the planned national inventory data and improvements at any point in future.

METHODOLOGY

The aboveground forest biomass (AGB) map has been developed following the VCS (Verified Carbon Standard) methodology (VT0005) by using by high-resolution airborne Light Detection and Ranging (LiDAR) inventory samples. The LiDAR flights were designed to capture the variability of forest structure using a systematic random sampling approach common in national forest inventory (NFI) techniques. Each LiDAR flight covered 2000 ha (1.7 km x 12 km) with flight orientation randomly selected between 0-180º and locations of flight lines randomly selected within a 1 deg x 1 deg (~ 1 million ha) grid area to cover more than 430, 000 ha of probability-based inventory samples of forest structure. Because of their random locations, orientation, and coverage, the flights sampled a large variety of forest types including terra firme, swamps, woodlands, land use gradients from deforestation, degradation, and tree plantations, and landscape and environmental gradients of elevation and slope, soil, and climate. DRC will be the first country in Central Africa to use LiDAR inventory sampling as their preferred rapid assessment.

The airborne data were collected by the South African Southern Mapping Company (SMC) between October 2014 and February 2015 using Optech LiDAR units and Rollei Phase 1 medium format cameras. In addition, SMC acquired about 3000 km of ferry lines between the random samples to cover approximately 170,000 ha of additional LiDAR data over forests of DRC. The LiDAR data were converted to AGB by collecting and compiling a new network of 1-ha field plots collected by various project partners and stakeholders co-located with LiDAR flights and covering different forest types in DRC. The plots were used to develop an unbiased model to estimate AGB from LiDAR data and create about 600,000 ha model-based inventory samples for quantifying and validating the carbon stocks in forests of DRC. The LiDAR samples were combined with satellite imagery and machine learning geospatial algorithms to map forest aboveground biomass and predict AGB everywhere in DRC at 1-ha spatial resolution. The methodology was established and operationalized by developing in-country capacity to implement all elements of AGB estimation, validation, and improvement of forest carbon map in future when additional plots, and LiDAR samples become available.

FINDINGS

The carbon map of DRC reveals a wide range of patterns of forest carbon density along climate, edaphic and disturbance gradients. Overall, forests of DRC contain a total of 23.3 ± 0.2 GtC carbon stored in humid tropical forests with a mean carbon density of 139 ± 1.2 MgC ha-1 in the aboveground live trees. At the landscape scale, the variations in forest carbon density follow disturbance and topographical gradients, where density of large trees dominating the magnitude of biomass varies from intact to logged forests, distance to roads and settlements, or geomorphological features associated with slopes, soil type and moisture conditions. The eastern regions of DRC has some of the largest trees in the country distributed amoung rugged terrains along the foothills of eastern mountains below 1000 m asl (above sea level). The land cover in the southern provinces of DRC are a mosaic of tree grass savanna, riparian forests, and Miombo woodlands. The carbon density in these forests are highly variable due to land use activities, slash and burn agriculture, and fire. The western region of DRC is dominated by wetland swamps with a combination of permanently and seasonality inundated forests and peatlands with approximately 132 ± 11 MgC/ha in hardwood and 36 ± 15 in palm dominated swamp forests. The high accuracy of LiDAR derived maps of forest height and aboveground biomass resulted in very low uncertainty of mapping forest height (~3 m RMSE) and 81% precision and biomass (~ 50 Mg/ha RMSE) and more than 72% precision. The derived LiDAR biomass model was

approximately unbiased when tested on inventory plots distributed across the country, making the overall map remain unbiased at regional scales.

We assessed the forest cover and carbon stored at the national and for all 26 provinces in DRC to provide baseline estimates for future forest management and protection. Results show that 4 provinces (Tshuapa, Tshopo, Ituri and Sankuru) have the highest mean AGB of more than 300 Mg/ha. The 10 other provinces (Mai-Ndombe, Equateur, Sud-Ubangi, Nord-Ubangi, Mongala, Bas-Uele, Nord-Kivu, Sud-Kivu, Maniema, and Kasai) have mean AGB estimates around 200 Mg/ha. These 14 provinces possess 75% of the total carbon in the country. The provinces with the lowest AGB density are Kinshasa, Kasai Oriental, Lomami and Kongo Central, which contribute less than 1% to the country-level carbon storage. At national level, the mean AGB is 236 Mg/ha for all forested regions, with less than 1% average modeling error when considering both the pixel-based error and the covariance between pixels.

The forest area of DRC including savanna woodlands and Miombo forests are estimated in this study to be approximately 167 million ha. This is significantly larger (> 12 million ha) than earlier estimates based on the Landsat based map. The difference between the maps is largely due to recent changes in the definition of forests from a minimum of 5 m to 3 m height threshold. With the minimum mapping area of 0.5 ha and the percent cover of 30%, a significantly larger area of woodland savanna is classified into forests.

The carbon distribution in forests of DRC is controlled by forest degradation and human activities. Environmental variables have weak and but significant relationships to forest carbon density. For humid tropical forests in DRC, mean temperature of driest quarter, topsoil organic carbon, landscape elevation variation and rainfall seasonality together explain about 28% of the carbon stock variations. The swamp forests, mainly distributed along the Congo river system in western DRC, have a more predictable pattern related to environmental variables with 66% of the carbon spatial variations explained by mean land elevation, land elevation variation, minimum temperature of coldest month, and annual precipitation. Carbon stored in Miombo forests in the south also have distinct environmental controls dominated by the rainfall seasonality and followed by subsoil silt fraction, mean land elevation, and the annual precipitation.

CONCLUSIONS

The systematic and probability based inventory of forest structure with airborne LiDAR data of DRC provided the first physiographical variations of the forest height and carbon density at landscape scales. Using the LiDAR inventory measurements calibrated with ground plots, we were able to develop the national-level forest biomass distribution at 100 m (1-ha) resolution with a formal uncertainty assessment at the pixel level for the entire country. The sampling density was designed to provide sub-national and province-level carbon statistics, as well as AGB estimates summarized by forest types. Together, the carbon map and the uncertainty can help the government of DRC for national and jurisdictional emission reduction programs, conservation and decision making for development programs.

The spatial products generated from this project, such as the forest height and the biomass helped us to estimate the area of forest cover based on the new definition of forests adopted by the country. These products have been validated using existing national inventory data collected in few regions and can be improved once new ground and remote sensing data become available. The methodology adopted here have been presented to the government through various workshops and meetings and all original data and products have been delivered to the government for developing the capacity within the forestry and environmental agencies for future resource management and forest monitoring.

LIST OF ACRONYMS

AFOLU: Agriculture, Forestry and Other Land use
AGB: Above Ground Biomass
ALOS: Advanced Land Observing Satellite
ALS: Airborne LiDAR Scanning
BGB: Below Ground Biomass
CAFI: Central African Forest Initiative
CARPE: Central African Regional Program for the Environment
CCBA: Communities, & Biodiversity Alliance
COMIFAC: Forestry Commission of Central Africa
DEM: Digital elevation Model
DIAF: Département des Inventaires et Aménagement Forestier
DRC: Democratic Republic of Congo
DSM: Digital Surface Model
DTM: Digital Terrain Model
ER: Emission Reduction
ERPD: Emission Reduction Project Document
FAO: Food and Agriculture Organization
FCCC: Framework Convention on Climate Change
GOFC-GOLD: Global Observation of Forest and Land Cover Dynamics
IPCC: Intergovernmental Panel on Climate Change
Kg: Kilogram
LiDAR: Light Detention and Ranging
LULC: Land Use and Land Cover
MEDD: Ministry of Environment & Sustainable Development
MRV: Magnetic Resonance Venogram
NASA: National Aeronautic and Space Adminstration
NFI: National Forest Inventory
OSFAC: Observatoire satellital des For. ts d'Afrique centrale
PALSAR: Phased Array type L-band Synthetic Aperture Radar
PD: Project Document
RaDAR: Radio Detection and Ranging
REDD+: Emissions Reductions from avoided Deforestation and Degradation
RMSE: Root Mean Square Error
SAR: Synthetic Aperture Radar
tCO2e: Ton of carbon dioxide equivalent
UNFCCC: UN Framework Convention on Climate Change
UCL: Universit. catholique de Louvain
VCS: Verified Carbon Standard
USAID: United States Agency for International Development
WD: Wood Specific Gravity or Wood Density
WRI: World Resource Institute
WWF: World Wide Fund for Nature

INTRODUCTION

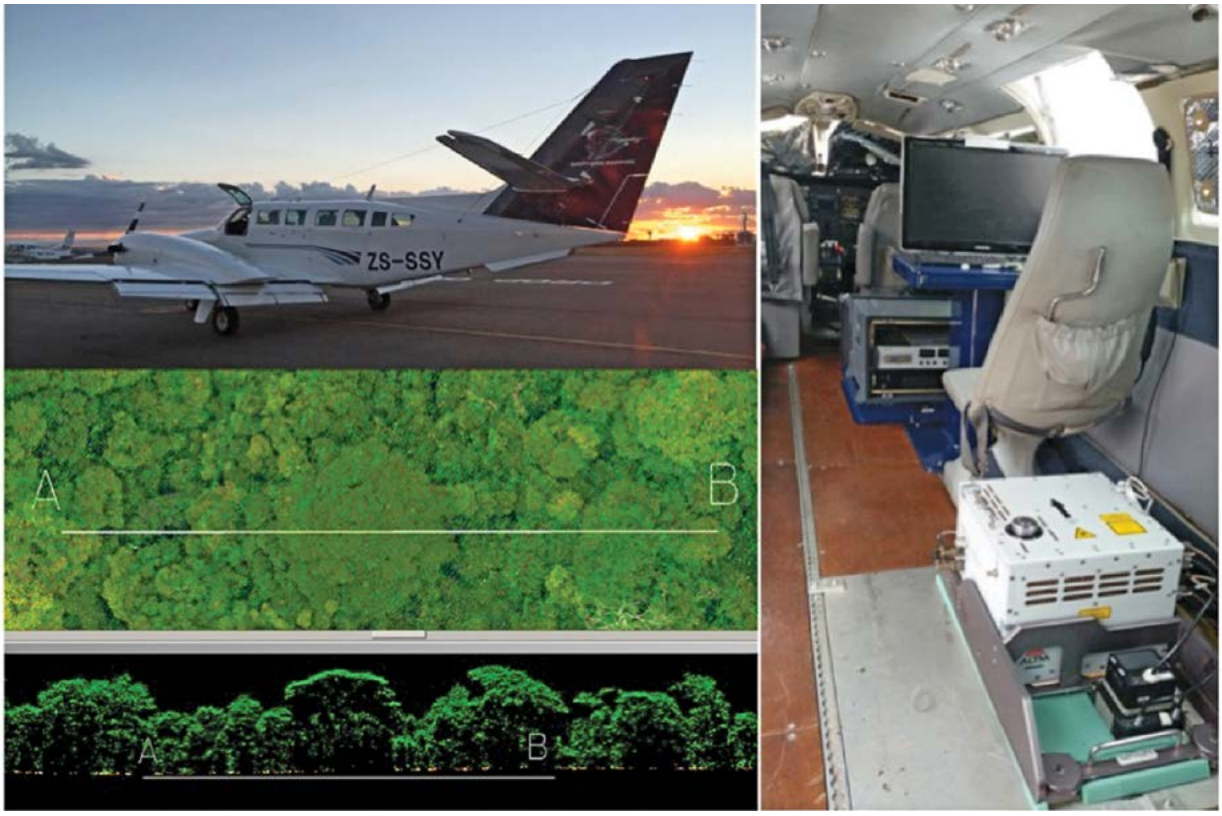

Tropical forests provide valuable ecosystem services, notably by storing vast amounts of biomass, serving an important role for climate change mitigation[1]. Accurate and precise quantification of emissions from deforestation has become a key policy issue in light of recent developments on the reduction of emissions from deforestation and degradation (REDD+) as a climate mitigation strategy[2]. In a national REDD+ policy framework, historical reference emission levels (potentially modified by one or several adjustment factors) will need to be set, and future emissions must be evaluated against the reference level as part of a monitoring (or measuring), reporting and verification (MRV) system to determine whether a country has or has not made significant emission reductions[3]. The uncertainty around reference emission levels and the resulting emissions from activity data such as land use and land cover change (LULC) must also be quantified. Because of the principle of conservativeness, results from the use of the lower uncertainty bounds for emission factors for the reference scenario must be adopted in order to avoid over-crediting future reductions. Meeting these conditions for national or regional scale REDD+ programs require a precise inventory of forest carbon stocks and changes that capture regional variability of forest aboveground biomass and land use patterns[4,5].

Figure 1: Airborne LiDAR scanning and optical imagery units of Southern Mapping and the aircraft used in 2014-2015 flight campaign in the Democratic Republic of Congo (DRC). The flights were designed based on systematic random sampling to collect more than 430,000 ha of the humid tropical forests of DRC. The LiDAR and optical imagery captures 3-D structure and visible characteristics of intact, degraded, swamp forests, and woodlands across more environmental and topographical gradients.

(Above) https://africa.quora.com/Congo-Basin
(Above right) https://africa.quora.com/Congo-Basin
(Below right) Photo © Jeff Walker / Center for International Forestry Research (CIFOR)

Many important technical and political questions remain to be answered regarding how REDD+-based emission reduction projects and programs will be implemented at the national level. Smaller voluntary-sector projects have been operating in many countries across the tropics since 2006 under the Verified Carbon Standard (VCS) and Carbon Communities, & Biodiversity Alliance (CCBA) Standards, amongst others, and provide much guidance as to how national-level schemes could operate. However, at the national level, emission estimates from land cover change require information on both the area of forest change and the corresponding carbon stocks of the ecosystems that are deforested. Such information is either not available or highly uncertain in many countries with extensive tropical forests. Much of the emphasis on emissions from tropical forests to date has focused primarily on improving the areal estimates of deforestation; yet significant errors exist in the carbon stock element, particularly when considering jurisdictional and national level emissions[6,7].

The carbon estimates and emission factors associated with land use change in tropical countries are often based on a small number of inventory plots or a combination of intensive in situ field sampling, paired with remote sensing methods (satellite or aerial), which are currently the only available options[8]. The general consensus in the scientific literature regarding monitoring forest cover change for reducing emissions from deforestation is that satellite imagery is practical, feasible and essential for determining baseline deforestation over time[9,10]. While methods to map carbon stocks directly have not been perfected nor made operational yet – this task would be impossible without a combination of airborne and satellite imagery, calibrated by field measurements at the national scale.

Current methodologies for mapping forest carbon stocks rely strongly on LiDAR satellite observations of forest structure converted to aboveground biomass (AGB) and extrapolated over the landscapes using satellite imagery[8,11–13]. This approach can suffer from uncertainty when LiDAR sampling is uneven or nonrandom, poor calibration of LiDAR data to forest biomass, and potential geographic bias introduced by the extrapolation approach and sensitivity of the satellite imagery to atmospheric conditions and vegetation phenology?[14].

TECHNICAL METHODOLOGY

SYNOPTIC VIEW

The estimation of carbon stocks in live biomass of forests of DRC follows the methodology outlined in VCS (Verified Carbon Standard) VT0005 tool developed by Sassan Saatchi and based on inventory sampling of forest structure by using high-resolution airborne Light Detection and Ranging (LiDAR) systems. The methodology was successfully tested in at a regional scale along the Pacific Coast of Colombia as part of the USAID BioREDD+ project Colombia (http://bioredd.org/projects/) and documented and verified as a VCS tool by Terra Global Capital in March 2015 (http://database.v-c-s.org). The airborne LiDAR techniques has recently emerged as a promising tool to acquire information on forest structure that can be converted into forest carbon density in a model-based and assisted estimation framework[16,17]. LiDAR provides horizontal and vertical information at high spatial resolutions and vertical accuracies through visible laser altimetry techniques (see Appendix for more information). In forestry applications, the measurements provide forest attributes such as canopy height at small footprints (< 1 m) that allow a detailed characterization forest structure that can be used to model aboveground biomass and canopy volume.

The LiDAR samples covered a large area (~2000 ha) and are collected based on a systematic random design matching a typical national forest inventory (NFI) technique in order to provide unbiased estimates of carbon density at the national and sub-national scales (Naesset et al. 2013; 2016; Stahl et al. 2011). We used LiDAR samples and a network of 1-ha field plots to develop unbiased models between LiDAR derived height metrics and forest aboveground biomass density. Estimation of Forest above ground and below ground biomass is performed at the national and sub-national levels using statistical and allometric models taking into account the uncertainty of models and sampling approach and spatial covariance. The LiDAR derived forest biomass samples are combined with existing high resolution satellite imagery and machine-learning algorithms to map the forest biomass at 100 m (1-ha) spatial resolution over the entire country.

STUDY REGION

LiDAR samples cover the humid tropical forests of the entire country of Democratic Republic of Congo (DRC). The forests of DRC cover a complex landscape of water-logged swamp forests of Congo River Basin in the west to topographically complex and Montane forests in the east reaching up to 3000 m in elevation. Forest cover in DRC is approximately 160 million ha, with about 48% in dense humid forests covering the swamps, terra firme old growth and secondary forests[19]. In the past decades, DRC had a gross forest loss of less than 2.5% concentrated around settlements and mining and concession areas. A significant area of the forests in central DRC is impacted by forest degradation along the main roads and in areas with intense logging[20]. Some of the most intact and biomass rich forests are in the sub-montane and montane forests in the east of DRC, where the altitude is higher than 900 m above the sea level. The north and south of DRC is covered by woodland savanna and grasslands with extensive coverage of Miombo forests in the southeastern regions.

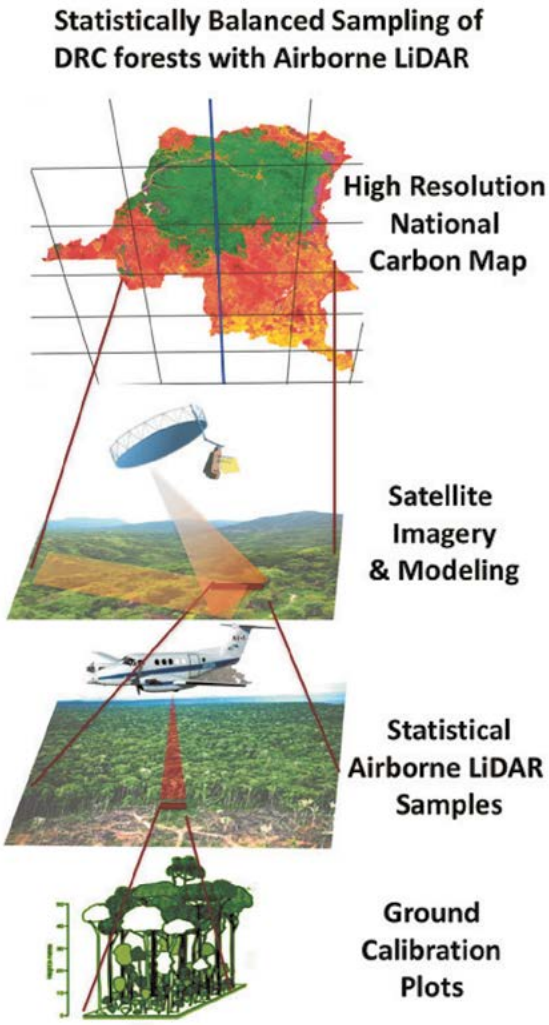

Figure 2: Schematic of the methodology for developing forest carbon map of DRC from sample plots to calibrate systematic design of airborne LiDAR data to wall-to-wall mapping using geospatial modeling with satellite imagery.

Figure 3: The sampling framework in VT0005 methodology showing a stratified or forested project area within which sampling should be conducted and for which an estimate of AGB is required. The remote sensing(RS) sampling units are shown with RS flightlines and the individual ground plots for calibration of the RS data are shown as solid circles randomly located within the flightlines

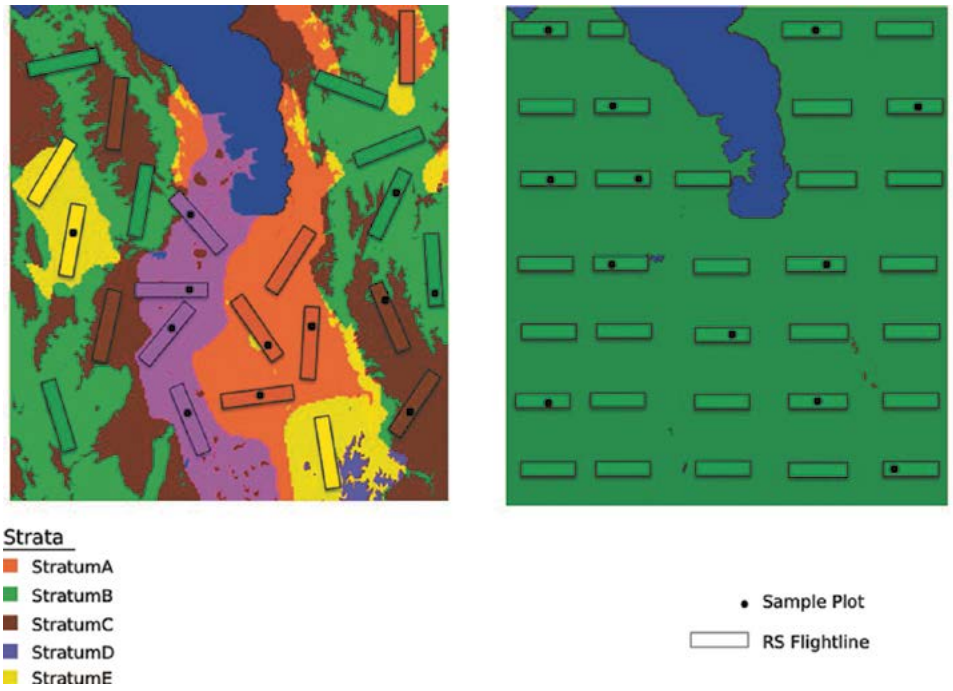

VT0005 VCS METHODOLOGY

The methodology VT0005 is a tool for measuring above ground live forest biomass using remote sensing data and is developed by Sassan Saatchi as part of the USAID Colombia BioREDD+ project (http://bioredd.org/projects/) and documented as a verified Carbon Standard(VCS) tool by Terra Global Capital in March 2015 (http://database.v-c-s.org)[13]. The methodology has been developed to produce precise estimation of carbon in aboveground live forest biomass (AGB) for implementation of many agriculture, forestry and land use (AFOLU) programs and in developing REDD projects . AGB is the primary factor for determining baseline levels for forest carbon pools. The geographic area of AFOLU projects must be large (>40,000 ha) and encompass a wide range of land use/land cover (LULC) types to allow for a cost-effective and efficient implementation of the methodology. Statistically valid sampling strategies for such large areas using traditional ground-based forest inventory plots are often not feasible due to cost and access constraints in tropical countries. As most VCS methodologies have no provision for the use of remote sensing methods to determine forest aboveground biomass and rely solely on traditional plot-based biomass measurements, the VT0005 tool is considered the only verifiable technique to provide unbiased estimates of carbon of forests. Here, we introduce a VCS (Verified Carbon Standard) tool intended to reduce the need for extensive ground-based sampling by leveraging remotely sensed data calibrated using a minimal number of ground-based sampling plots.

The tool also uses the latest versions of the following tools and methodology:

1. CDM tool Calculation of the number of sample plots for measurements within A/R CDM project activities (https://cdm.unfccc.int/methodologies/ARmethodologies/tools/ar-am-tool-03-v2.1.0.pdf/).
2. CDM tool Estimation of carbon stocks and change in carbon stocks of trees and shrubs in A/R CDM project activities(https://cdm.unfccc.int/methodologies/ARmethodologies/tools/ar-am-tool-14-v2.1.0.pdf/).
3. VCS methodology VM0006 Carbon Accounting in Project Activities that Reduce Emissions from Mosaic Deforestation and Degradation (http://database.v-c-s.org/).

The VT0005 tool provides a method for determining average AGB density at the stratum or area of interest through a combination of remote sensing probability based sampling and field measurements in limited inventory plots for calibration of remote sensing data. In this tool, sampling unit is used to refer a spatially contiguous area within a stratum for which remote sensing data has been collected (see figure for a schematic representation of the RSSU). Simple random sampling, systematic sampling, or stratified random sampling can be employed in designing the samples. In general, AGB estimation based solely on sampling units is assumed to have larger errors than estimation based only on field inventory data for an equal area (e.g. 1 ha). However, the use of larger remote sensing sampling units reduces the estimator error[21].

For this tool, the remote sensing sampling unit must be large enough to allow for cost effective flight design. The pixels covered within each unit are inherently clustered due to the swathing or field-of-view configuration of airborne sensors. Therefore, the size of each unit necessary to achieve the required precision are inversely related: the smaller the sample size, the larger the number of samples. For a schematic representation of the variation of

AGB at the landscape scale, the estimator of AGB at the landscape scale must also include the spatial correlation among remote sensing pixels within each unit. In general, the area of each sampling unit with a stratum must be larger than the spatial correlation length (range of the semivariogram) of estimator error (see equations in VT0005 tool). The combined area samples from number of units and the number of pixels within each unit within a stratum must be of a minimum size to allow unbiased estimation of mean AGB with required precision. Determination of the extent of remote sensing data collection is also dependent on the desired confidence in the estimate produced by this tool and on the use of AGB estimates known *a-priori* either from a pilot study, from appropriate literature, or using default values provided by the tool.

Airborne LiDAR Sampling

To apply the VT0005 tool in DRC, our team at the University of California, Los Angeles designed an airborne LiDAR-based national inventory using a systematic random sampling approach (See Appendix on LiDAR Remote Sensing). The country was divided into 1oX1o (~ 10,000 km2) grid cells and each cell a random point was selected using the Reverse Randomized Quadrat Recursive Raster (RRQRR) approach, GIS-based tool.

The LiDAR flights were collected only in humid tropical zones and all samples in savanna regions and Miombo forests were eliminated due to the cost and lack of field support for savanna regions. A total 216 random points that were used to center the LiDAR flight transects of approximately 2000 ha in area coverage (1.7 km x 12 km) and with flight orientation randomly selected between 0-180°. The transect size (~2000 ha) was selected for allowing less < 1% uncertainty for biomass estimation over the entire LiDAR transect based on models that include spatial correlation among the LiDAR pixels[13,41,42]. Because of their random locations, orientation, and coverage, the flights sampled a large variety of forest types (terra firme, swamps, and woodlands), land use gradients from deforestation, degradation, and tree plantations, and landscape and environmental gradients of elevation and slope, soil, and climate[43]. DRC is the first country in the tropical belt to use LiDAR inventory sampling as their preferred rapid assessment of forest

Frans Lanting
Flowering trees in lowland rainforest (aerial),
Wamba, Congo (DRC)

cover and carbon stocks. A total of 432,000 ha of inventory samples were collected by the Airborne LiDAR in a discrete return mode with approximately two pulses or about 4 returns per 1-m^2. The average point density of 4 was enough to provide accurate measurements of the forest height by quantifying the digital terrain model (DTM) and the digital surface model (DSM). The difference between DTM and DSM provided the maximum height or top canopy height at 1-m^2 grid cell.

We received airborne small-footprint LiDAR measurements from DRC with a total of 216 plots and 96 Ferry lines. It covers the entire tropical forest region of DRC with spatially balanced samples. The Southern Mapping Company (SMC) conducted the airborne LiDAR surveys using the Optech ALTM 3100 LiDAR scanner from June 2014 to February 2015. The preprocessing of LiDAR data from SMC included trajectory calculation, LiDAR point calibration, and LiDAR point classification (separating ground and vegetation points). The final classified LiDAR points were delivered in LAS format to the University of California, Los Angeles (UCLA).

The data were further filtered for any artifacts in ground classification and ground points were interpolated to improve the development of DSM and DTM. We produced three raster products in 2-meter spatial resolution from the LiDAR point cloud including DTM, DSM, and the canopy height model (CHM). We used the existing classification labels from SMC, and created the digital terrain model (DTM) using mean elevation of LiDAR points labeled as class 2 (ground) in each 2-meter pixel. Pixels with missing data were interpolated by natural neighbor interpolation. (2) LiDAR points classified as 2 (ground),) in each 2-meter pixel. Pixels with missing data were interpolated by natural neighbor interpolation. (2) LiDAR points classified as 2 (ground), 3 (low vegetation), and 4 (medium vegetation) were used all together to create digital surface model (DSM). The maximum elevation of the used LiDAR points in each 2-meter pixel was picked as the DSM value. (3) As a result, the canopy height model (CHM) was calculated as the height difference between DSM and DTM.

The decision of creating 2-meter raster products was based on the designed airborne data acquisition in DRC. With an average coverage of approximately 4 LiDAR points per square meter, raster creations in 1-meter resolution are not appropriate. We found unexpected stripes of data

Figure 4: Distribution of LIDAR transects and ferry lines across the humid tropical forests of DRC.

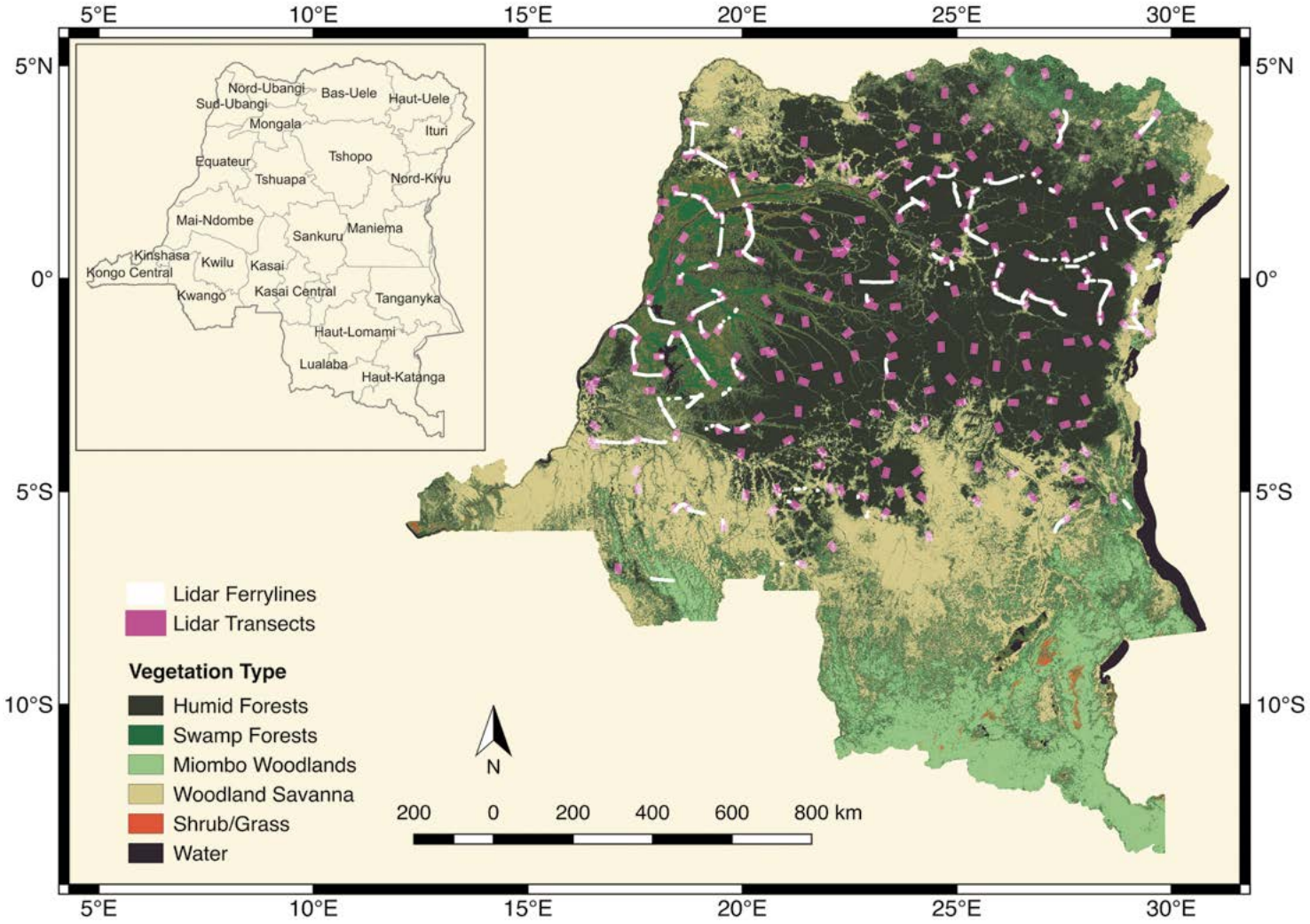

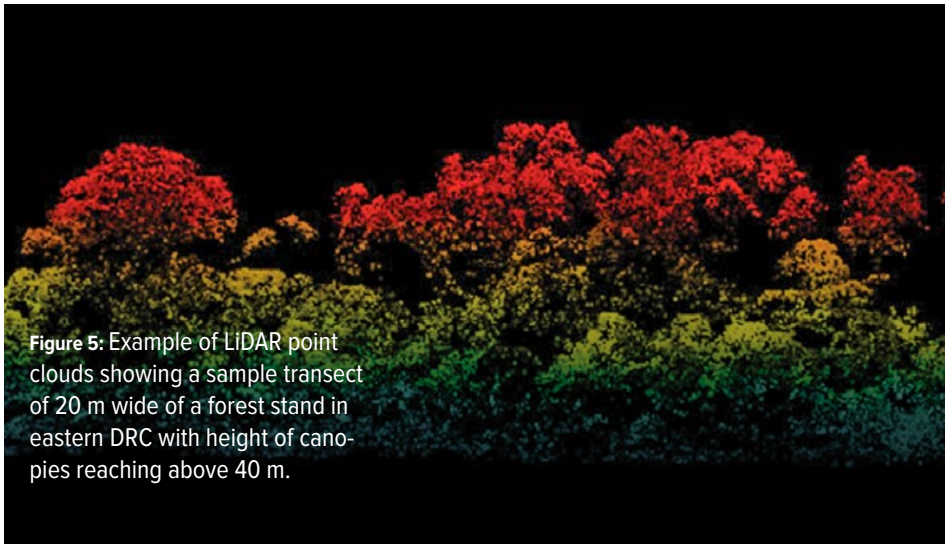

Figure 5: Example of LiDAR point clouds showing a sample transect of 20 m wide of a forest stand in eastern DRC with height of canopies reaching above 40 m.

gaps from 1-meter CHM, because of missing vegetation LiDAR points in these pixels. These data gaps cannot be corrected by the spatial interpolation method, because ground points exist in some of these gaps. Such ground points in gaps lead to extremely low CHM values compared to nearby pixels, while they are apparently canopy pixels observed from aerial photos. We decided to use the 2-meter spatial resolution when a sufficient number of LiDAR points are available in each pixel to determine the maximum height. Results show that the CHM raster images in 2-meter resolution can eliminate most of the undesired gap signals without sacrificing too much spatial detail. The 2-meter posting products were the most reliable

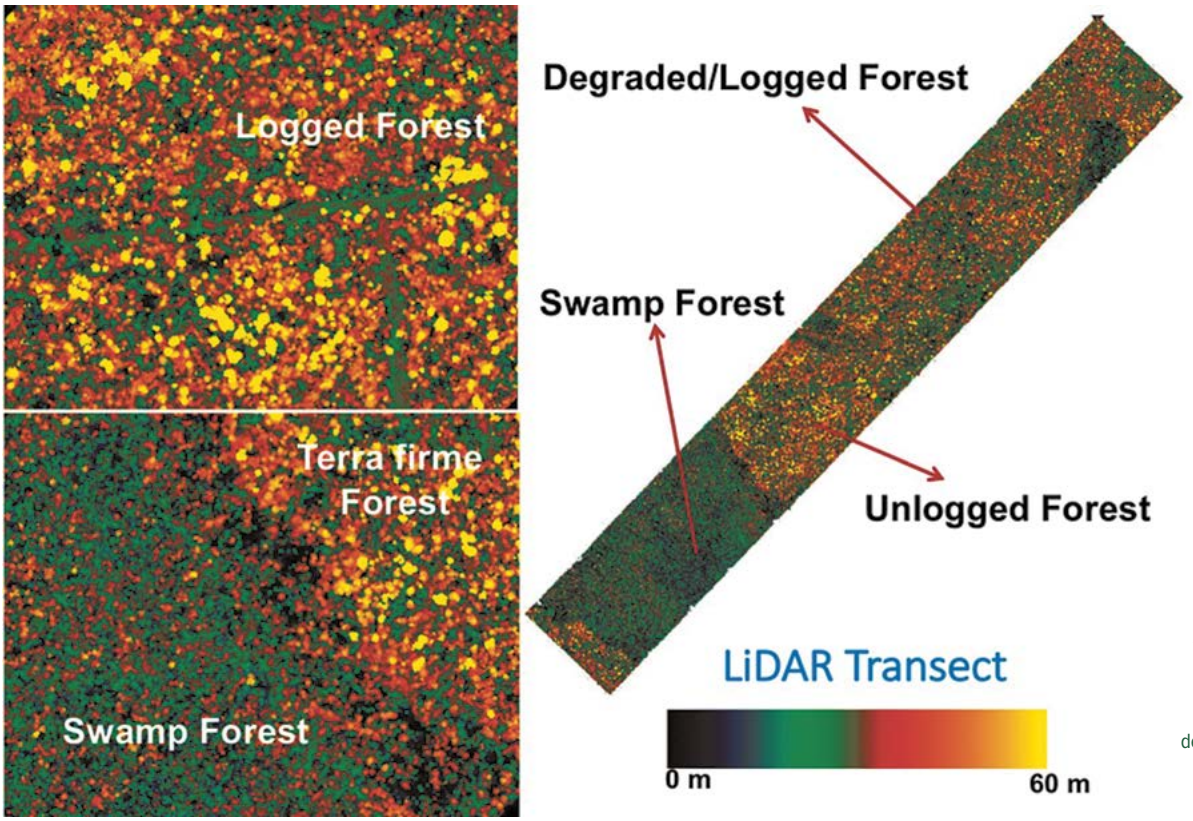

Figure 6: Example of LiDAR random sample covering an area of approximately 2000 ha of intact, degraded and swamp forests. The detailed information in LiDAR point clouds allow for identifying different degrees of degradation and separating forest types based on their 3-D structure.

data sets in terms of uniform pulse density, geolocation accuracy and the precision of height and structure.

For 1-ha (100-meter) spatial resolution, we used approximately 2500 2-meter observations for each hectare of forest. To ensure that the MCH values can well represent the mean characteristics of 1-ha pixels, we set MCH observations valid only when 90% of the 1-ha pixels are covered by airborne LiDAR measurements, i.e., we excluded most of the edge pixels with partial coverage in the 1-ha mapping process. The final LiDAR-derived 1-ha map of DRC has a total of about 665,000 valid 1-ha pixels from random sampling and ferrylines that can be used in national-level MCH and carbon mappings.

Ground Plots

Ground inventory plots distributed over DRC were collected to calibrate the LiDAR data. All the ground data was collected from various partners, listed in appendix, between 2011 and 2016. The requirement for the field data included two sets of plots. One permanent plot at 1-ha (100 m x 100 m) and four auxiliary plots at 0.25 ha (50 m x 50 m) distributed on the eastern and western axis from the center of the permanent plots at 250 m and 500 m intervals. However, the ground plots we are using here vary in size, shape and design because they are coming from different sources and collaborators. We are using a total of 4684 ground plots, varying between sizes of 0.04ha and 1ha. 139 of these plots meet our 1ha plot size requirements for biomass model calibration, of which 47 are set aside for independent validation (ground estimated AGB vs Maximum Entropy estimated AGB) because they do not fall into any LiDAR scene. The smaller plots could not be used for calibration of the LiDAR data because of their size and potential geolocation uncertainty. However, smaller plots were used to retrieve information on wood density, assuming that plot size does not affect this metric.

Locations of inventory plots collected for this project were selected randomly in the LiDAR transects to make sure that the process of calibration and validation does not introduce any artificial bias. We also used pre-existing plots that fell within the LiDAR transects for calibration of the LiDAR. In all cases, the measurement of the trees followed the standard protocols provided by the IPCC guidelines to provide diameter, sample heights, and species identification.

Plot location is known for all the plots and is characterized by four corners of the plots (square or rectangular plots). Although the accuracy of geolocation is supposed to be between 3 and 8m, in most cases, the error was larger and measured distance between corners were used to better locate the plots on the LiDAR transect. We used only 1-ha plots to calibrate the LiDAR data because larger plots provide a better relationship with LiDAR metrics, reducing the overall uncertainty of biomass estimation and errors associated with the allometry, edge effects and geolocation errors[22,23].

Forest Biomass Allometry

Specific equations for Central African forests are rare because of the lack of availability of destructive sampling of trees of different size and rigorous statistical approaches for developing the regression models and testing for random errors and bias[24-26]. One of the most reliable allometric equations widely used in most studies in tropical forests is developed by Chave et al. (2014)[24], improving upon earlier equations used for estimation of aboveground biomass across tropical forests. The new equation includes a large numbers of trees from Central Africa, which is an improvement over earlier work[27], which only included trees from Asia and Americas. The mean percent bias and variance of this model was only slightly higher than that of locally fitted models[24].

Wood specific gravity was an important predictor of aboveground biomass, especially when including a much broader range of vegetation types than previous studies.

Height-diameter Allometry

Within each plot, all stems > 10 cm in diameter (D) at breast height (dbh) were measured at 130 cm from ground or above the buttress or trunk deformations. In addition, the total height (H) of some trees were measured using instruments such as the Laser ACE 2D Hypsometer (MDL, York, UK ie. Bastin plots). In all plots established under this project, tree height was measured by sampling 10 trees within each DBH class from 10-50 cm at 10 cm interval, 10 trees for 50-70 cm class and all trees > 70 cm diameter. Emphasis on measurements of the height of large trees was designed to improve the ground-estimated biomass estimation as large trees contribute significantly more to the overall biomass. Height of trees that were not measured in the field was estimated using local H-D models developed typically for each plot or sub-region. DBH-H allometric model follows a logarithmic function:

$$H = aln(D) + b$$

However, some plots did not have any reliable measurements of trees and had no neighboring plots that could be used to assign a local H-D model. For trees in these sites (i.e. Ituri, PARAP Luhudi and PARAP Maniema, FRM, etc.), AGB was estimated using a allometric models without tree height.

Tree species were identified and recorded for wood density calculations. Wood density was assigned using the World Wood Density database for tropical trees (Chave et al, 2009) and the FAO database, at the highest level possible, species level being the most precise level, followed by genus and family level. In the cases where tree identification was missing or did not match any name in our databases, the mean wood density of the plot was assigned.

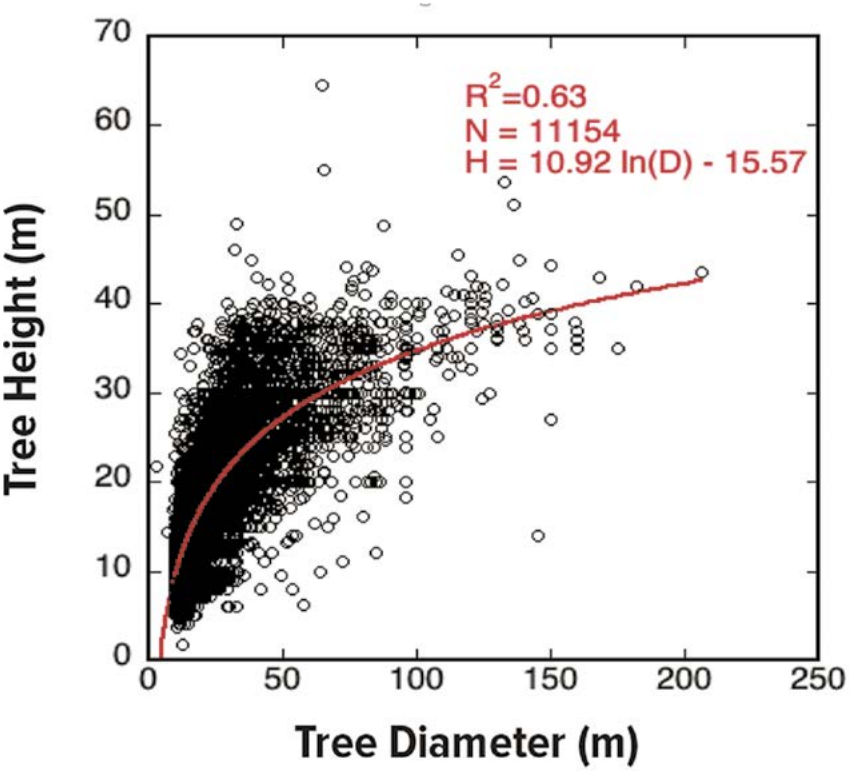

Figure 7: Relation between forest tree height and diameter in western DRC using measurements of 11154 trees from 32 1-ha plots established by Bastin et al. (2014)28.

Above Ground Live Biomass

Here, AGB was calculated using the allometric models developed by Chave et al, 2014.

$$AGBH_{est} = \frac{10^{-3}}{A}\sum_{i=1}^{N} 0.0673 \times (\rho_i D_i^2 H_i)^{0.976}$$

$$AGB_{est} = \frac{10^{-3}}{A}\sum_{i=1}^{N} e(-1.803 - 0.976\,E + 0.976\,ln(\rho_i) + 2.673 \times ln\,(D_i) \\ 0.0299(ln\,(D_i))^2)$$

Where AGBest is the above ground biomass in units of Mg ha-1, A is the area of the plot in hectare (ha), D_i is the diameter of each tree in the plot in centimeter (cm), Hi is the height of each tree in meter (m), and ρ_i is the wood density of each tree in g cm^{-3}. In Equation 2), E is a measure of environmental stress, taking into account temperature seasonality, precipitation seasonality and climatic water deficit, at any location on the globe[24]. Equation 2 was used for sites where no tree height measurement or when the measurements were considered unreliable.

Biomass Correction for Small Trees

The aboveground biomass was further augmented for all trees with DBH < 10 cm. Trees < 10 cm in diameter and height > 1.3 m were not measured in most of the plots. However, the data provided for the 40 ha plot in Ituri included a complete set with all trees > 1 cm. We used a model relating the AGB of all trees > 1 cm to trees > 10 cm at 1-ha scale and applied the model to all 1-ha ground-estimated AGB values. Small trees add approximately 3-7% on the average to the aboveground biomass values.

$$AGB_{1cm} = 1.872(AGB_{10cm})^{0.906}$$

Below Ground Live Biomass

For belowground estimation of tree biomass and carbon stocks, we used established allometry based on the aboveground biomass using root to shoot ratios. It is not practical to measure below ground biomass in most tropical forests on a routine basis. It is also very difficult to develop an appropriate, country-specific allometric equation for root biomass. Instead below-ground biomass is estimated from a well-accepted ratio for moist tropical forests[29,30] ; which reliably predicts root biomass based on shoot biomass. The equations below show how the belowground biomass (BGB) can be estimated from AGB.

$$BGB = 0.235 \times AGB \;\; if \; AGB > 125 \; Mg \; ha^{-1}$$

$$BGB = 0.205 \times AGB \; if \; AGB \leq 125 \; Mg \; ha^{-1}$$

$$BGB = 0.489 \times AGB^{0.89}$$

LIDAR BIOMASS ESTIMATOR

Calibration plots of 1ha were used to develop the LiDAR-biomass model. Out of the 139 plots of 1ha available in DRC, 92 plots fell within LiDAR flightlines. Each of these plots represents a region of interest (ROI) in our LiDAR 2m resolution CHM dataset. For each ROI, pixels were extracted and used to calculate the LiDAR mean canopy height (MCH) for each plot. Calibration of LiDAR data for biomass estimation consists in finding the relationship between LiDAR MCH and ground estimated AGB across DRC (see Appendix for available data). We tested a model that includes wood density as a weighting parameter to allow the model to be used for different forest types with different average wood density. If general wood density variations can be determined from existing historical field surveys, the LiDAR model can be readily adjusted to produce unbiased estimate of the biomass. The overall form of the model is:

$$AGB = a(h)^b + \epsilon$$

$$AGB = a(WD \times h)^b + \epsilon$$

$$WD = \frac{1}{N}\sum_{i=1}^{N} \rho_i$$

where WD represents the plot mean value of wood density of individual trees (ρ_i) in units of g cm-3, h represents the mean top canopy height MCH in units of m from LiDAR observation, and $\varepsilon \sim N(0,\sigma^2)$ represents the uncertainty in measurements.

The LiDAR biomass model is the key element of the overall estimation of biomass for stratified forest types and for the national mapping. The model will introduce both random and systematic errors to the estimation of biomass. Due to the large sample size, the impact of the random estimation error is relatively negligible. However, the bias and systematic much be quantified to allow for removal of the biomass on the estimation of biomass and reduce its effect on the national carbon map.

The source of the systematic error in the model is the representativeness of plots over the entire range of available biomass and the quality of the model fit to the data. We quantified the systematic error in the model through a boot-strapped cross-validation process by removing 20 percent of the data for validation for 100 times and quantifying RMSE and the bias.

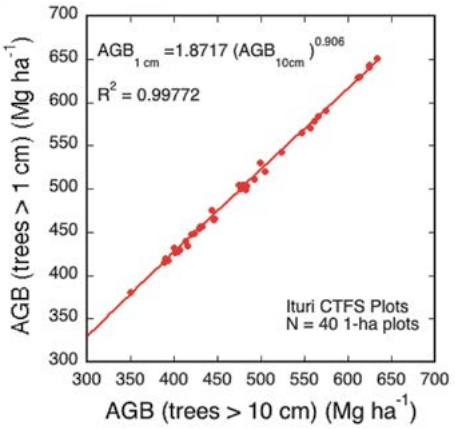

Figure 8: Model to scale the forest biomass to all trees > 10 cm in diameter from measurements of trees > 20 cm in diameter. Plots inlcude data from ROC forest inventory and research plots in Congo (Afritron) and border regions in Gabon and DRC in similar forest types. The plots include both terra firme and swamp forests.

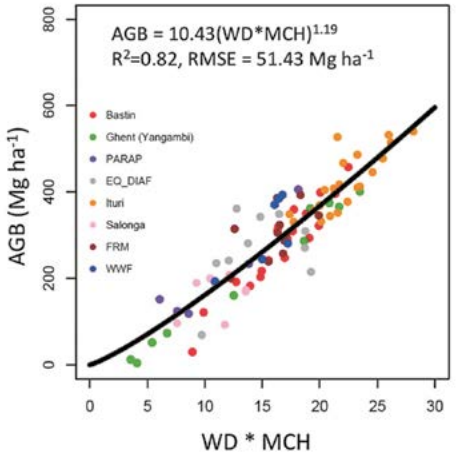

Figure 9: Calibration of airborne LiDAR measurements of mean top canopy height (MCH) in meter to above ground biomass density (AGB) in Mg/ha using 92 1-ha plots distributed in DRC and collected in 2014-present to coincide in time with LiDAR flights. The Ituri plot data were acquired from the Smithsonian Institute. The power-law model fit was based on a non-linear fit (black line) that provided approximately no bias in estimation of AGB.

Model Type	Allometry	a	b	R^2	rmse (Mg/ha)	bias (Mg/ha)	Cross-val R^2	Cross-val rmse (Mg/ha)	Cross-val bias (Mg/ha)
$AGB = a(h)^b$	E factor	2.58	1.47	0.78	56.64	-0.83	0.77	57.86	-1.05
	Height	0.86	1.78	0.71	61	-1.05	0.69	62.73	-1.24
	combo	2.06	1.53	0.75	59.73	-0.72	0.75	60.73	-0.89
$AGB = a(WD \times h)^b$	E factor	13.36	1.12	0.83	49.47	-0.67	0.82	50.52	-0.79
	Height	8.26	1.26	0.77	54.25	-1.29	0.75	55.91	-1.7
	combo	10.43	1.19	0.82	51.49	-0.69	0.81	52.54	-0.69

MAPPING CARBON DENSITY

To produce the national carbon map at 1-ha (100-meter) spatial resolution, we built a synergistic model for estimating biomass and total carbon from a variety of data sources, including the *in-situ* measurements of key forest attributes such as AGB and wood density, airborne small-footprint LiDAR systematic sampling with a wider spatial coverage at the country level. We also included the spatial data from contemporary satellite imagery covering the DRC in the optical and microwave spectral domain with sensitivity to forest structure that will allow the process of mapping forest biomass. The key steps of our workflow is shown below.

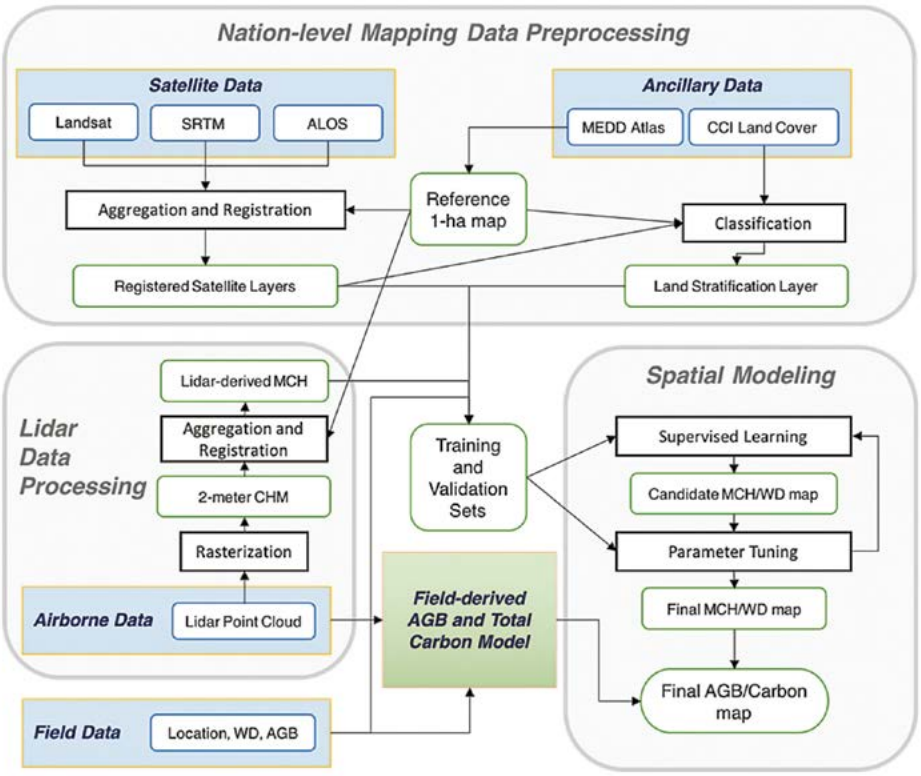

Figure 10: Workflow and the processing steps to develop carbon estimates in forests of DRC and produce spatially explicit map at 1-ha resolution along with uncertainty assessment.

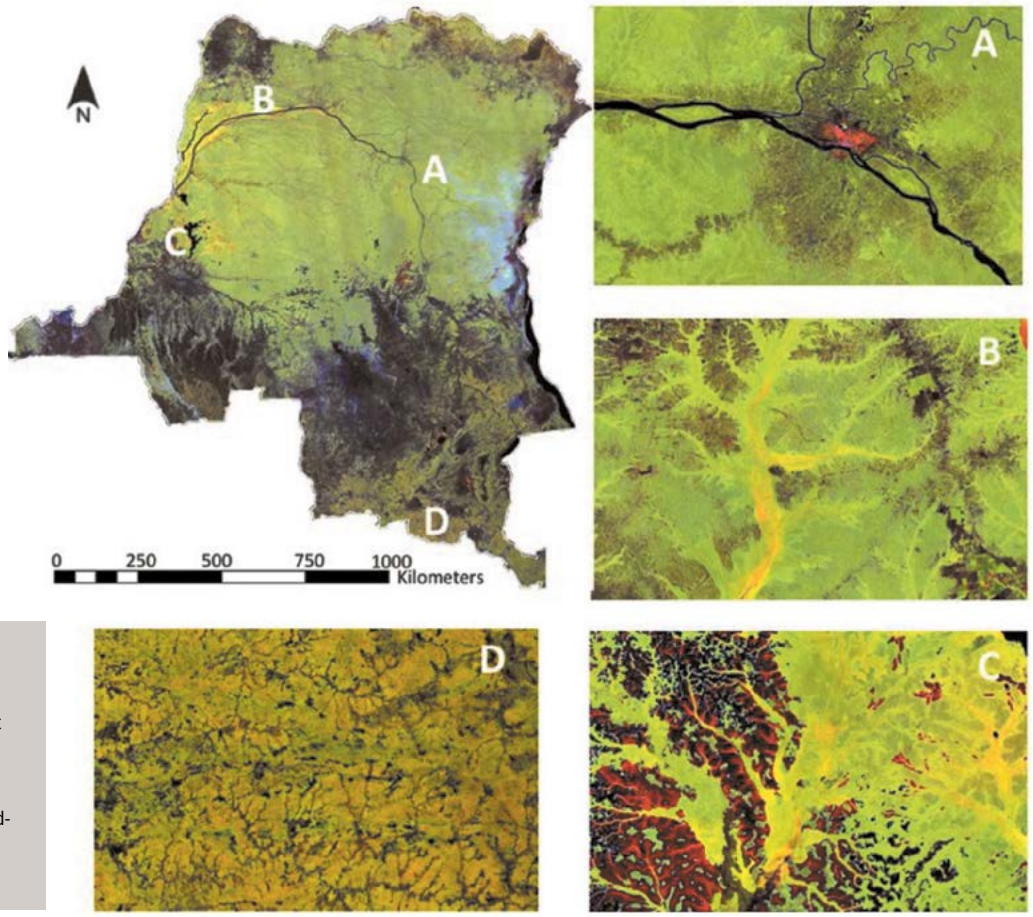

Figure 11: ALOS PALSAR mosaic imagery acquired in 2007-2010 and aggregated to about 100 m spatial resolution showing variations of intact (A), degraded (A),B), swamp forests (B), Forest-savanna boundary (C), and Miombo woodlands (D) in four panels across DRC.

Satellite Image Data

Environmental layers in our study include satellite data and ancillary mapping products of administrative boundary and major land cover types based on forest atlas data from the Ministère de l'Environnement et Développement Durable (Potapov et al. 2012)[20]. We also used MEDD data from WRI to define the boundary of the country and provinces[31]. From the source vector data in shapefile format, we rasterized the map in 100-meter resolution with binary numbers. We assigned the value of 1 to each pixel within the country boundary, and the value of 0 to the rest of pixels. The final output is under the geographic coordinate system (GCS) with WGS84 datum (pixel resolution in 0.0008983°). This becomes our reference 1-ha map, and every other data set should be registered to this map.

We used three sources of satellite data as our inputs to the synergistic model.
The first input is the radar backscatter data from the Phased Array L-band Synthetic Aperture Radar (PALSAR) sensor aboard the Advanced Land Observing Satellite "DAICHI" (ALOS). ALOS has the L-band SAR observations at the wavelength of 1270 MHz for five years' operation from January 2006 to May 2011 and starting again . The Japan Aerospace Exploration Agency (JAXA) has produced the ortho- and slope-corrected backscattering coefficient of PALSAR global mosaics in both HH and HV polarizations from 2007 to 2010[32]. We used the 4-year mean (2007-2010) of PALSAR data gridded at 100 m as input layer for geospatial modeling.

The second input is the mosaic of Landsat-8 top-of-atmosphere (TOA) reflectance data averaged from April 2013 to August 2016. We used the simple cloud-score algorithm on the Google Earth Engine[33] for cloud screening, and kept the median values over the 3 years as valid observations. The final cloud-free imagery of Landsat-8 contains 4 bands including band 4 (Red), 5 (NIR), 6 (SWIR-1), and 7 (SWIR-2) at 30-meter spatial resolution. To account for the BRDF (bidirectional reflectance distribution function) effect of Landsat data, we corrected our Landsat-8 mosaic using the MODerate-resolution Imaging Spectroradiometer (MODIS) Nadir BRDF-Adjusted Reflectance (NBAR) product (MCD43A4)[34,35]. By obtaining the MODIS NBAR mosaic similar to Landsat-8 for the same time period, we applied a simple correction as follows:

$$L_{corr} = L \times \frac{N_{fmean}}{L_{fmean}}$$

where L and L_{corr} are the Landsat reflectance before and after the correction, L_{fmean} and N_{fmean} are the focal means of original Landsat and NBAR reflectance, and we used the window size of 2500x2500 meters for both data sets.

The third input is the digital elevation model (DEM) data derived from the Shuttle Radar Topography Mission (SRTM). The global mosaic of SRTM land elevation product36 has a spatial resolution of 30 meters processed by the National Aeronautics and Space Administration (NASA). Although the latest release

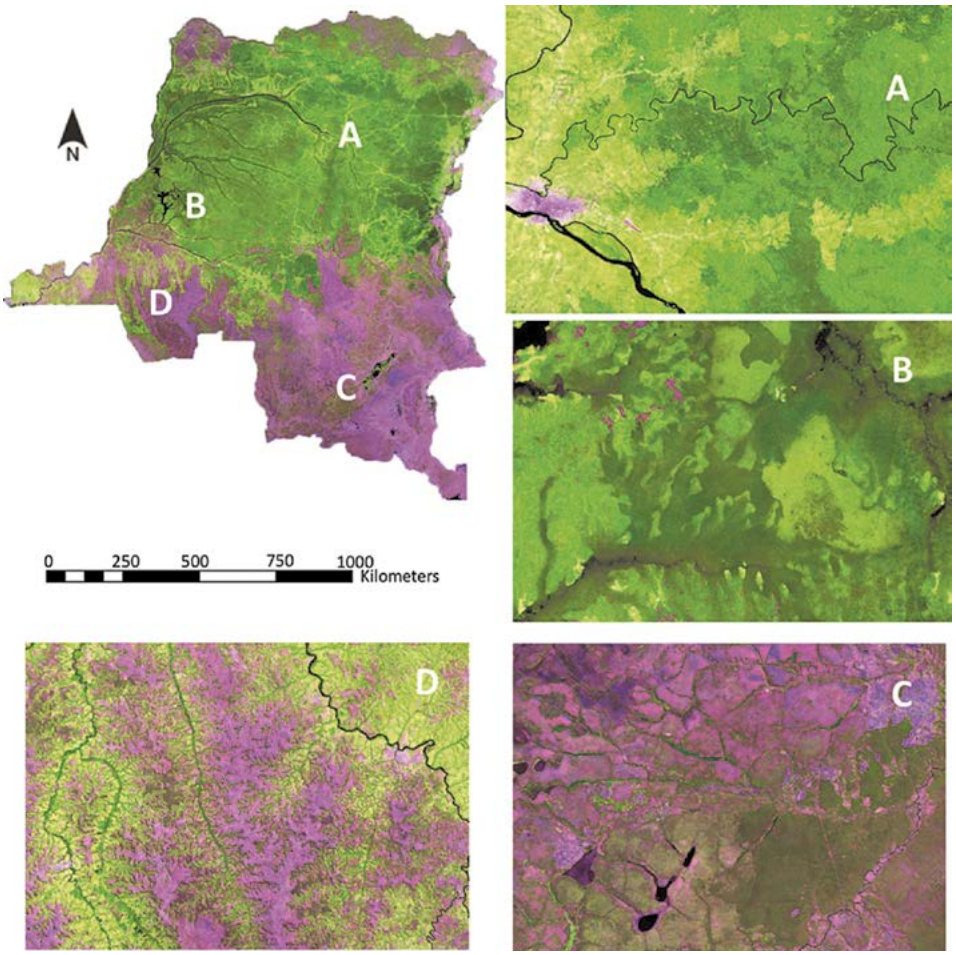

Figure 12: Cloud free Landsat 8 image mosaic aggregated to about 100 m using four bands and samples of image quality over areas of intact (A), degraded (A), swamps (B), Miombo woodlands (C), and forest-savanna mosaic vegetation (D).

of SRTM land elevation is the void-filled product (SRTM v3), there are regions with missing data in DRC (e.g. regions in the eastern part of the country. We used the ASTER GDEM v2 (Global Digital Elevation Model Version 2) data to further fill the gaps in these areas.

The preprocessing of satellite data includes spatial aggregation and image registration. We aggregated 4 bands of Landsat-8 mosaic, 2 bands (HH/HV) of ALOS PALSAR, and the SRTM v3 DEM data into 100-meter spatial resolution using spatial average. We also kept the local standard deviation of SRTM data as an additional layer, creating a final set of satellite inputs with 8 layers. Using the 1-ha reference map created from the MEDD country boundary, we registered all our satellite layers to the same raster grid.

Geospatial Modeling

With the availability of environmental layers and LiDAR-derived MCH, we were able to build a supervised learning model as the spatial estimator to predict the unknown MCH for locations where we have environmental data. Maximum Entropy (ME), as a supervised learning algorithm, is a probability-based algorithm that seeks the probability distribution by maximizing the information contained in the existing measurements[37,38]. In the ME algorithm, a measurement A of class k has the probability of occurrence $p(A_k)$ with the constraint that probabilities of all $p(A_k)$ must sum to 1 ($\sum_k p(A_k) = 1$). From information theory, the most uncertain probability distribution is the one that maximizes the entropy term:

$$E = -\sum_k p(A_k) \ln p(A_k)$$

With some knowledge of additional information, i.e. the training set of MCH measurements with corresponding environmental data X, the probability distributions are "conditioned" on the available observations:

$$p(A_k|X) = p_k(X)p_0(A_k)/p(X)$$

The right part of the above equation follows the Bayes' theorem, meaning that the posterior probability $p(A_k|X)$ depends on the distribution of X and equals to the product of prior probability $p_0(A_k)$ and the probability distribution $p_k(X)$ that finds X to be in the class k, and normalized by the probability distribution of X for the entire domain of measurement variables (environmental layers). For our interested metric MCH, we categorize the numeric values into a set of classes: $k_1, k_2, k_3, \ldots, k_n$, where $0 < k1 \leq MCH1 < k2 \leq MCH2 < \bullet\bullet\bullet < kn \leq MCH_{max}$. And each class has a nominal value of MCH – usually the mean value of each class, MCH_k. To predict the MCH value for any pixel i with known measurements X_i, we calculate it as the expectation of all classes given the ME results retrieved from the training set:

$$\langle MCH_i \rangle = \frac{\sum_{k=1}^{N} p(A_k|X_i)\overline{MCH}_k}{\sum_{k=1}^{N} p(A_k|X_i)}$$

Empirical tests have found that the model performs better when assigning higher weights to more probable classes,

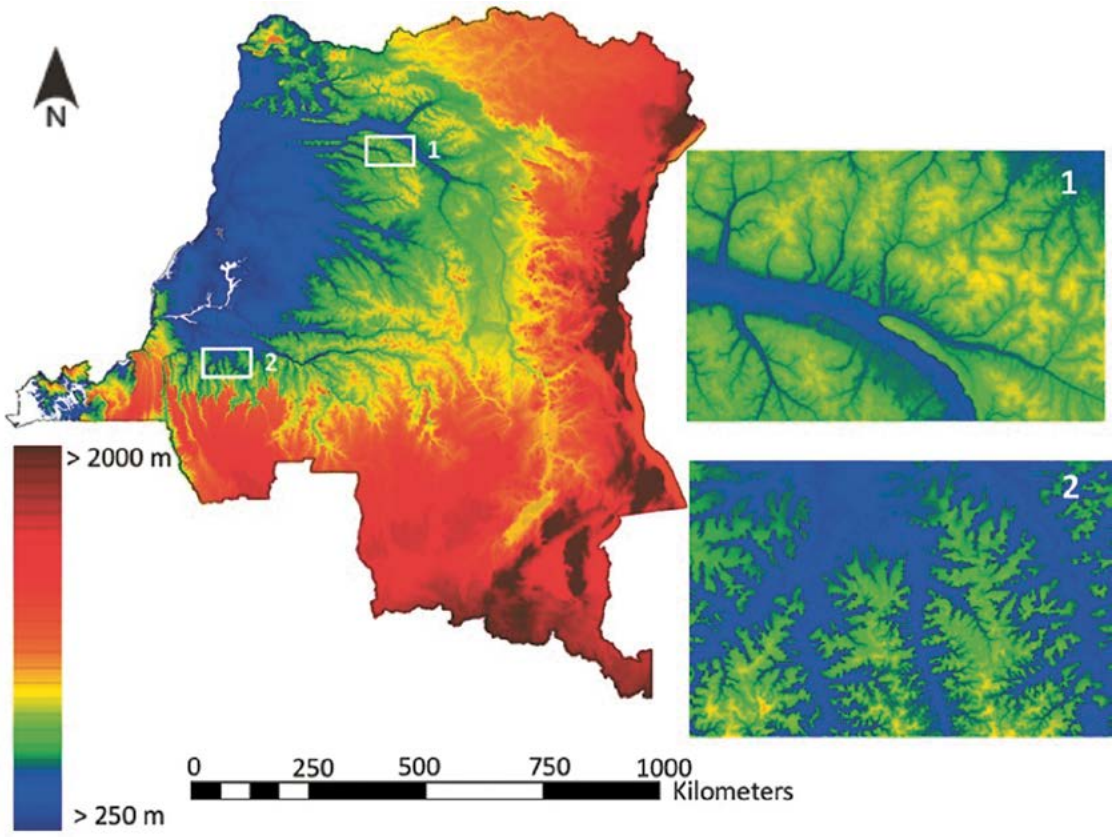

Figure 13: Images of digital elevation data from SRTM showing the overall topographical gradients across DRC and regions dominated by wetlands (1) and a combination of swamp forests and forest-savanna mosaics (2).

$$\langle MCH_i \rangle = \frac{\sum_{k=1}^{N}[p(A_k|X_i)]^m \overline{MCH}_k}{\sum_{k=1}^{N}[p(A_k|X_i)]^m}$$

The parameter optimization procedure suggests m=3 as the best parameter with the smallest average relative error and keeping most test points aligned with the 1-to-1 line39,40. We evaluated 3 statistical measures in our parameter tuning procedure, including the coefficient of determination (R^2), the root-mean-square error (RMSE), and the mean signed deviation (MSD). Besides the overall MSD applied to all test samples, we assessed two additional MSD measures for both small trees (MSD1) and large trees (MSD2). We define MSD1 as the MSD calculated for test samples with the sum of predicted MCH and measured MCH to be less than 20 meters. Similarly, MSD2 is defined as MSD for samples with the sum of predicted MCH and measured MCH to be less than 60 meters. Results also suggest that we use a relatively larger regularization multiplier (~5) and a large background number to avoid overfitting.

The mapping of WD adopted the same spatial modeling procedure as MCH. But WD training data were from field measurements of 1-ha plots covering the whole country. A total of 4287 1-ha WD samples of ground measured WD was extrapolated using a bias-corrected Random Forest estimator to the country-level map.

The LiDAR-based biomass estimator is expressed as a power-law function with MCH and WD as input variables. With the availability of both MCH and WD maps at the country level, we can produce the final AGB map by applying the allometric equation.

FOREST CARBON DISTRIBUTION OF DRC

The AGB map of DRC provides the detailed spatial variability of carbon stored in the forests at landscape and regional scales (see figure below) and follows disturbance and topographical gradients, where density of large trees dominating the magnitude of AGB may be impacted. The AGB distribution across forest degradation, roads and settlements, or geomorphological features associated with slopes, soil type and moisture conditions can be readily identified in the map.

The overall variation of AGB across forest types[20] ranges from as low as 1±10 Mg/ha for shrublands to as high as 296±86 Mg/ha for evergreen forests. Within the humid tropical zone of the country extended between the latitudinal bands of 5°S and 5°N, there is a strong spatial variation of carbon storage, showing significant differences by geographical regions.

The largest stretch of high AGB is across the eastern border region of DRC, starting from the northeastern Ituri to nord- and sud-Kivu provinces (Table 1). These forests are distributed over rugged terrains along the foothills of eastern mountains below 1000 m asl (above sea level) and stretch west into Tshopo, Maniema, and southern Sankuru provinces. The average AGB is about 320 Mg/ha

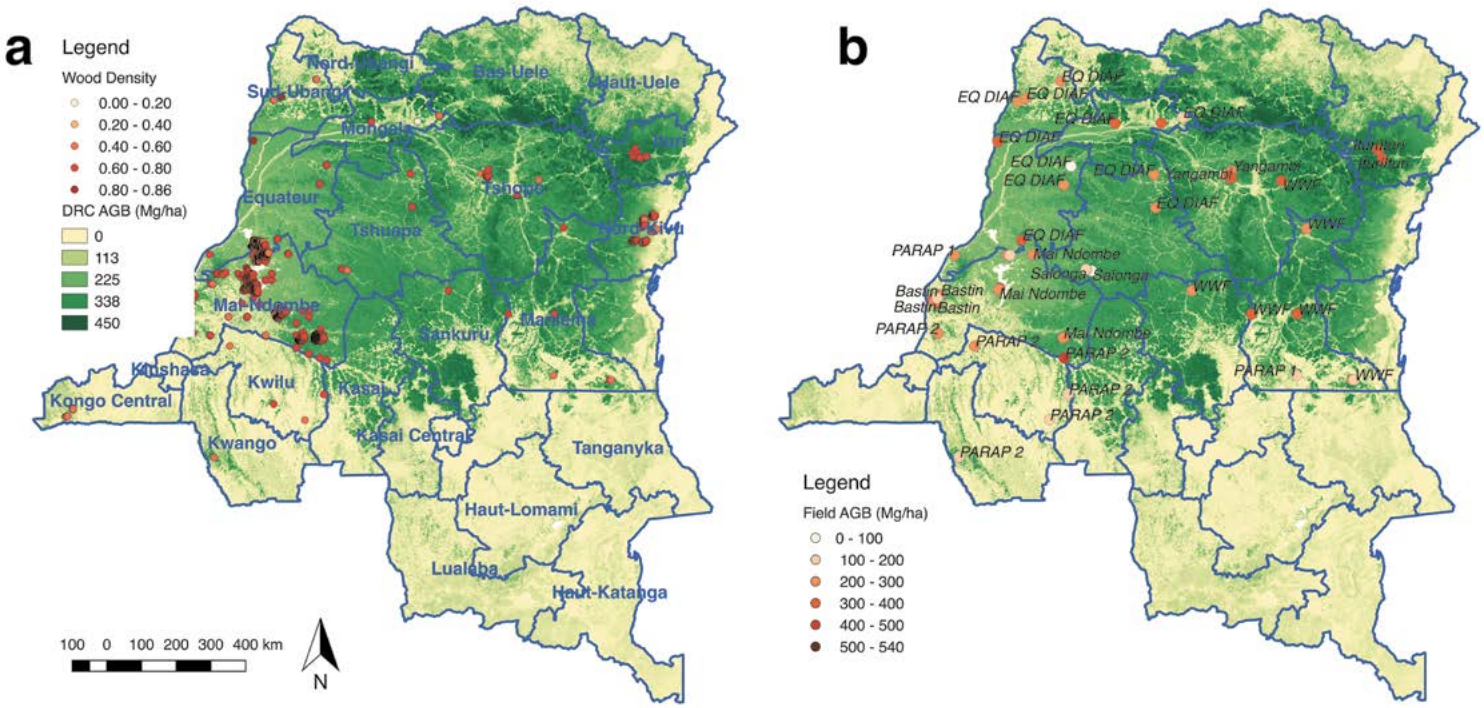

Figure 14: Locations of available field data in DRC: (a) All available wood density field data in DRC. (b) All available 1ha field plots of AGB measurements. The colored based map is our prediction map of AGB, the blue labels on the left panel are province names, and the black labels on the right panel are the source names of field measurements.

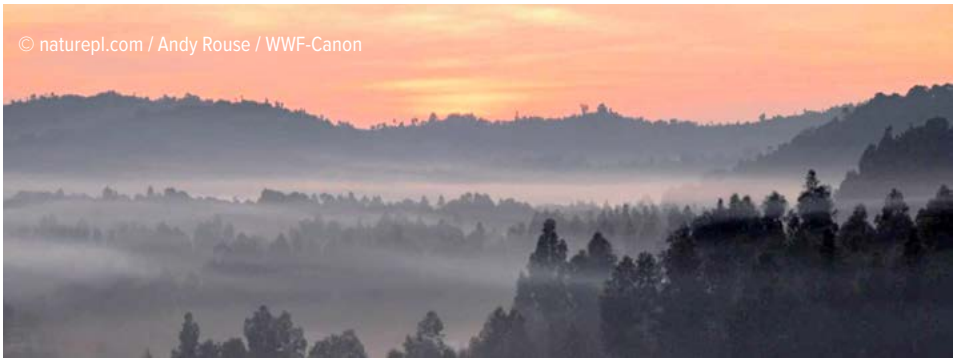

and the AGB values of greater than 450 Mg/ha are observed over significant number of 1-ha pixels. Another distinct pattern of high biomass extends in the northern DRC along the remaining intact terra firme forests of Bas-Uele, Nord-Ubangi and Mongala provinces. These forests occupy relatively flat terrain over Humic acrisols and Hapic Ferralsols soils with mean biomass exceeding 380 Mg/ha and extensive areas with greater than 500 Mg/ha.

The eastern mountains and the northern elevated plateau slope gently towards the interior and to the west of the country where the central depression of the Congo Basin forms the Cuvette Congolaise swamp (wetlands) forests[24]. The swamp or edaphic forests distributed along the Congo, Ubangi, other large tributaries such as Ruki, Lulonga, Maringa, and Tshuapa river systems and within the Lake Tumba and Lake Mai Ndombe basins have a slightly smaller mean carbon density compared to the evergreen forests (206±64 Mg/ha). The entire swamp forests cover about 9.5 million hectares in DRC divided into hardwood and palm dominated swamps over an extensive area of peatlands[25]. We consulted the map of swamp forests provided by and estimated the mean AGB for hardwood dominated swamps is 264 ± 21 Mg/ha and for palm dominated swamp is 71± 29 Mg/ha.

The largest contrast in forest biomass is mainly in the southern provinces of DRC where a mosaic of tree grass savanna and riparian forests dominate the landscape in southern Bandudu provinces towards the extensive southeastern deciduous Miombo woodlands in Lualaba and Katanga. These forests have significantly lower biomass stock (44±37 Mg/ha and 21±30 Mg/ha, respectively), though they cover an equally large region

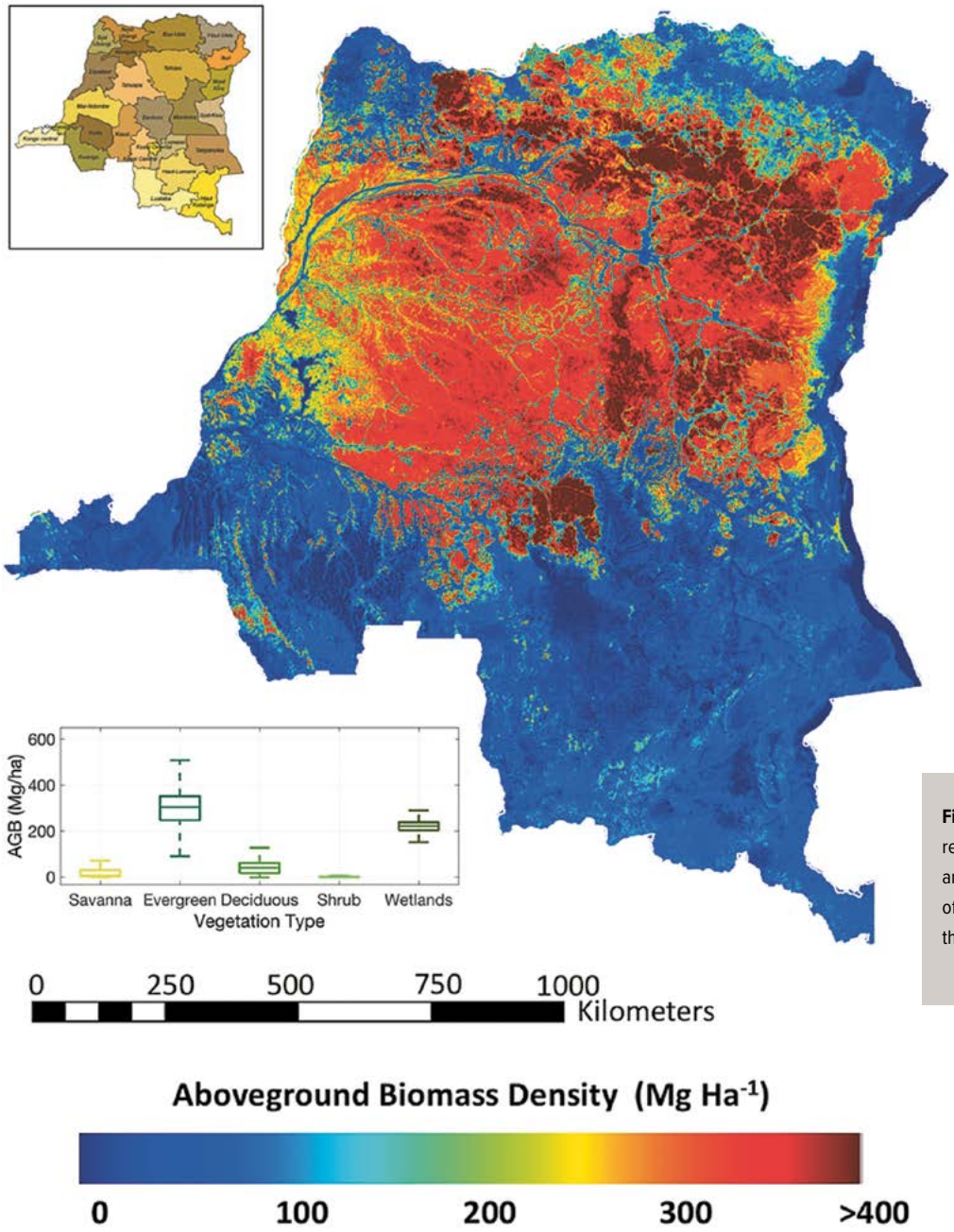

Figure 15: National AGB map at 1-ha spatial resolution showing spatial patterns of AGB in DRC and within provinces along with mean estimates of AGB for each land cover types identified using the national map of DRC.

(117 million ha) in DRC compared to the humid tropical forests (115 million ha). The airborne LiDAR samples were only conducted in forest and forest-savanna boundary regions and did not cover the Miombo forests. However, the limited sampling and the higher sensitivity of ALOS PALSAR imagery to woodland biomass range provided reasonable training data set for the machine learning algorithm to estimate spatial distribution of AGB in these other types of forests. The large variability in the estimate is mainly due to the heterogeneity of forest cover and the impact of frequent disturbance such as fire and land use change such as slash and burn agriculture which is particularly prevelent across forest-savanna boundaries and within the Miombo woodlands.

If our LiDAR biomass estimator is free of error, the biomass map gives unbiased estimates of all available ground plots with an overall accuracy of 63 Mg/ha for AGB density. Using the carbon factor of 0.49, we summarize the recent total carbon storage in DRC to be approximately 23.3 Pg for the forested region.

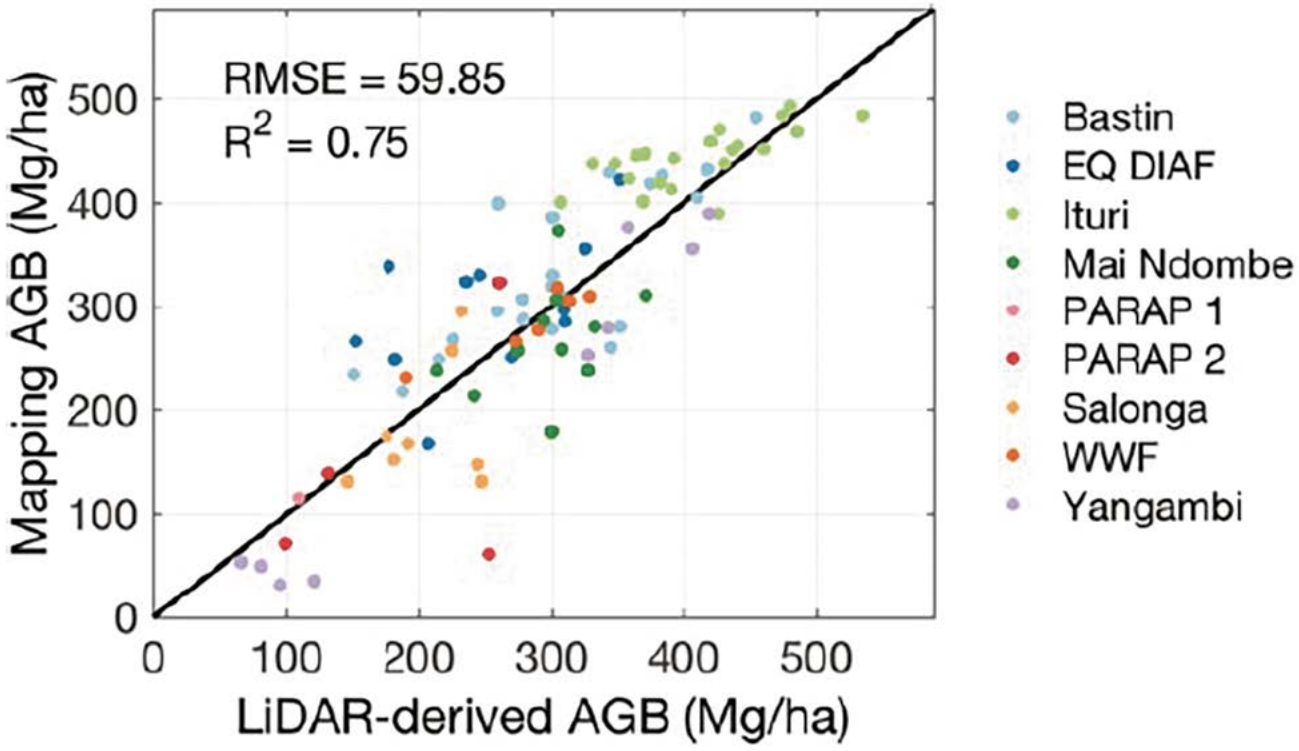

Figure 16: Scatter plot of mapped AGB vs. field LiDAR-derived AGB values showing the validation of the national carbon map of DRC across forest types using field LiDAR pixels calibrated by field inventory plots.

UNCERTAINTY

The LiDAR probability sampling approach follows design-based inventory sampling to ensure unbiased estimates of forest structure. However, similar to the national inventory in design-based ground sample plots, the estimation of AGB at local or regional scale depends strongly on the use of an allometric model. The LiDAR-AGB model plays the same role as the ground allometric model and the overall uncertainty of AGB estimate depends on how well the model was developed. Here, we provide the uncertainty of forest biomass at two levels: 1. We quantify the uncertainty associated with the LiDAR-AGB model using ground plots distributed across DRC. 2. We estimate the uncertainty associated with the MaxEnt prediction at the pixel and jurisdictional scales over the entire country.

LiDAR-AGB Model Uncertainty

LiDAR-AGB model was developed using ground plots distributed randomly within a LiDAR transect across but only in transects that were not limited by access or security. We tested for the uncertainty of the model using a bootstrapping (1000 times) cross-validation approach with randomly selecting 80% of data for model fits and 20% for validation. The result suggests that model has a standard error of 52.54 Mg ha^{-1} at 95% confidence interval but remains relatively unbiased (-0.62 Mg ha^{-1}) across all regions. The use of wood density as a weight to LiDAR-derived mean canopy height is contributing to reduce the bias that may have been introduced in the model due to variations in tree composition.

Pixel-level Uncertainty

We first evaluated the uncertainty associated with the spatial modeling of AGB using cross-validation (CV) approach. CV results from LiDAR plot-based sampling give the best overall prediction compared to the other methods, with an average RMSE of 61±1 Mg/ha. Considering the possible existence of residual spatial autocorrelation, CV results from latitudinal sampling have a relatively larger prediction error, with an average RMSE of 70±6 Mg/ha. The two CV results also confirmed that the predictions were statistically unbiased over the entire sample size, with the mean signed deviation (MSD) at 0.4±3.2 Mg/ha for LiDAR plot-based sampling and -4.5±15.2 Mg/ha for latitudinal sampling approaches. To further explain the differences between the two CV methods, we used a variogram-based analysis showing the spatial autocorrelation with paired distance. The spatial autocorrelation in the original AGB map can extend for more than 200 kilometers, and the covariance between spatially On the other hand, the residuals between our prediction and LiDAR samples show a similar range of spatial autocorrelation but less than 10% of the original covariance. This residual spatial autocorrelation can cause larger prediction uncertainty for pixels far away from the training data, resulting in the differences between two CV methods.

Other sources of uncertainty come from (1) the uncertainty of the field-derived Li-

Figure 17: AGB uncertainty map showing the spatial variation of pixel level uncertainty from MaxEnt Bayesian estimation approach. The uncertainty at the pixel represents the RMSE of AGB estimation by taking into account errors from all sources including allometry. The uncertainty is overlaid on the shaded relief to highlight the potential impact of topography on uncertainty.

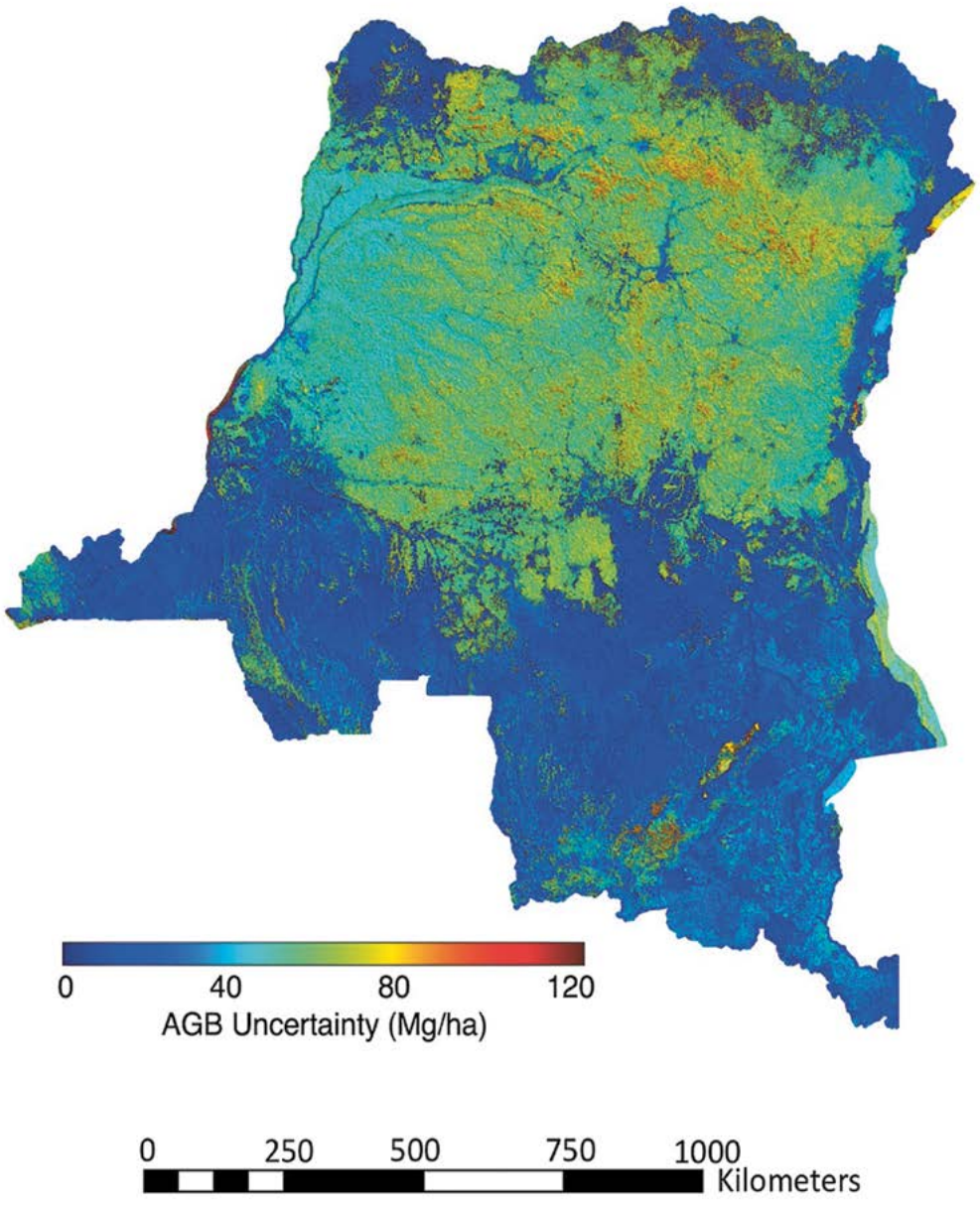

DAR-AGB model, (2) the geolocation errors between field-derived LiDAR modeling and spatial mapping, and (3) the interpolation error of airborne LiDAR sampling for rasterization. The field-derived LiDAR-AGB model has an average RMSE of 51 Mg/ha, which then propagates to the national mapping with a potential sub-pixel geolocation error. The average sub-pixel geolocation error can be approximated as the nugget effect of zero distance in the semi-variogram analysis, and is roughly 50 Mg/ha as well. The interpolation error can be modeled using ordinary kriging. Under the original 2-meter resolution for LiDAR raster product, we found regions with missing ground return could have uncertainty as high as 1 meters. However, the spatial aggregation of 2-meter products to 1-ha resolution makes this part of uncertainty rather small. Therefore, compared to other sources of uncertainty, LiDAR height measurements provides the most accurate estimation

The spatial modeling uncertainty of AGB represented by pixel level prediction error is the last source of uncertainty. The results show that majority of the AGB modeling uncertainty of humid tropical forests is bounded between 50 to 90 Mg/ha. However, compared to the pixel values with ground-estimated AGB at the 1-ha plots, the uncertainty is larger (90 Mg/ha) when compared the validation field plots, and about 105 Mg/ha when compared with an independent data set. If we assume different processes impacting the uncertainty of our AGB map are unrelated, the propagation of uncertainty from field-derived LiDAR AGB modeling error (~50 Mg/ha), pixel mismatch error (~50 Mg/ha), to the average spatial mapping error (~70 Mg/ha), is theoretically about 100 Mg/ha, similar to what we found from independent field validation.

CARBON STOCKS IN NATIONAL FORESTS

We report the carbon and biomass estimates for each province in DRC, to provide baselines for future forest management and protection (see table below). Results

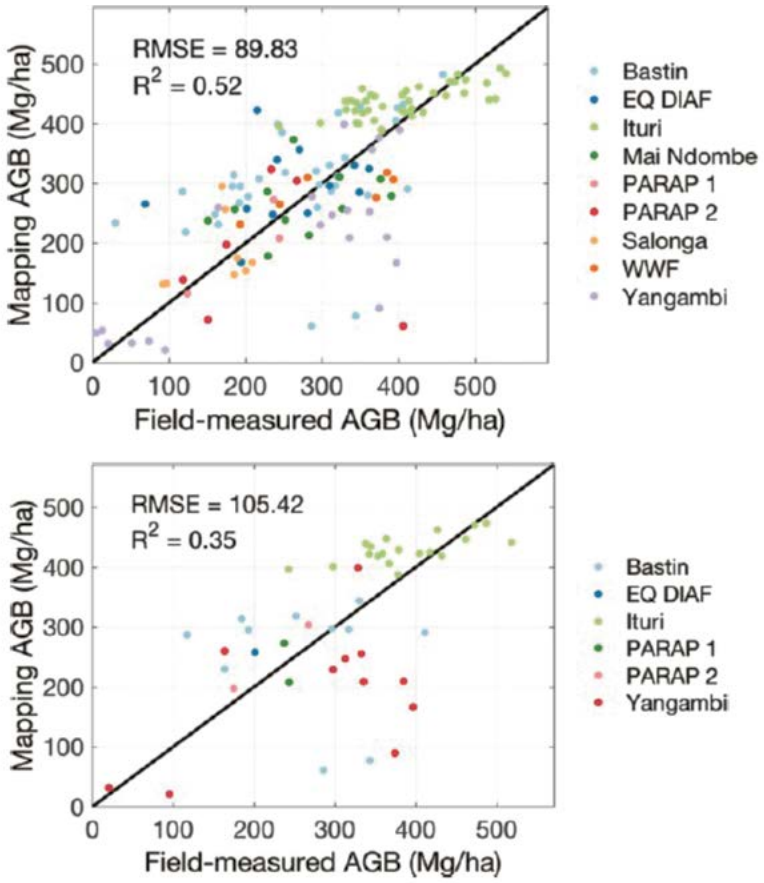

Figure 18: Validation of the biomass map against all available 1-ha plots in DRC (top) and against all 1-ha plots not used in developing the LiDAR-biomass model. None of the 1-ha plots were used directly in the MaxEnt machine learning algorithm and considered as reliable test of the map pixel level uncertainty.

show that 4 provinces (Tshuapa, Tshopo, Ituri and Sankuru) have the highest mean AGB of more than 300 Mg/ha. The 10 other provinces (Mai-Ndombe, Equateur, Sud-Ubangi, Nord-Ubangi, Mongala, Bas-Uele, Nord-Kivu, Sud-Kivu, Maniema, and Kasai) have mean AGB estimates around 200 Mg/ha. These 14 provinces possess 75% of the total carbon in the country. The remaining 12 provinces have lower AGB density and total carbon than the others, and nevertheless, contain more than 30% of thetropical forested area. The provinces the the lowest AGB density are Kinshasa, Kasai Oriental, Lomami and Kongo Central, which contribute less than 1% to the country-level carbon storage. At national level, the mean AGB is 236 Mg/ha for all forested regions, with less than 1% average modeling error when considering both the pixel-based error and the covariance between pixels.

To assess the uncertainty of regional mean of carbon stored in the forests at the province scale, we need to account for the covariance

$$\bar{\sigma}^2 = \frac{1}{N(N-1)}\left(\sum_{i=1}^{N}\sigma_i^2 + \sum_{i=1}^{N}\sum_{j(j\neq i)}^{N}\rho_{ij}\sigma_i\sigma_j\right)$$

where N is the total number of pixels, ρ_*ij* is the correlation coefficient between pixels *i* and *j*, and it can be approximated from the normalized C(*h*) under the assumption that spatial autocorrelation only changes with distance *h*. When our retrievals have little or no spatial autocorrelations between the predicted pixel-level errors, the variance of regional mean is simply the average of all pixel-level variance.

$$(\bar{\sigma}^2 = \frac{1}{N}\sum_{i=1}^{N}\sigma_i^2)$$

The total carbon estimate for each province is different from mean values, as it is area-weighted. Tshopo, Tshuapa and Bas-Uele thus become the top 3 provinces which store the most terrestrial carbon, each containing more than 2 PgC due to its large area of tropical forests. Mai-Ndombe, Equateur, Maniema and Sankuru also have 1.4-1.8 PgC in each province with a large forest coverage of over 9 to 10 Mha. However, the forest type is also important to estimating total carbon. Note that Lualaba, Tanganyka and Haut-Katanga all have 6-7 Mha of forests, comparable to the forest coverage in Haut-Uele and Kasai, but the total carbon storage is only 0.3 PgC – approximately one third of the total carbon for those tropical forest counterparts. The total carbon of the entire DRC is around 23.3±0.2 PgC. Although the modeling error for this total number is also 1%, consistent with the mean AGB estimates, the uncertainty of total carbon varies with both the mean uncertainty and the number of pixels. For example, Bas-Uele and Mongala have similar estimates of mean AGB and the associated errors, but the forested region in Bas-Uele is more than double. As expected, the total carbon uncertainty in Bas-Uele is twice of Mongala.

Province	Forest area CM&M (Mha)	AGB Mean (Mg ha^{-1})	Carbon Mean (Mg ha^{-1})	Total AGB (Pg)	Total Carbon (Pg)
Bas-Uele	13.56	268.93±8.37	162.50±3.95	3.645±0.114	2.203±0.054
Equateur	9.61	246.09±7.18	148.85±3.50	2.366±0.069	1.431±0.034
Haut-Katanga	6.2	60.06±4.63	35.48±2.18	0.372±0.029	0.220±0.014
Haut-Lomami	4.22	80.70±6.53	48.04±3.24	0.340±0.028	0.202±0.014
Haut-Uele	7.45	173.01±7.64	104.22±3.79	1.289±0.057	0.777±0.028
Ituri	4.68	312.41±11.96	188.92±6.05	1.461±0.056	0.883±0.028
Kasai	7.18	249.40±8.25	150.67±4.11	1.792±0.060	1.082±0.030
Kasai Central	3.75	182.47±9.57	109.95±4.31	0.684±0.036	0.412±0.016
Kasai Oriental	0.12	83.66±9.56	49.99±5.05	0.010±0.001	0.006±0.001
Kinshasa	0.2	67.87±8.85	40.45±4.36	0.013±0.002	0.008±0.001
Kongo Central	2.3	76.49±6.90	45.61±3.43	0.176±0.016	0.105±0.008
Kwango	4.6	114.68±7.89	68.68±3.73	0.528±0.037	0.316±0.017
Kwilu	3.46	112.22±7.44	67.39±3.64	0.389±0.026	0.233±0.013
Lomami	1.26	119.74±8.02	71.85±4.18	0.151±0.010	0.091±0.005
Lualaba	6.93	89.39±6.27	53.21±3.35	0.619±0.044	0.369±0.024
Mai-Ndombe	10.06	237.93±7.44	143.85±3.57	2.393±0.075	1.447±0.036
Maniema	10.4	285.01±8.28	172.29±3.91	2.963±0.087	1.791±0.041
Mongala	5.39	261.53±9.47	158.10±4.76	1.410±0.051	0.852±0.026
Nord-Kivu	4.71	253.54±9.84	153.22±4.88	1.194±0.047	0.722±0.023
Nord-Ubangi	3.85	275.37±10.93	166.45±5.56	1.060±0.042	0.641±0.022
Sankuru	9.31	310.00±9.14	187.46±4.44	2.885±0.086	1.744±0.042
Sud-Kivu	4.51	251.25±11.75	151.83±5.41	1.134±0.053	0.685±0.025
Sud-Ubangi	3.85	212.64±9.69	128.43±4.71	0.819±0.038	0.495±0.018
Tanganyka	6.04	76.67±5.76	45.60±2.77	0.463±0.035	0.276±0.017
Tshopo	19.82	323.55±7.46	195.74±3.45	6.413±0.149	3.879±0.069
Tshuapa	13.26	306.14±7.68	185.21±3.69	4.058±0.103	2.455±0.049
All Provinces	**166.58**	**231.67±2.46**	**139.90±1.19**	**38.592±0.415**	**23.304±0.200**

Table 1. Forest area, biomass and carbon statistics of DRC provinces. The forest area estimates are based on the DRC forest definition of minimum mapping area of 0.5 ha, canopy cover > 30% and forest height > 3 m. Forest carbon includes above ground and below ground root biomass.

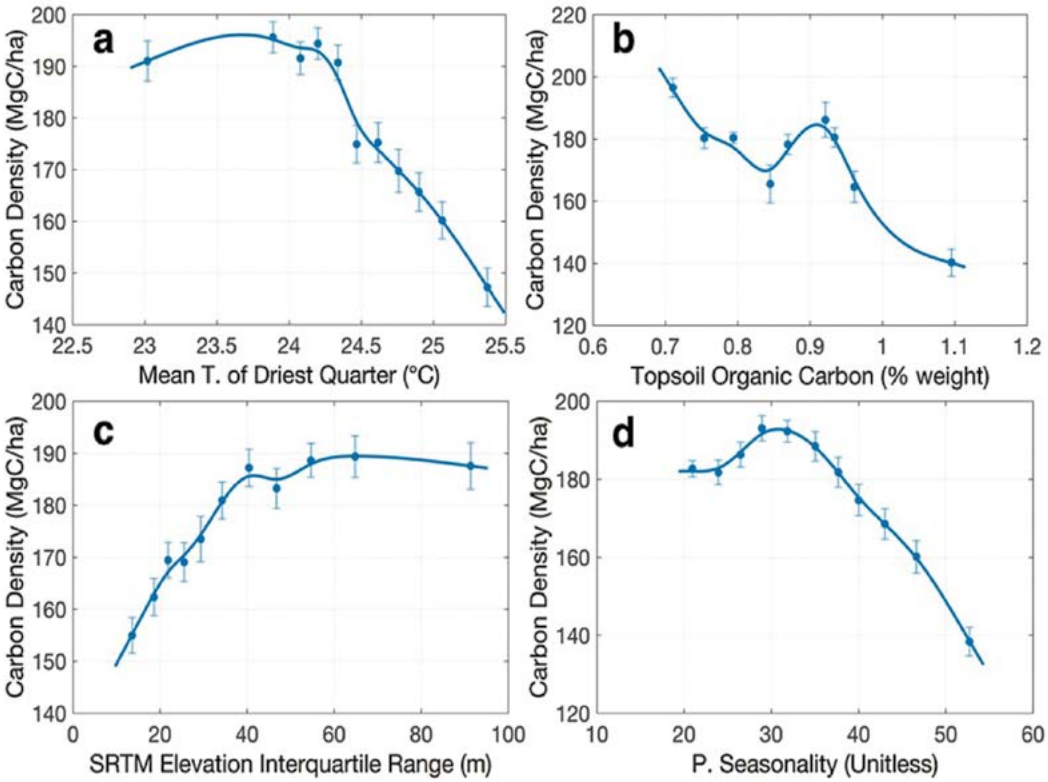

Figure 19: Average relationships between carbon density and environmental variables in Evergreen tropical forests in DRC. Panels show carbon density vs. (a) mean temperature of driest quarter, (b) topsoil organic carbon, (c) land elevation variation, and (d) precipitation seasonality. The plots show the relationships between mean values within each interval of environmental variables. The errorbar associated with carbon density is the standard error of mean estimation from bootstrapping samples.

ENVIRONMENTAL CONTROLS

The climate and edaphic characteristics in DRC may partly explain the spatial variability of forest carbon stock. By upscaling our carbon density map to a quarter-degree, matching the spatial resolution of available products for climate and soil variables, we found weak but significant relationships between carbon stocks and environmental variables. Our analysis shows the most important environmental variables for determining spatial distribution of carbon in evergreen forests are mean temperature of driest quarter, topsoil organic carbon, land elevation variation and rainfall seasonality. These 4 variables explain about 28% of the carbon stock variation in evergreen tropical forests. Although the power of explanation is not very strong, likely due to the heterogeneity of forest structure and composition, all 4 variables significantly regulate the distribution of carbon at least from the mean characteristics. The mean temperature of the driest quarter is the most important variable, showing negative correlation with carbon density and suggesting that areas with higher temperature are less suitable for biomass accumulation. This may follow the observations that forests have an optimum range of temperature for CO_2 uptake[49,50].

Rainfall seasonality is also well correlated with carbon density showing a similar negative relationship suggests that more carbon is stored in less seasonal forests. Interestingly, among soil properties, the topsoil organic carbon also plays an important role in the carbon storage of the Congo basin, consistent with our findings in the tropical Amazon region[51], which shows a significant negative effect of soil organic carbon to dominant tree height. The peatlands found in Congolese swamp forests[48] can partly explain this particular relationship, showing increasing topsoil carbon corresponding to smaller trees. Higher temperatures in tropical forests near swamp-dominated areas could also protect soil organic carbon from decomposition[52]. The variation in land elevation, related to various landscape structure, affecting incoming solar radiation, hydrological features, as well as soil compounds, shows a positive relationship with carbon density, meaning more forest carbon stored over complex terrains. This effect may also be due to the higher probability of forest degradation and logging in areas with flat terrain that could not be readily verified in this study.

The swamp forests (wetlands), mainly distributed along the Congo river system, have a more predictable pattern related to environmental variables. Results show that 66% of the carbon spatial variation in these forests can be explained by 4 variables: mean land elevation, land elevation variation, minimum temperature of coldest month, and annual precipitation. The most important variable, mean land elevation, can explain about 49% of the carbon variation. showing a linear increase of carbon stock density with elevation over the range of about 50 m. Unlike evergreen forests, swamp forests show a negative relationship between carbon and elevation

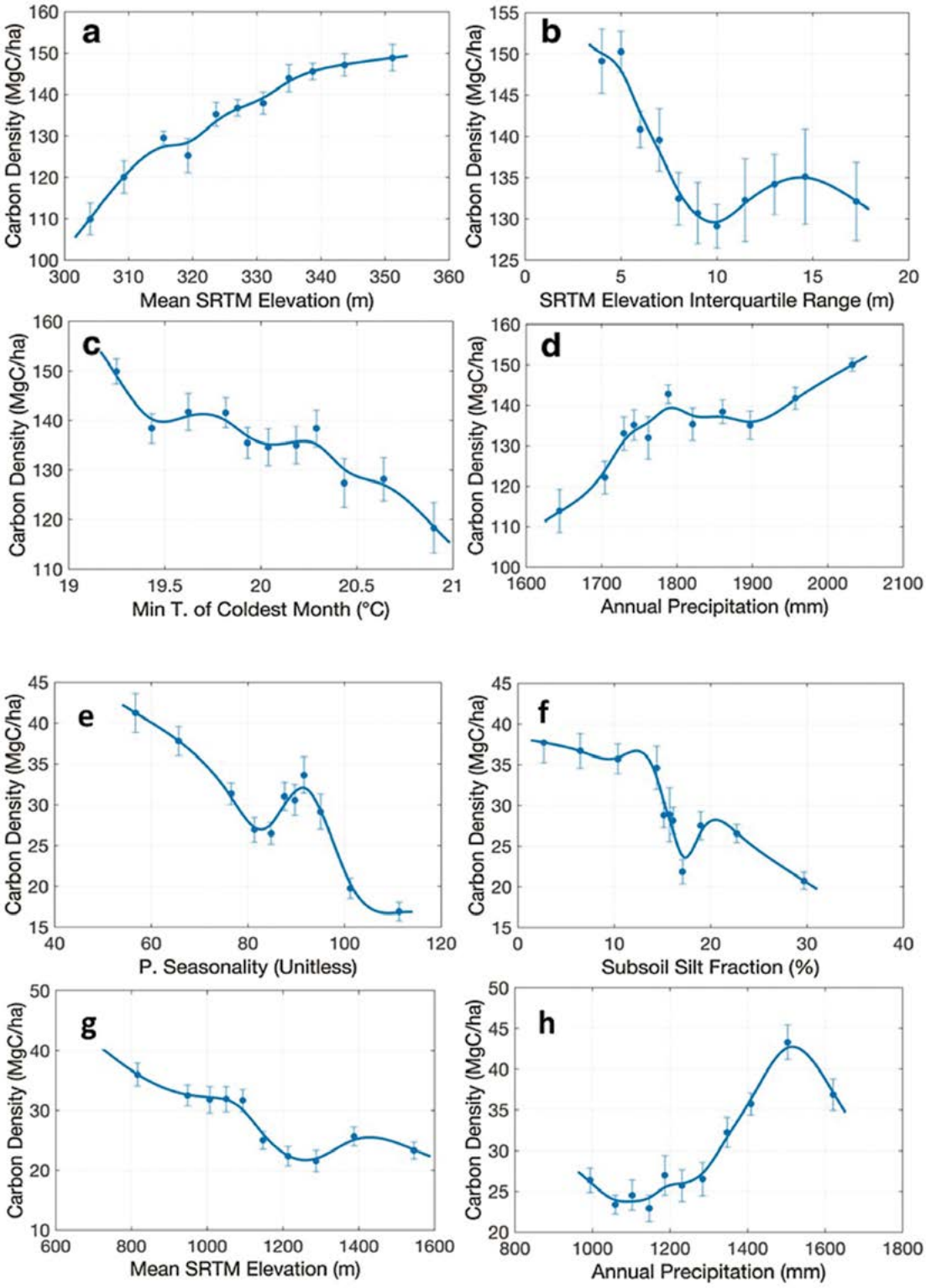

Figure 20: Average relationships between carbon density and environmental variables in Swamp forests with (a) mean land elevation, (b) land elevation variation, (c) minimum temperature of coldest month, and (d) annual precipitation, and Miombo forests with (e) precipitation seasonality, (f) subsoil silt fraction, (g) mean land elevation, and (h) annual precipitation.

(Above) Sunrise behind Mount Mikeno, Virunga National Park, Democratic Republic of Congo

variation, suggesting more wetland forests growing on the flat terrain that allows persistent inundation seasonally or over the entire year. The minimum temperature of the coldest month in wetlands is closely correlated with annual mean temperature, temperature diurnal range and annual range. The negative correlation with carbon density is consistent with what we found in the evergreen forests. Annual precipitation, though high enough, still shows a positive relationship with carbon density in wetland forests. The soil properties in these forests are highly correlated with each other and temperature variables, probably due to their similar geographical distribution, and therefore, could not significantly explain the variations of carbon density in swamp forests. The Miombo woodlands in DRC cover mostly the southern part of the country. Compared to evergreen and wetland forests, these forests have much lower carbon density. As expected, there are distinct environmental variables that determine the variations of forest carbon in these forests. Rainfall seasonality becomes the most important variable, followed by subsoil silt fraction, mean land elevation and annual precipitation. Surprisingly, no temperature variable plays an important role in the carbon distribution. But since these seasonal forests are distributed over a large range of elevation, we found that most temperature seasonality features are correlated strongly with precipitation seasonality, and mean temperature features are tightly correlated with mean land elevation. The soil, silt fraction, is well correlated with the soil nutrient availability such as the cation-exchange capacity, and the soil organic carbon. These soil variables occur in areas with lower annual precipitation.

DIAF INDEPENDENT VALIDATION

The forest aboveground biomass map and uncertainty were delivered to the national agencies of DRC for reviews and validation. DIAF, the ministry of forestry in DRC took the responsibility of estimating the uncertainty of the carbon map over regions were field inventory data are available. However, due to lack of NFI data in DRC, only a small number of samples within the province of Mai Ndombe were selected to examine the quality of the map in terms of the overall bias in estimating carbon. The plot data used are not based on any systematic or any probabilistic design and hence cannot be a rigorous estimation of the bias of the map. Nevertheless, this effort was helpful in understanding how the plot level data can be compared with the map and to what extent the plot size and location accuracy can influence the estimation of errors. The results of the comparison with independent ground plots from DIAF are summarized in the table below

The validation included data sets from Bastin plots that were not used in the development of the map and plots collected by the Japan International Cooperation Agency (JICA). There were a total of 25 1-ha plots from the research groups distributed in DRC and 90 0.36-ha clustered plots from the DIAF-JICA inventory data. The figure below shows the estimates of mean biomass from these plots using different allometric models and comparison with the forest biomass map produced in our project. The results suggest that the overall bias of the map is very small (1% for Bastin plots and 3% for JICA plots). The bias may be partially due to the plot size in the case of JICA) plots, orientation with respect to the 100 m pixel of the map and the geolocation error.

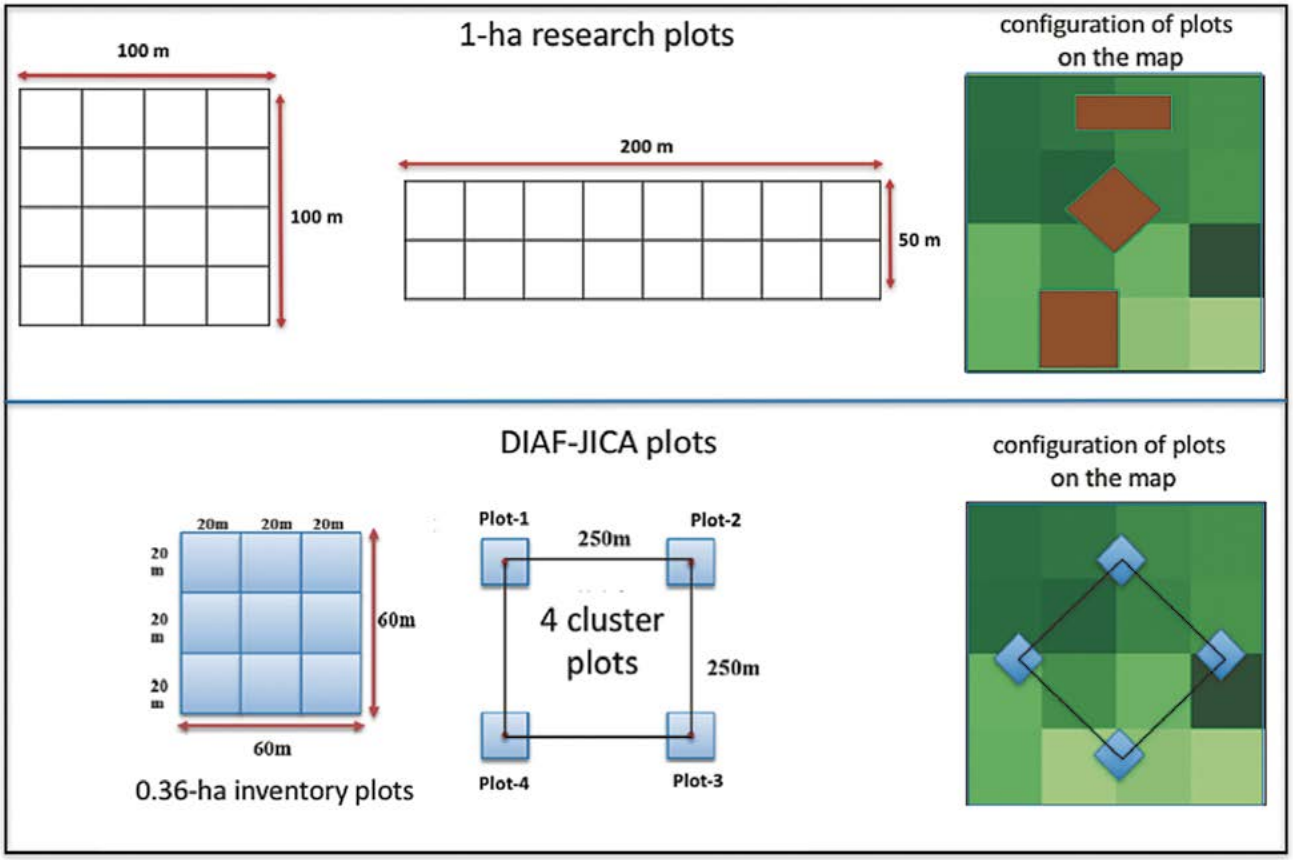

Figure 21: Size and shape of plots used in the validation of the national biomass map.

Source	AGB E-factor (Mg/ha)	AGB H-Model (Mg/ha)	AGB: Combined (Mg/ha)	AGB Map Estimate (Mg/ha)	AGB Diff E-factor (%)	AGB Diff H-model (%)	AGB Diff Combined (%)
Research Plots: 25 1-ha plots							
Research Plots	336.41	281.23	308.82	299.5	-10.97	6.49	-3.01
DIAF-JICA: 90 0.36-ha plots							
Dense Humid Forests	328.72	276.96	302.84	291.67	-11.27	5.31	-3.69
Open Forests	113.61	133.04	123.32	104.6	-7.93	-21.38	-15.19
Secondary Forests	118.2	86.71	102.45	72.36	-38.78	-16.43	-29.28
Savanna	65.83	36.9	51.36	48.29	-26.64	30.87	-5.99

DIAF validation of the national map.

CONCLUSIONS

We developed the first national-level forest biomass distribution and uncertainty assessment in a tropical country from systematic sampling of airborne LiDAR data. We also report province-level carbon statistics, as well as AGB estimates summarized by different forest types. By examining the environmental condition such as the climate and edaphic variables, we identified key climate (temperature and precipitation), terrain (elevation and interquartile range) and soil properties contributing to spatial distribution forest carbon stocks, and environmental variables which can differentiate forest types. The development of carbon estimates and the national map follows a verified methodology that defines the LiDAR sampling approach, conversion of LiDAR measurement to AGB and assessment of the uncertainty. Our results indicate that the methodology can be applied to other tropical countries to provide cost-effective and efficient assessment of forest carbon storage and changes over large areas.

ACKNOWLEDGEMENTS

The authors wish to the thank the International Climate Initiative (IKI) of the German Federal Ministry for the Environment, Nature Conservation, Building and Nuclear Safety. Additionally, the contribution of field plot data and expertise by Ghent University (ISOFYS and CaveLab), INERA-Yangambi, WWF-DRC (PARAP), le Département des Inventaires et Aménagement Forestier (DIAF), Forest Ressources Management (FRM); Wildlife Conservation Society, Office National des Forets (ONFI), Conservation International (CI), Project Earth Observation for Reducing Emissions from Deforestation and forest Degradation (EO4REDD), Forest and Biodiversity Program of German Cooperation (PBF/GIZ), Universite Libre de Bruxelles (ULB), Wildlife Works Carbon (WWC), the Smithsonian Institution and the World Bank (WB). We also wish to acknowledge the Food and Agriculture Organization (FAO), the World Bank (WB) for supporting field data collection and validation efforts, and the dedicated pilots, engineers of Southern Mapping Company.

APPENDIX

SUB-NATIONAL GOVERNMENT REGIONS

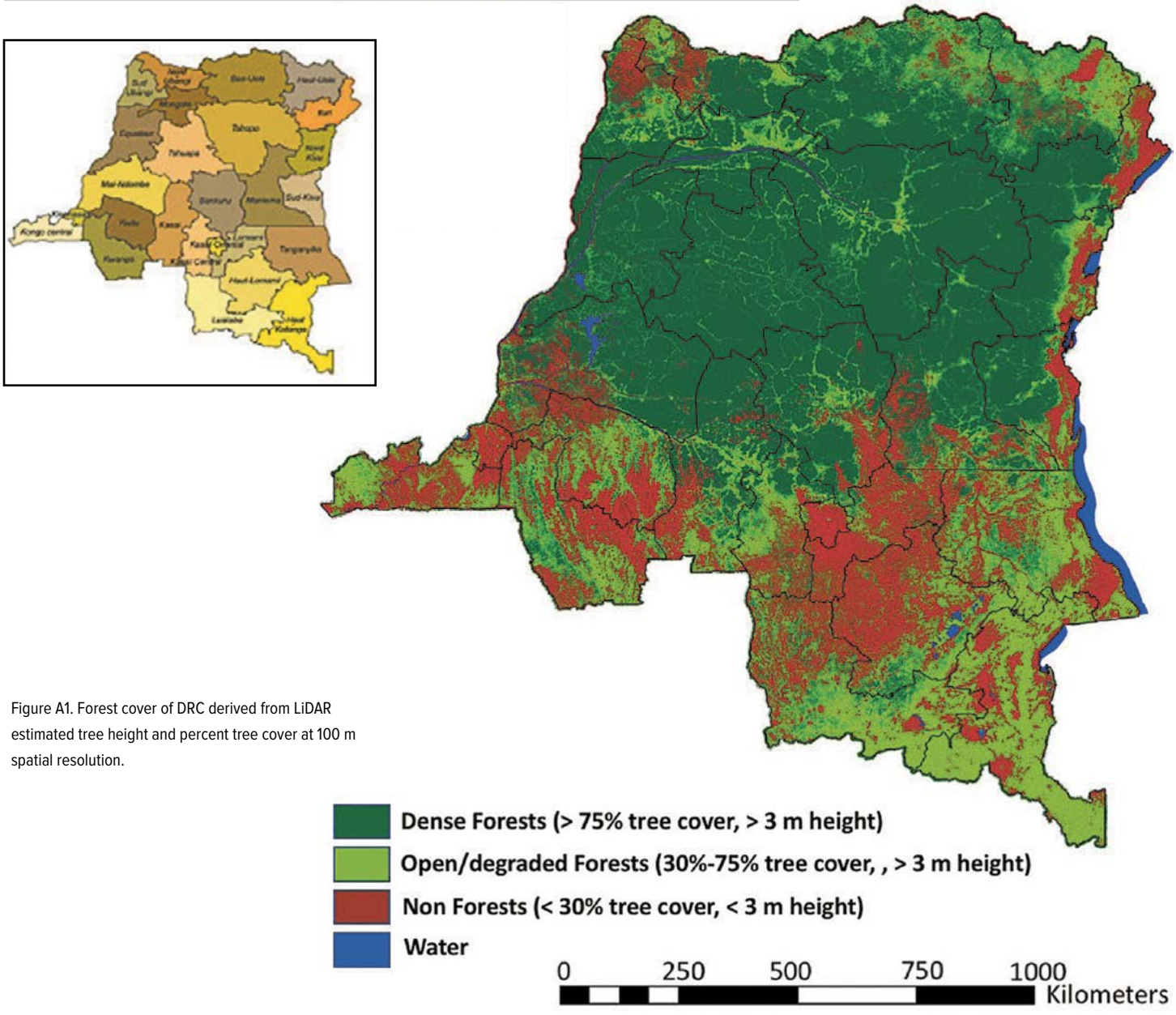

Figure A1. Forest cover of DRC derived from LiDAR estimated tree height and percent tree cover at 100 m spatial resolution.

FOREST AREA IN DRC

The quantification of the carbon stored in forests of DRC depend strongly on the precision of mapping forest areas. Forests in DRC are defined of covering a minimum mapping unit area of 0.5 ha, have an average height of greater than 3 m, and tree canopy cover of more than 30%. These three components of definition cannot be readily mapped using the conventional remote sensing data and techniques. Most global and regional maps are derived from remote sensing data with limited to no sensitivity to forest height or tree canopy cover. However, the classification of the remote sensing data is often calibrated extensively with training data over areas that are identified as forests by experts in the country in order to produce forest cover maps that closely follow the national definition of forest.

The current estimate of the national forest area is based on the FACET forest map produced by OSFAC using forest cover change techniques from multi-temporal Landsat ETM data from 2000 to 2010 at 60 m spatial resolution (Potapov et al. 2012). For the FACET map, forest was defined as 30% or greater canopy cover for trees of 5 m or greater in height. This definition has been changed in recent years to 3 m threshold for tree height and a minimum mapping unit of 0.5 ha compatible with the national plans for REDD+ and national or jurisdictional emission reduction (ER) programs.

As part of CM&M program, the UCLA team has developed national level maps of forest height and canopy cover using the statistical sampling of high resolution LiDAR data. These maps are produced using geospatial modeling of more than 600,000 ha of height and canopy cover samples using Landsat, ALOS PALSAR, and SRTM imagery at 100 m spatial resolutions. Using the maps, we combined the 30% canopy cover and 3 m height thresholds to estimate the forest cover area at the national scale and for all provinces summarized in table 1. The overall difference between the approach and the forest definitions used in FACET and the CM&M maps results in more than 10 million ha of forests distributed extensively along the forest-savanna boundary in southern provinces and degraded areas. The following table (Appendix A) summarizes differences in forest cover and provides the mean and total carbon stored in DRC based on the FACET map.

Province	Forest area FACET (Mha)	AGB Mean (Mg ha^{-1})	Carbon Mean (Mg ha^{-1})	Total AGB (Pg)	Total Carbon (Pg)
Bas-Uele	12.36	289.17	174.79	3.573	2.160
Equateur	9.37	249.82	151.13	2.341	1.416
Haut-Katanga	8.22	46.53	27.48	0.383	0.226
Haut-Lomami	3.84	74.43	44.31	0.286	0.170
Haut-Uele	6.52	189.43	114.19	1.235	0.745
Ituri	4.56	317.74	192.17	1.448	0.876
Kasai	6.27	277.31	167.63	1.738	1.051
Kasai Central	2.86	221.73	133.77	0.634	0.382
Kasai Oriental	0.08	98.30	58.87	0.008	0.005
Kinshasa	0.08	91.19	54.59	0.007	0.004
Kongo Central	0.76	90.18	53.87	0.069	0.041
Kwango	3.65	128.10	76.82	0.467	0.280
Kwilu	2.59	132.86	79.90	0.345	0.207
Lomami	0.86	145.43	87.48	0.126	0.076
Lualaba	6.63	84.85	50.53	0.562	0.335
Mai-Ndombe	9.42	248.55	150.32	2.342	1.417
Maniema	9.75	298.66	180.59	2.912	1.761
Mongala	4.97	279.44	168.96	1.389	0.840
Nord-Kivu	4.37	267.00	161.41	1.168	0.706
Nord-Ubangi	3.37	308.03	186.26	1.039	0.628
Sankuru	8.88	321.56	194.48	2.854	1.726
Sud-Kivu	4.30	256.82	155.25	1.104	0.667
Sud-Ubangi	3.40	233.89	141.33	0.796	0.481
Tanganyka	6.77	67.13	39.93	0.454	0.270
Tshopo	19.40	328.98	199.03	6.382	3.861
Tshuapa	13.11	308.47	186.63	4.045	2.447
All Provinces	**156.26**	**241.08**	**145.63**	**37.67**	**22.75**

Table 2. Forest area, biomass and carbon statistics of DRC provinces. Forested area is calculated by using the FACET forest cover map produced by OSFAC and adding all pixels associated with the intact humid tropical forests, secondary forests, and woodland savanna areas. FACET map is based on the national Landsat time series data capturing forest cover change from 2000 to 2010. The classification of Landsat data assumes areas with more than 30% forest cover and tree height of greater than 5 m (Potapov et al. 2012).

BAS UELE

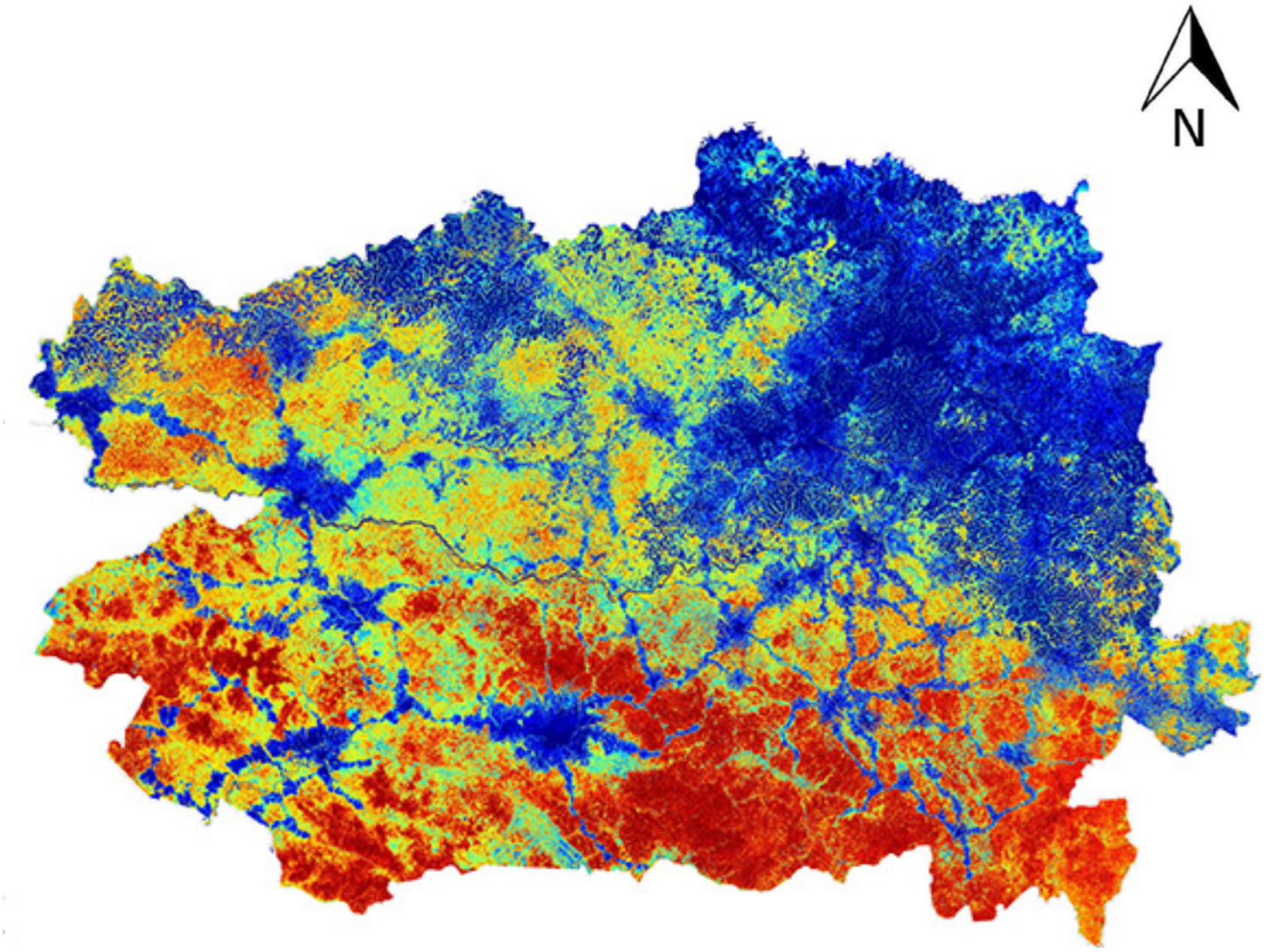

EQUATEUR

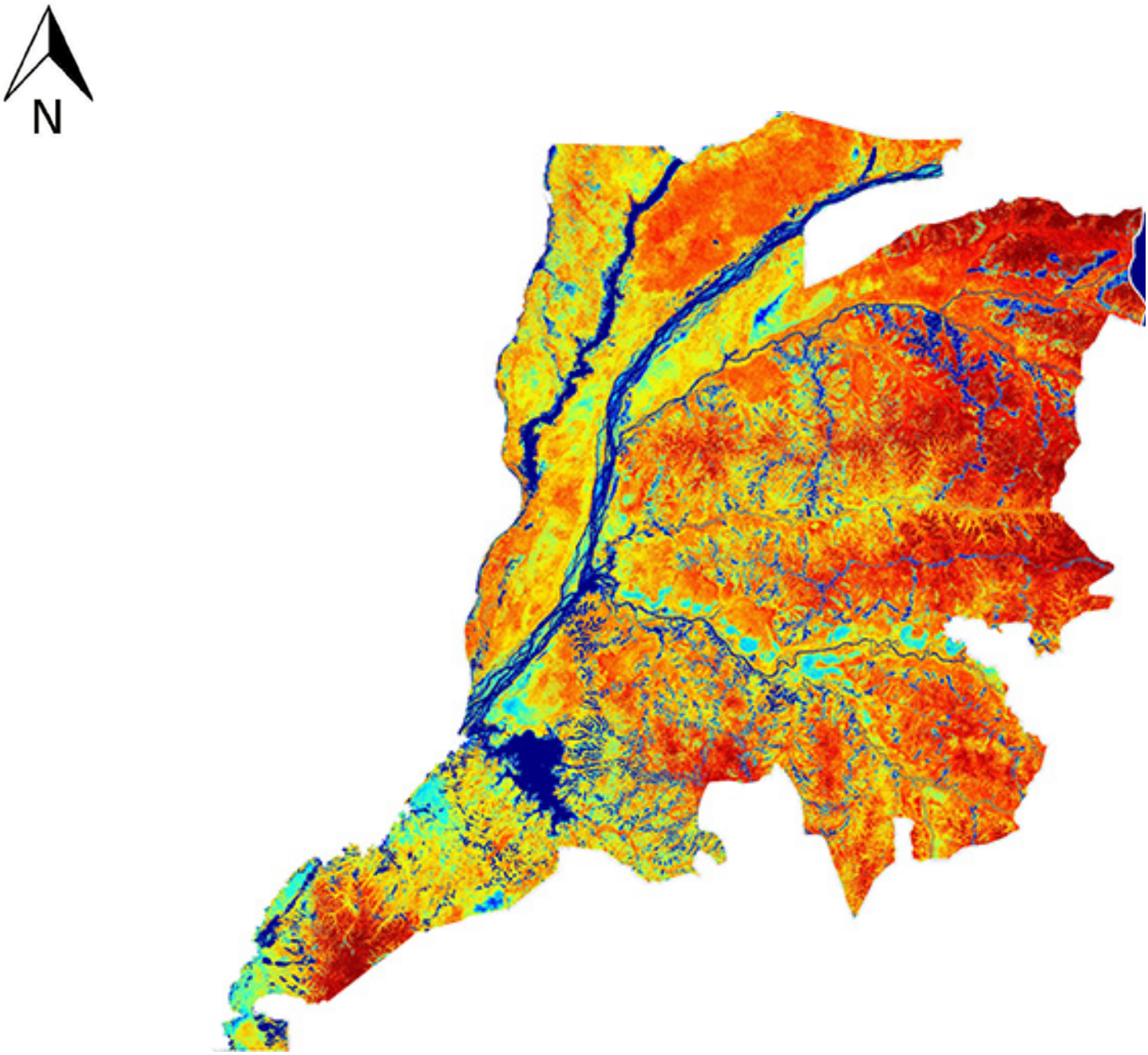

HAUT-KATANGA

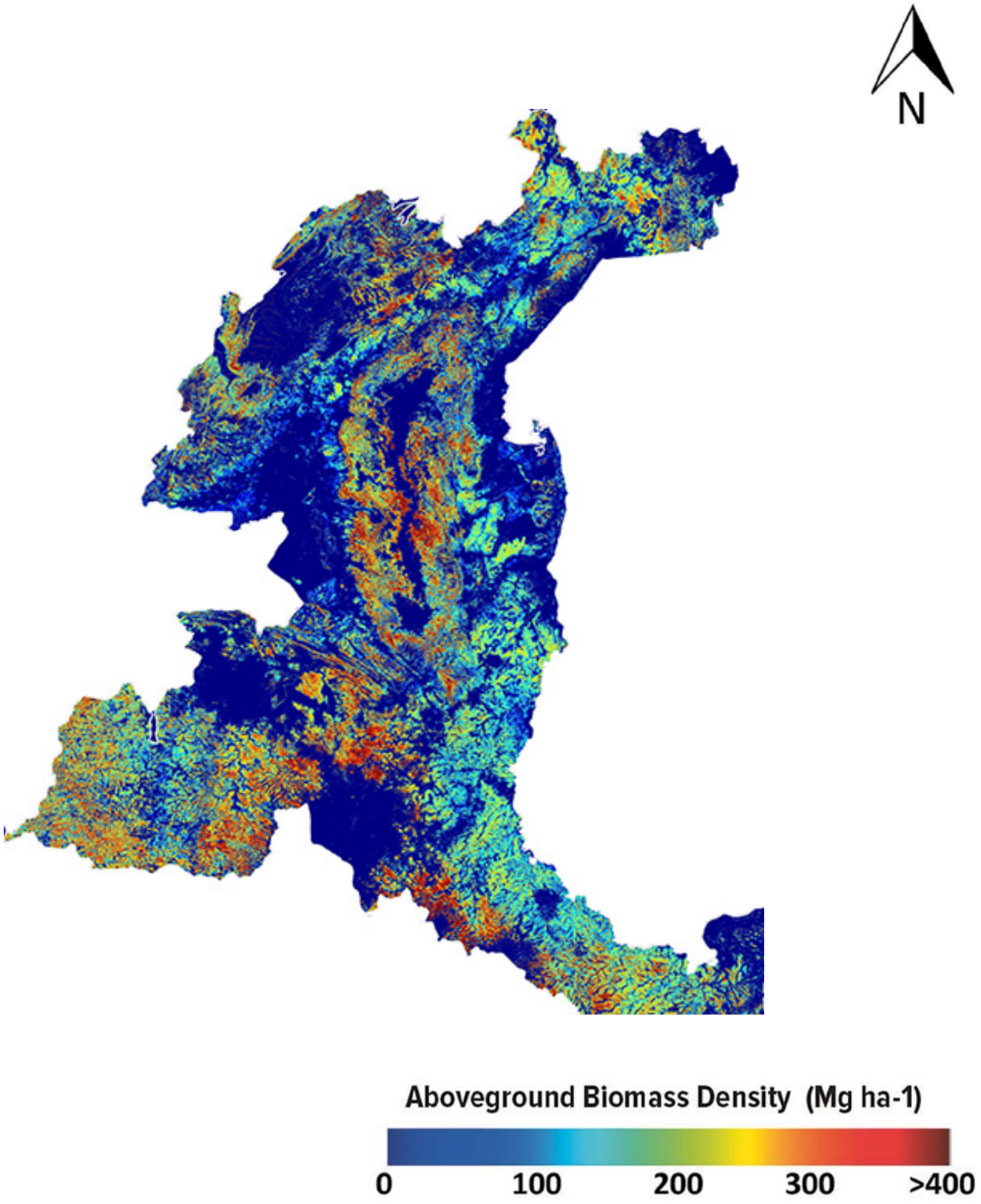

HAUT-UELE

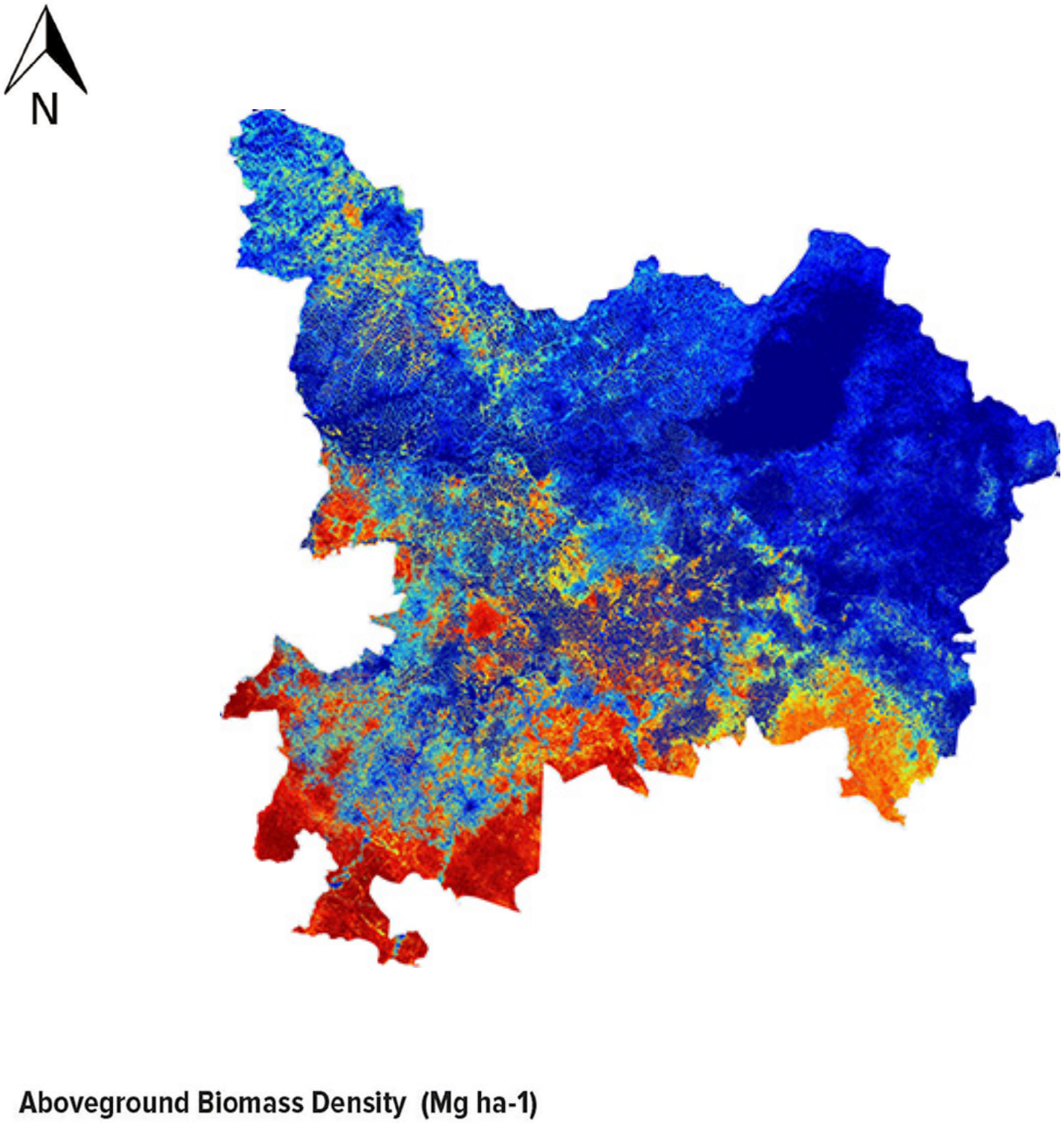

HAUT-LOMAMI

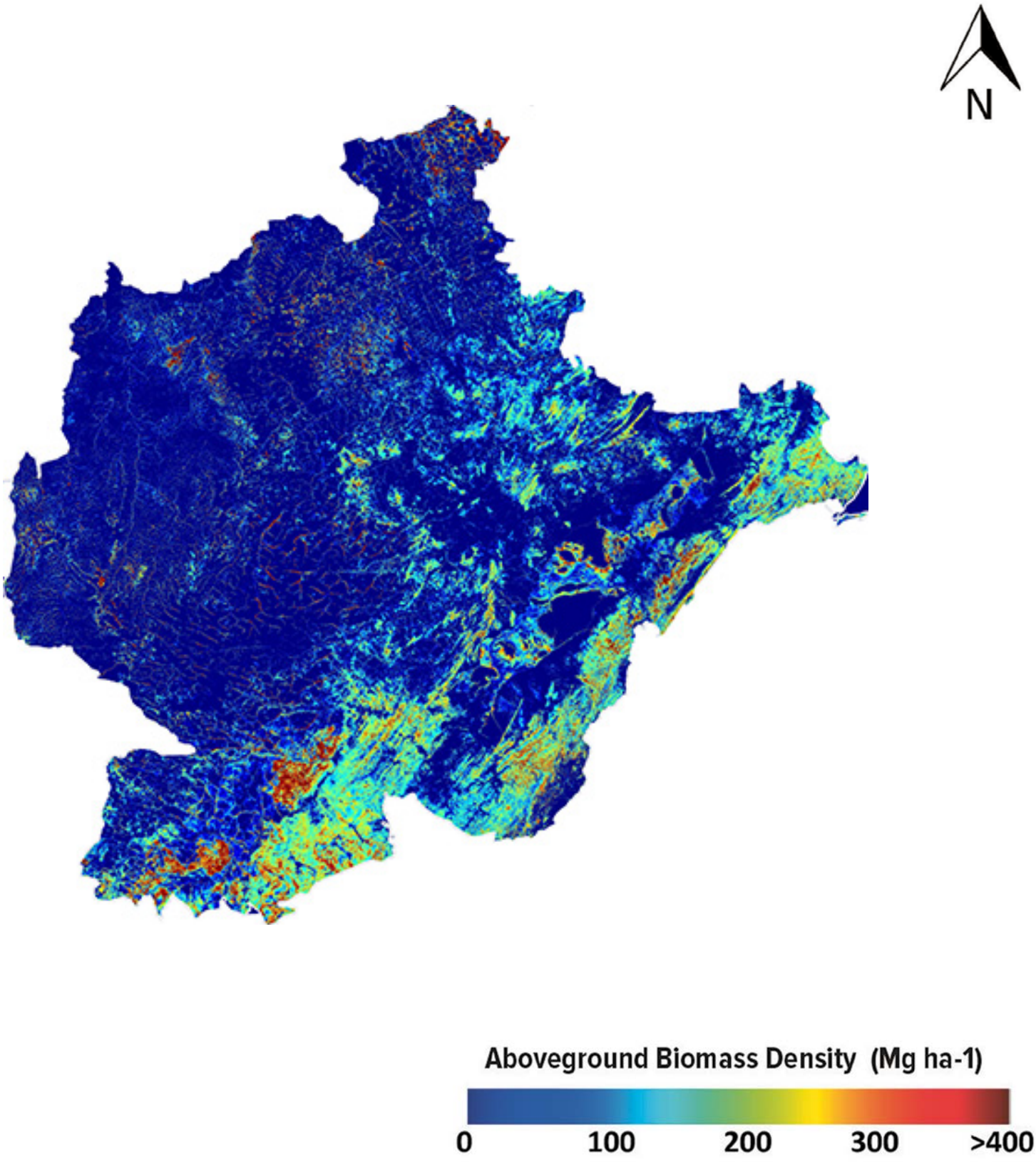

ITURI

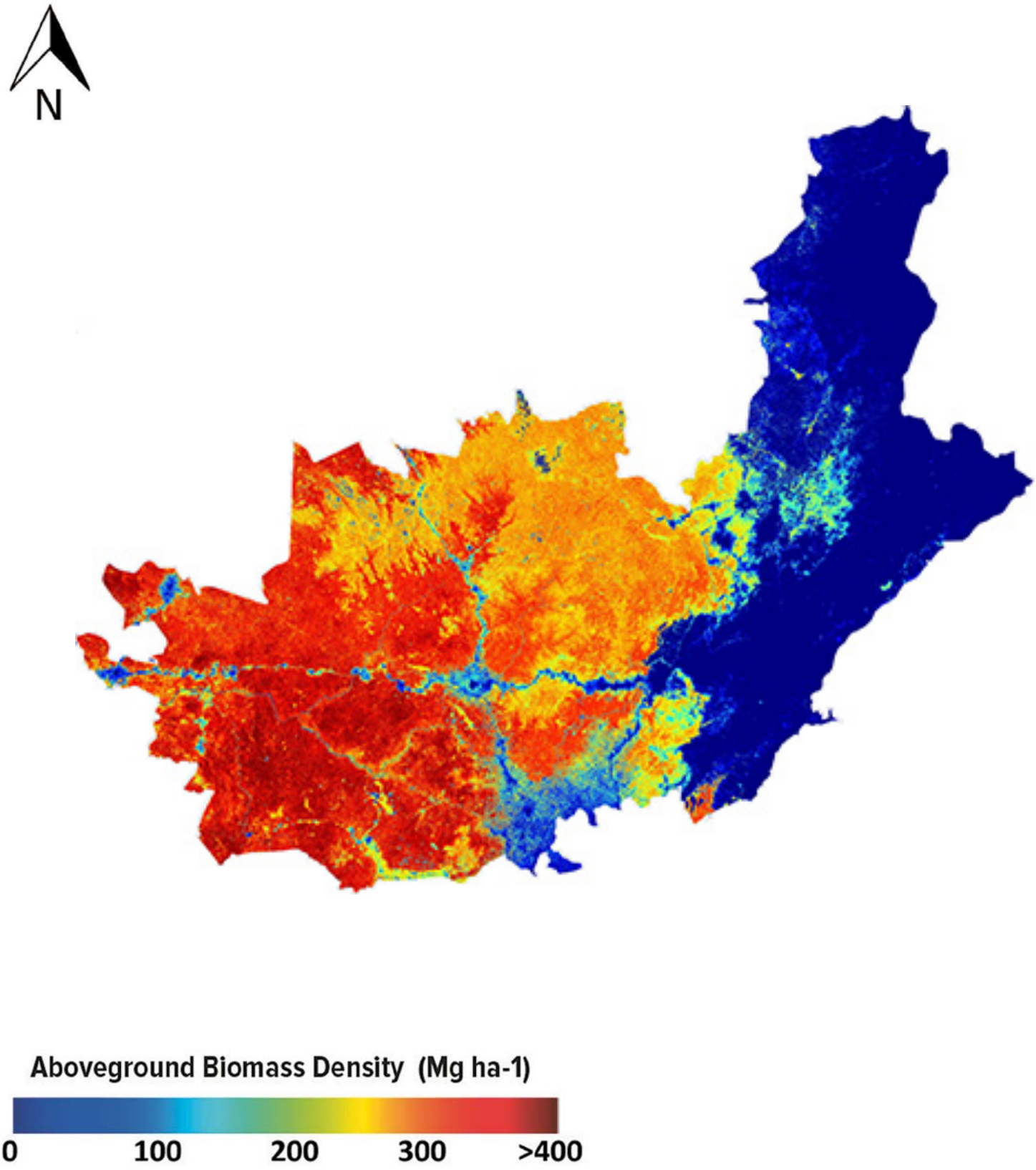

KASAI CENTRAL & ORIENTAL

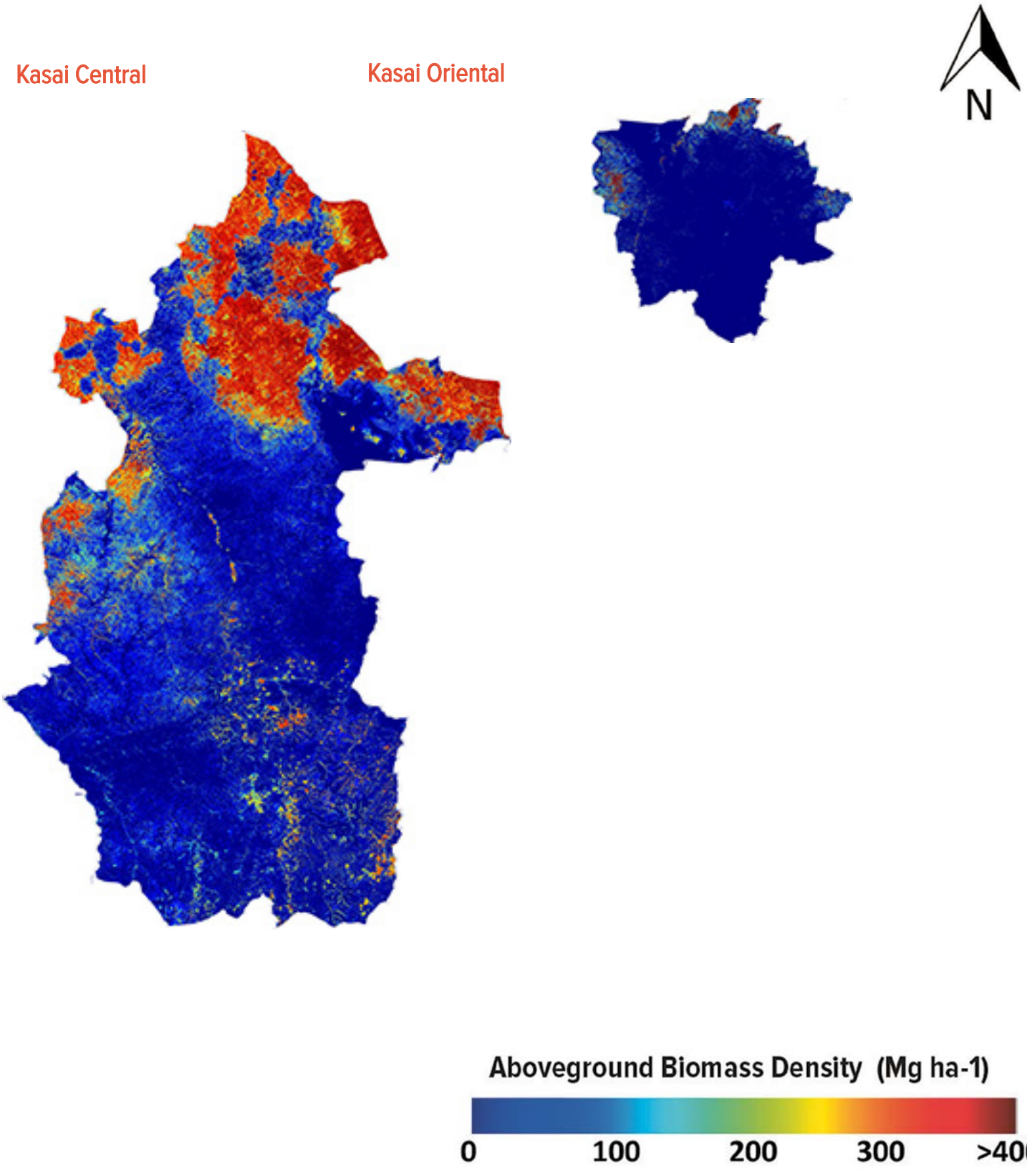

KASAI ORIENTAL

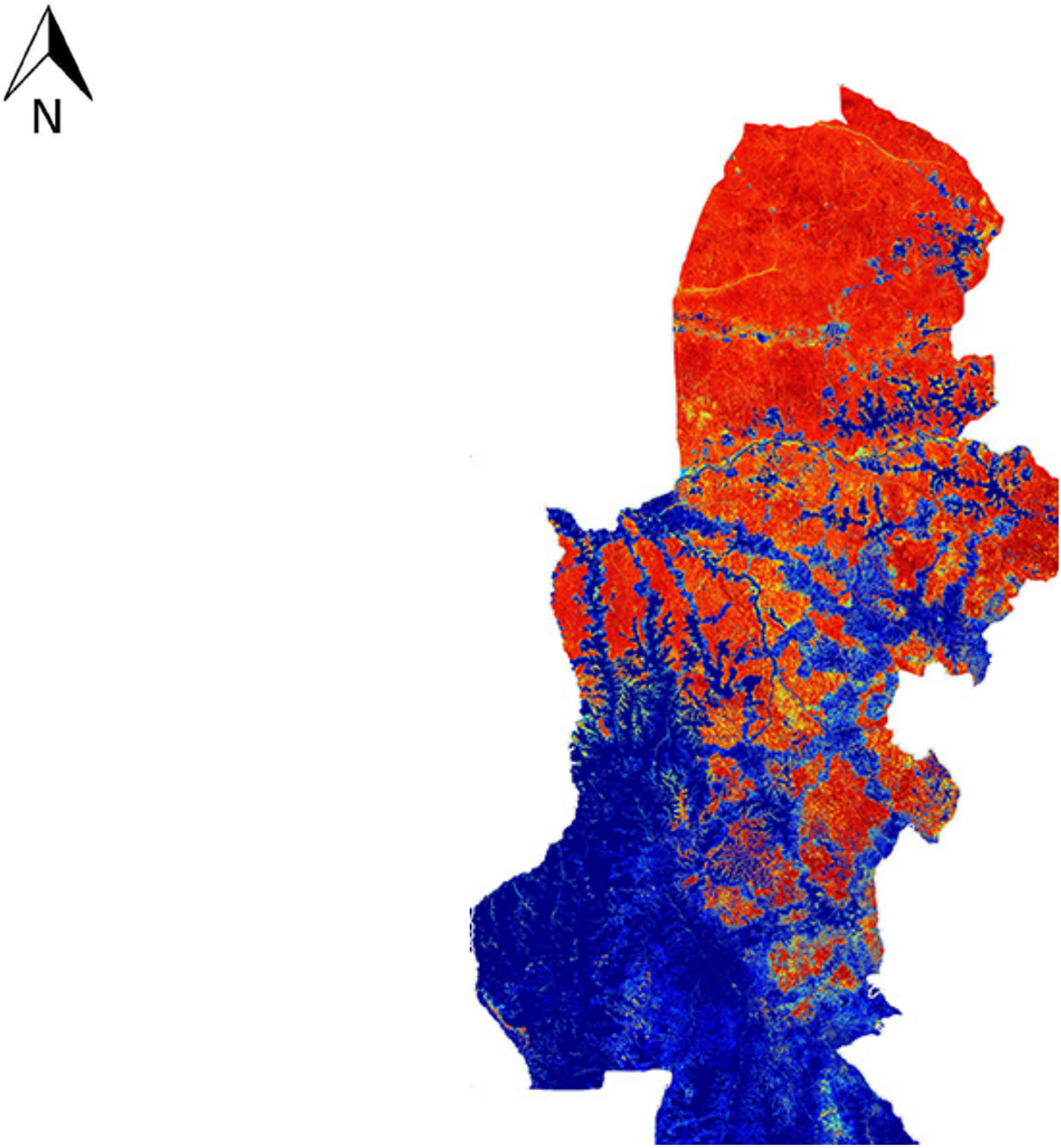

KINSHASA & KONGO CENTRAL

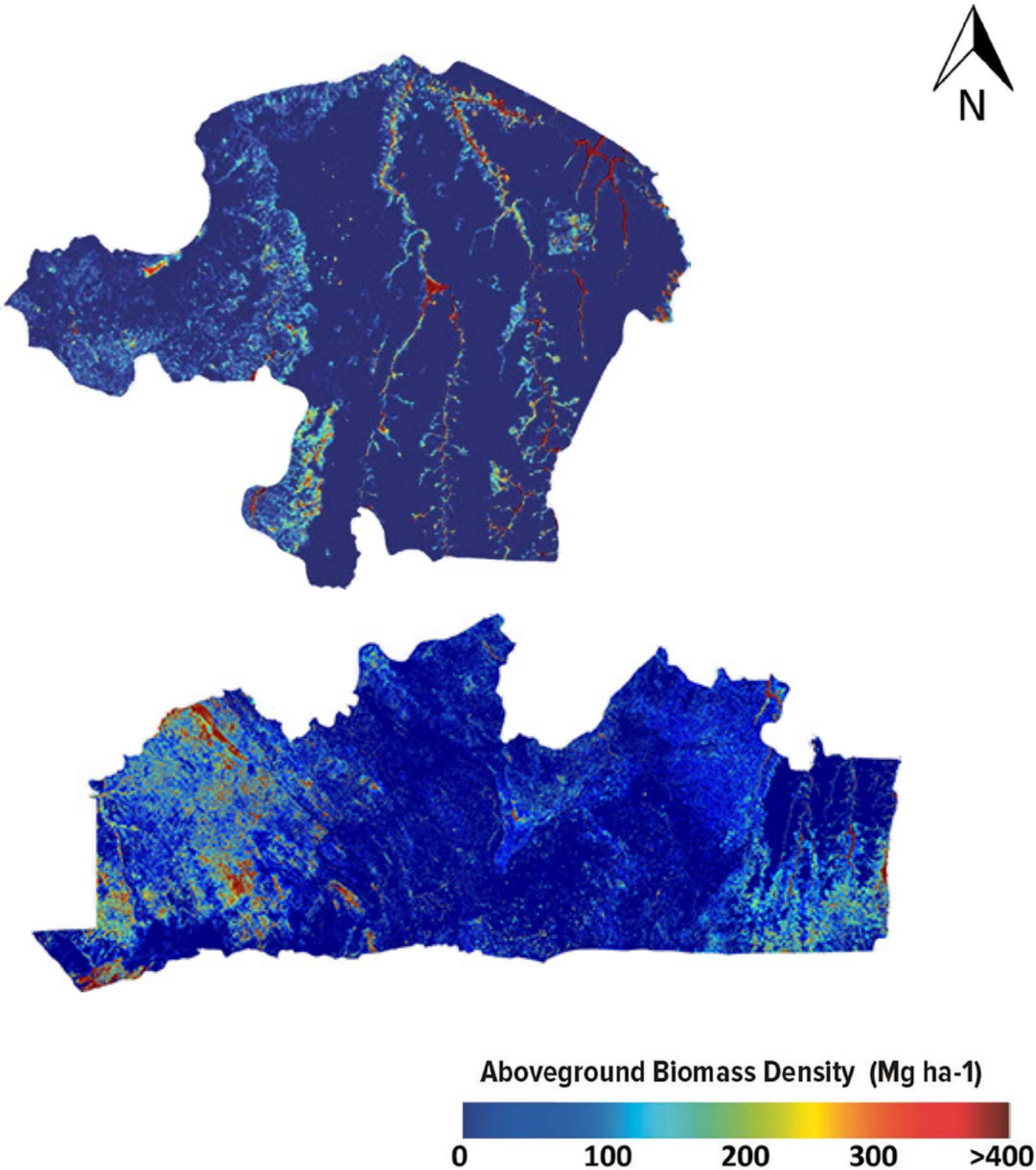

KWANGA

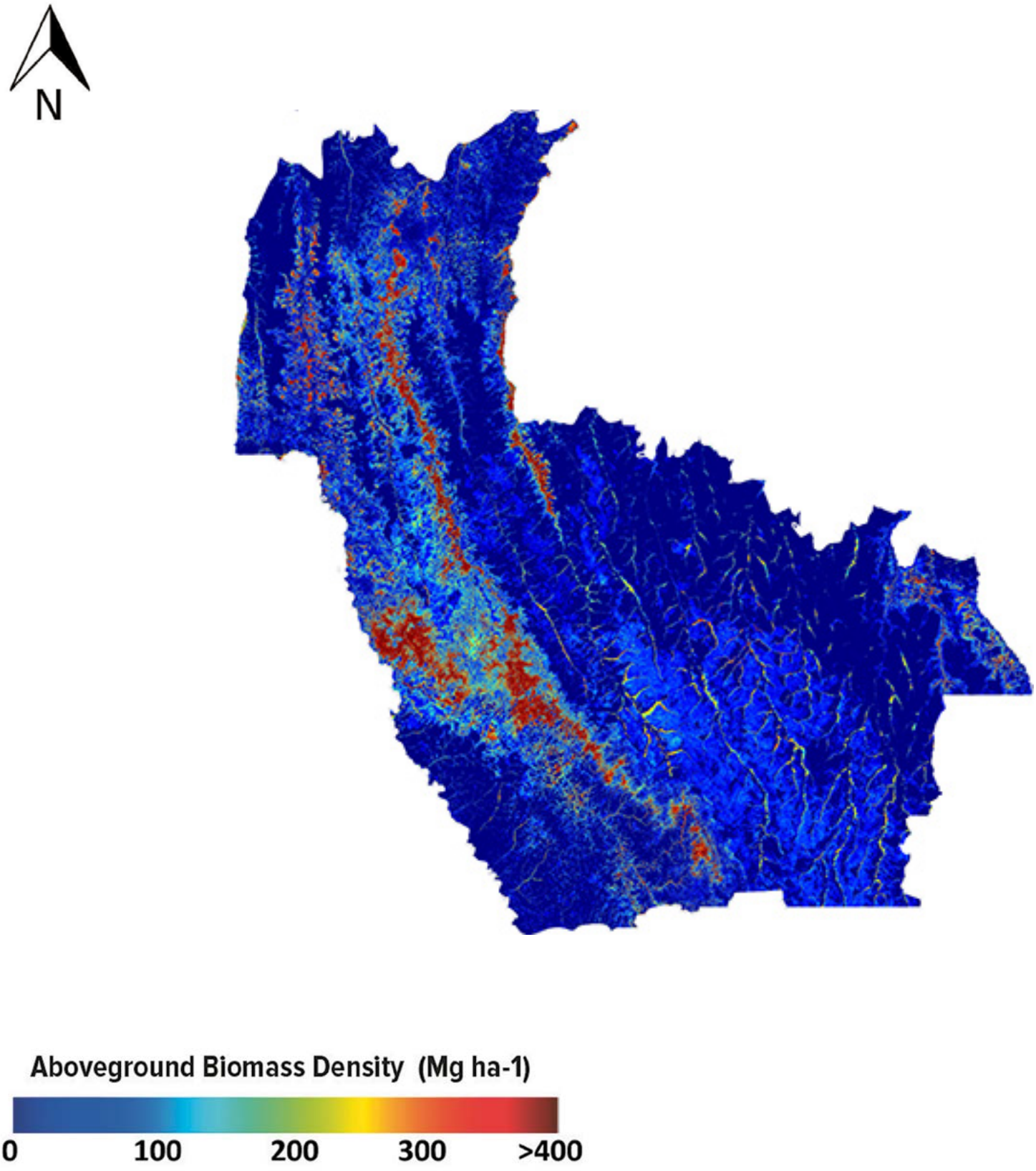

KWILU

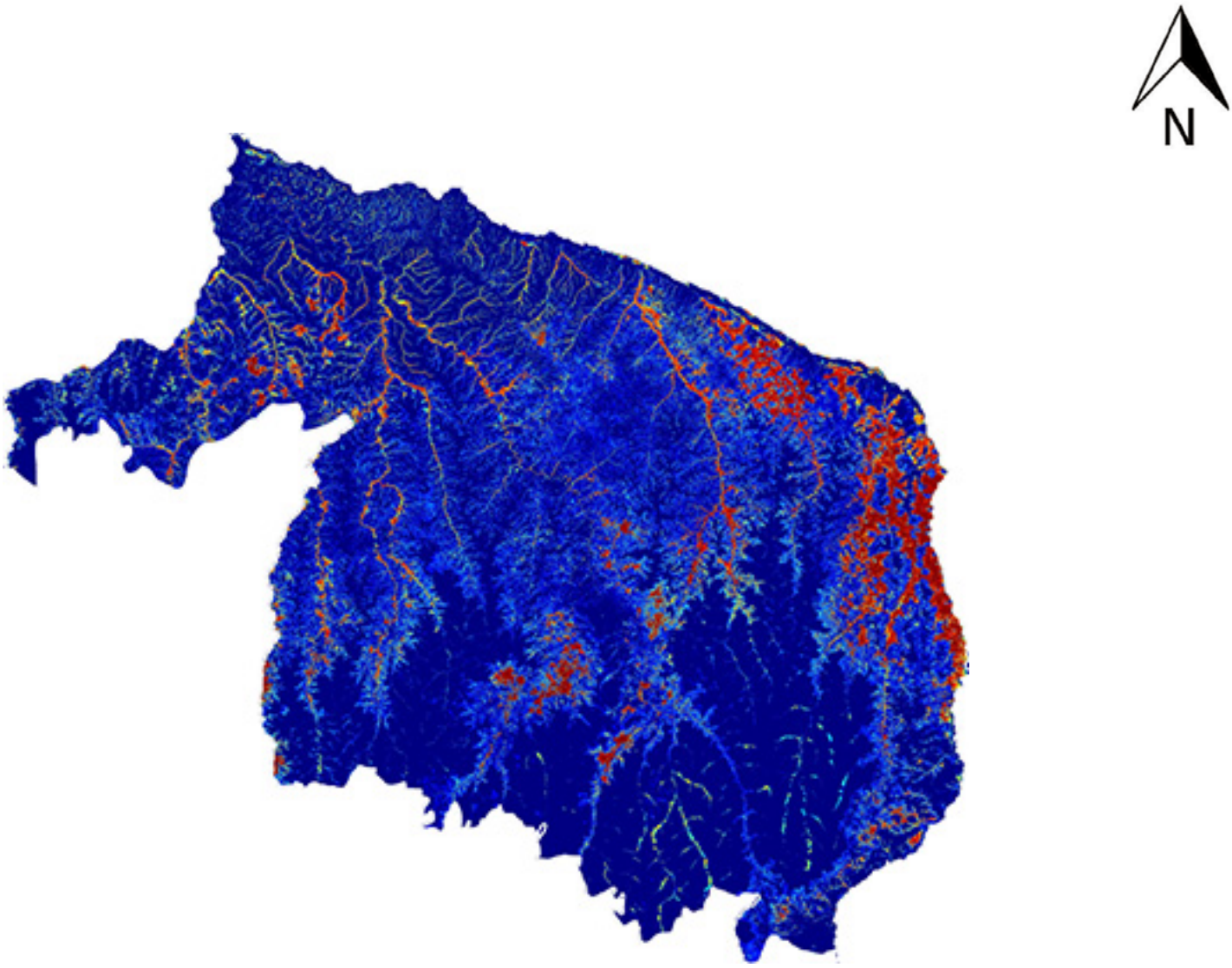

LOMAMI

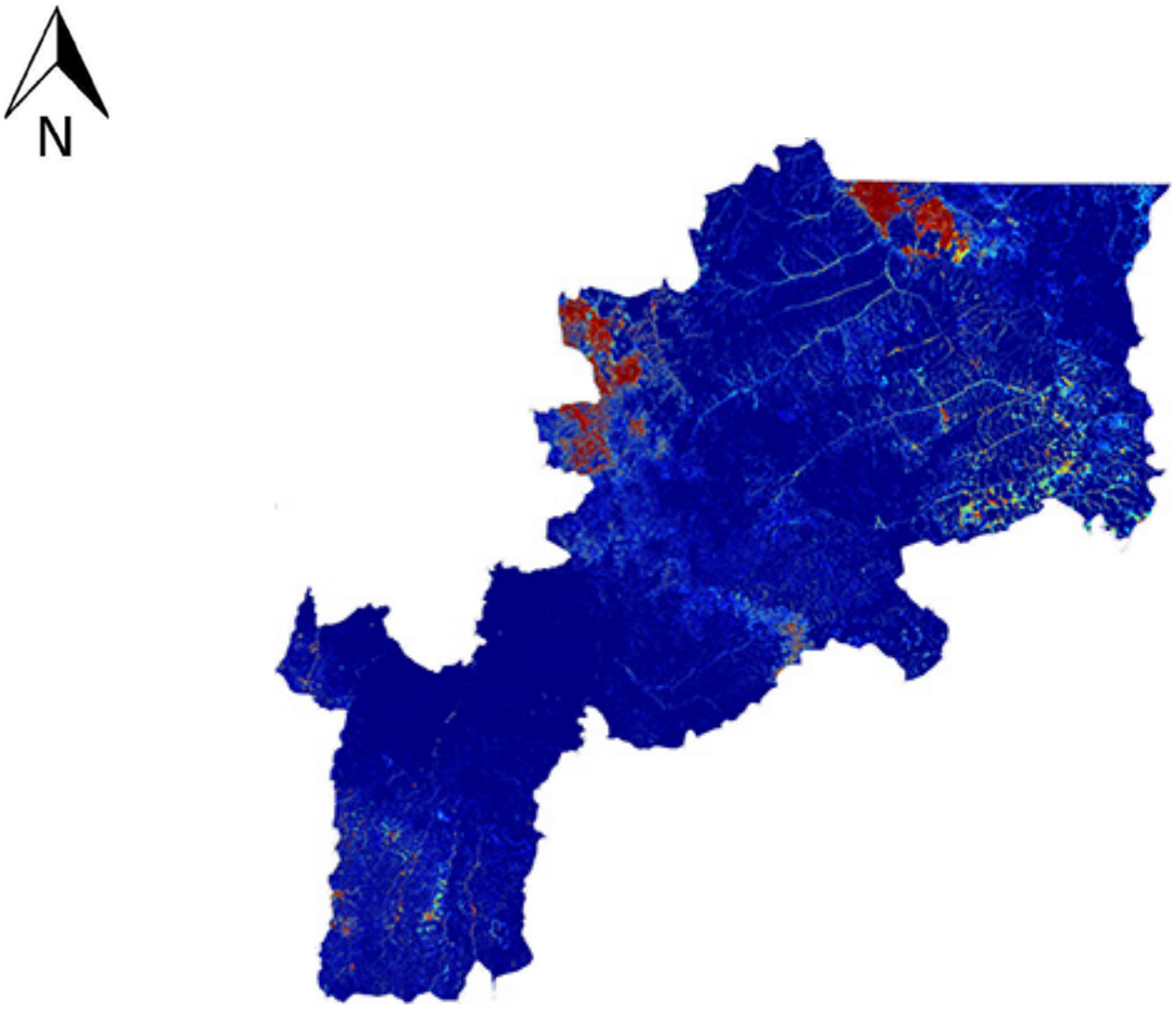

LUALABA

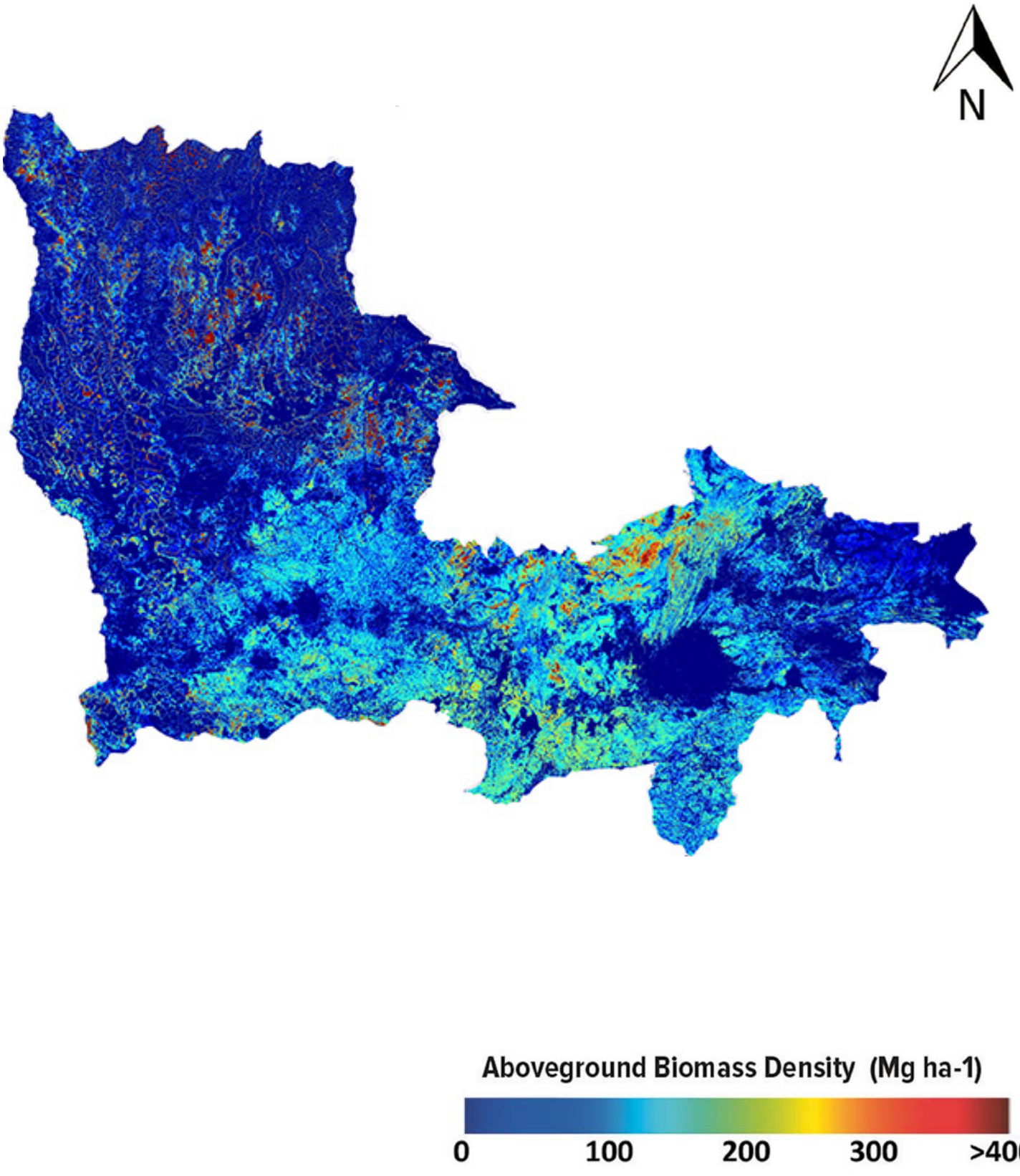

MAI NDOMBE

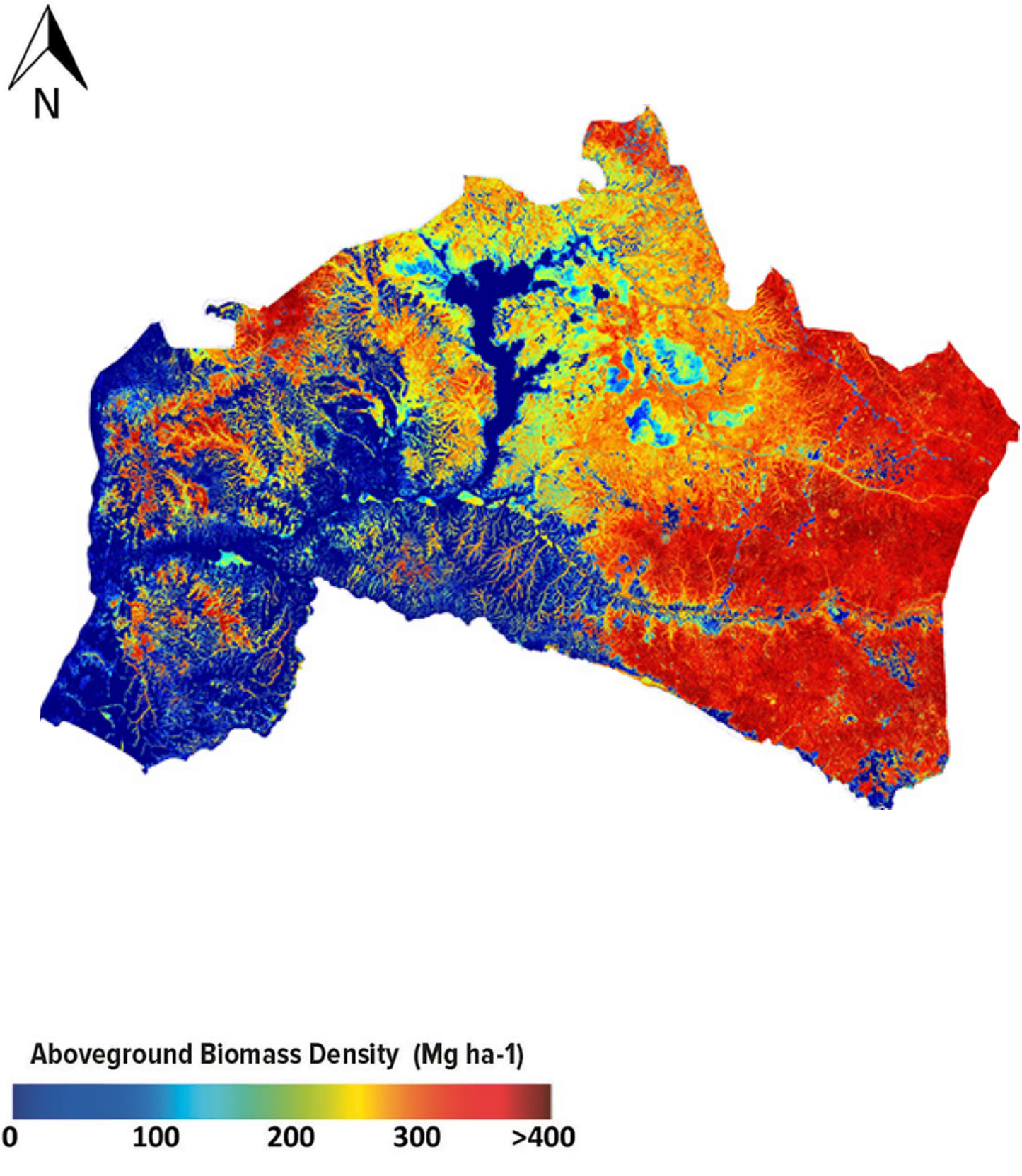

MANIEMA

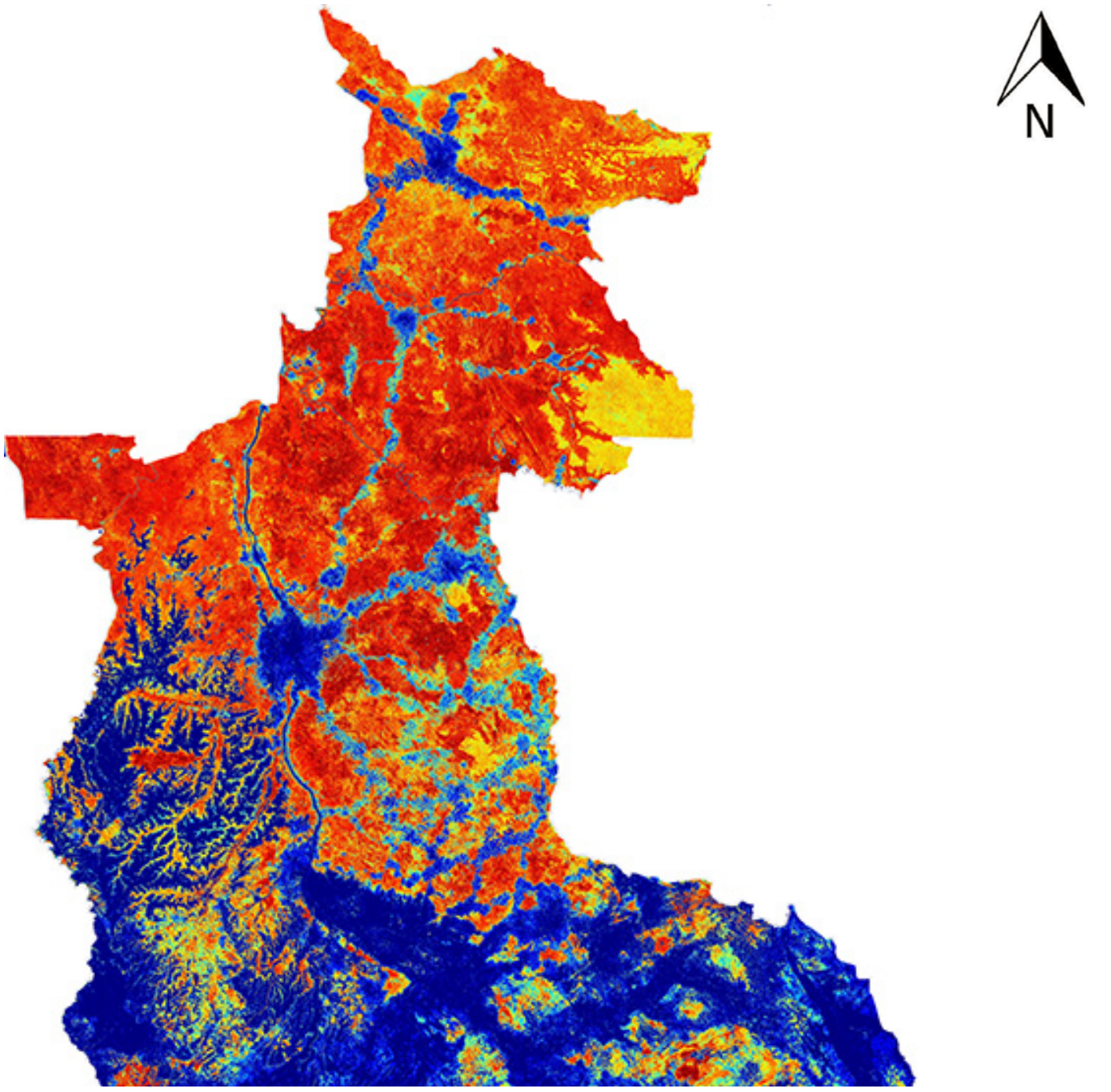

MONGALA

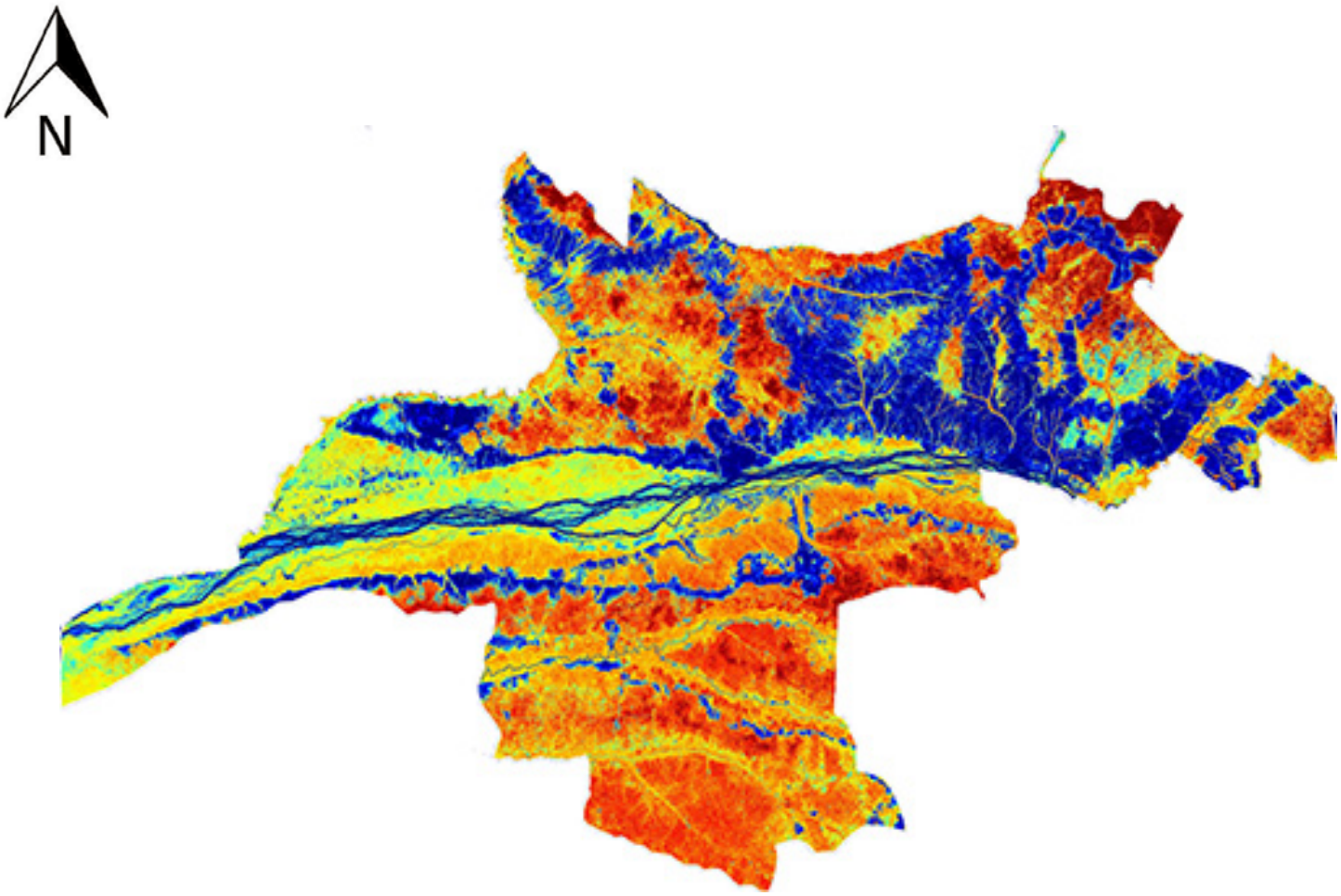

Aboveground Biomass Density (Mg ha-1)

0 100 200 300 >400

NORD-KIVU

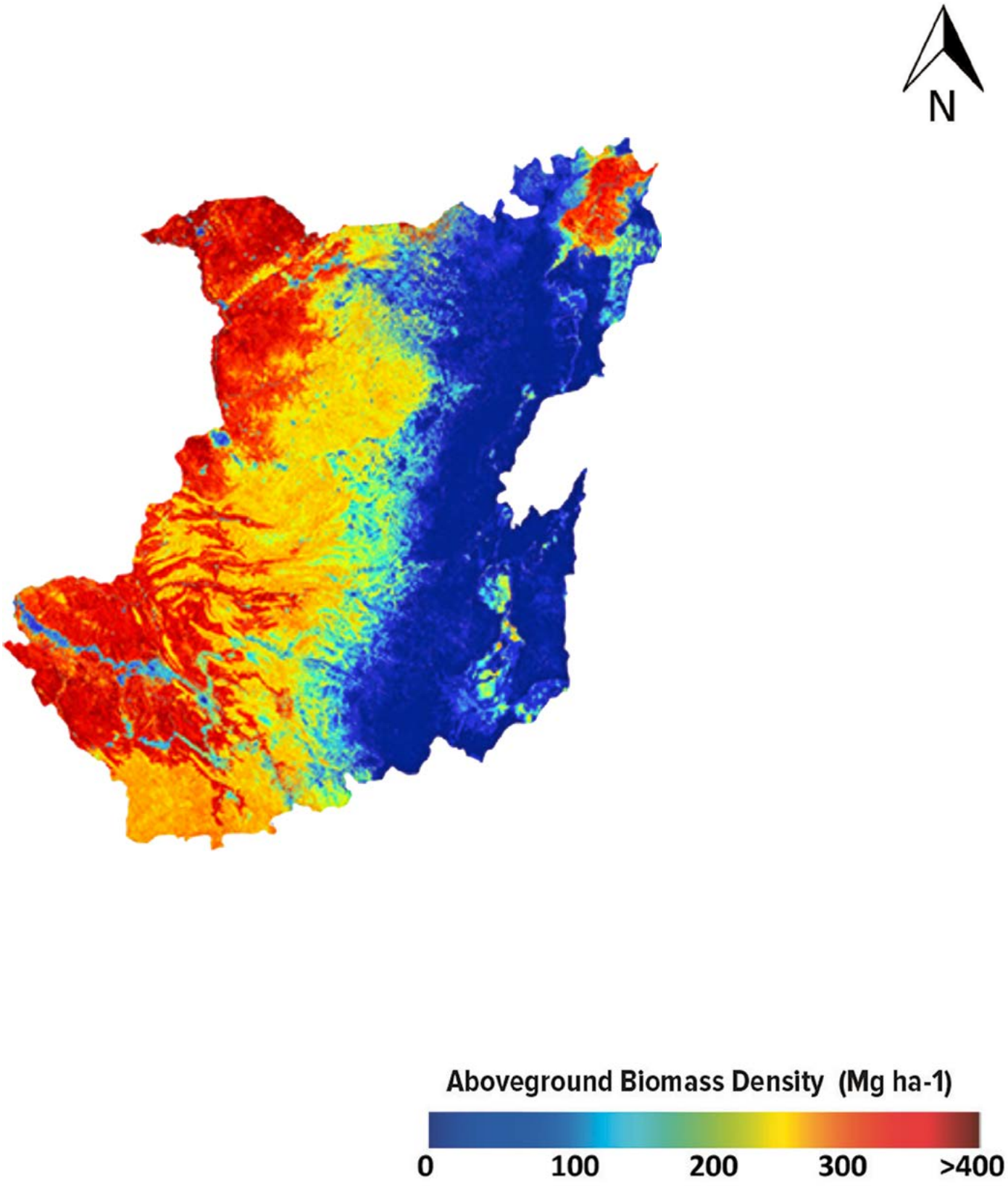

NORD UBANGI

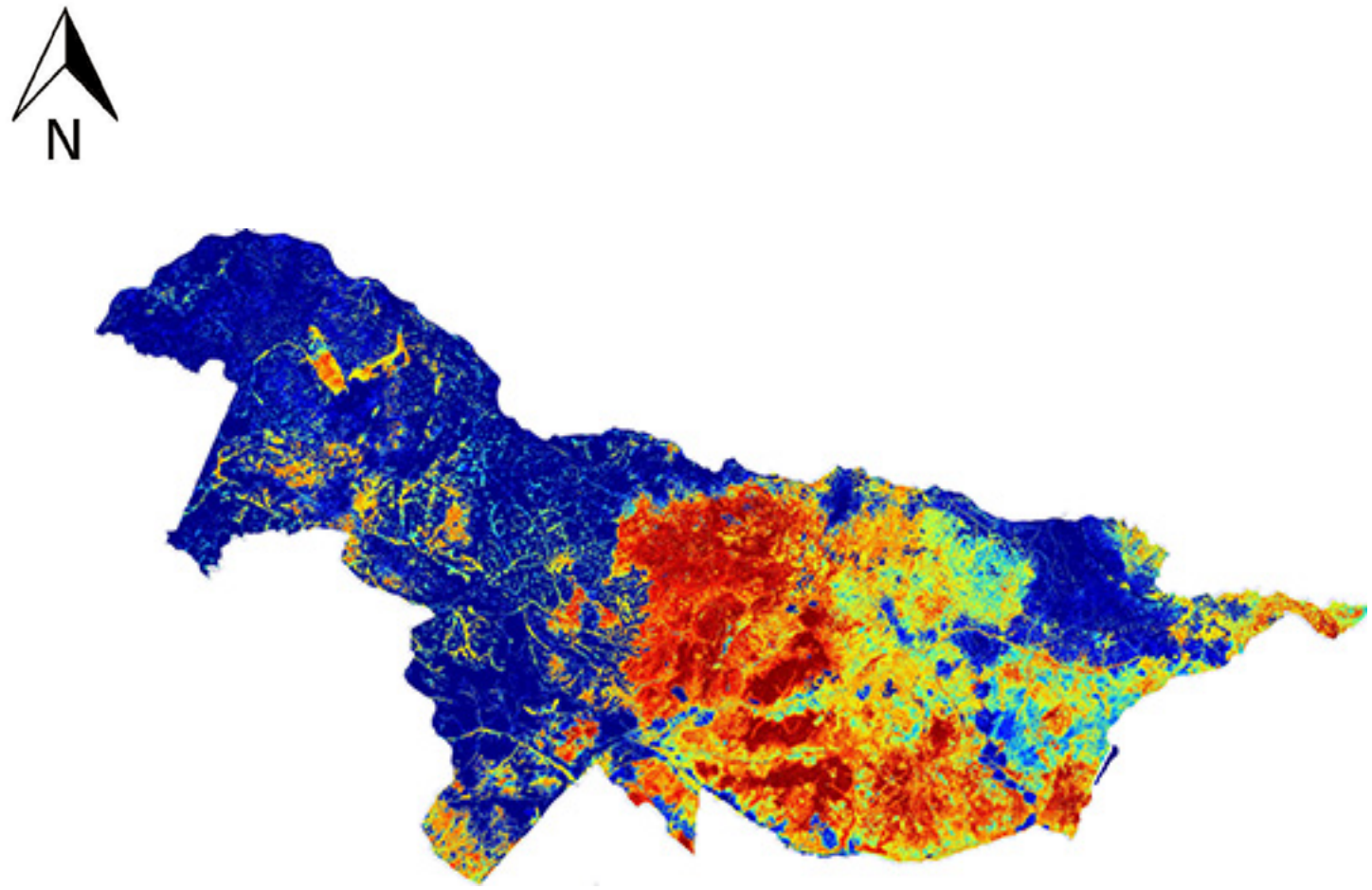

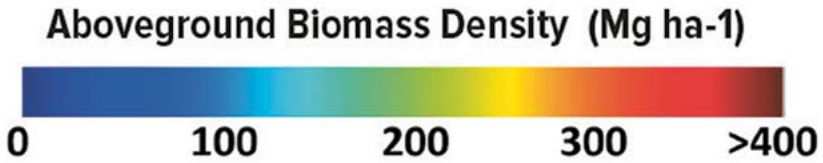

SANKURU

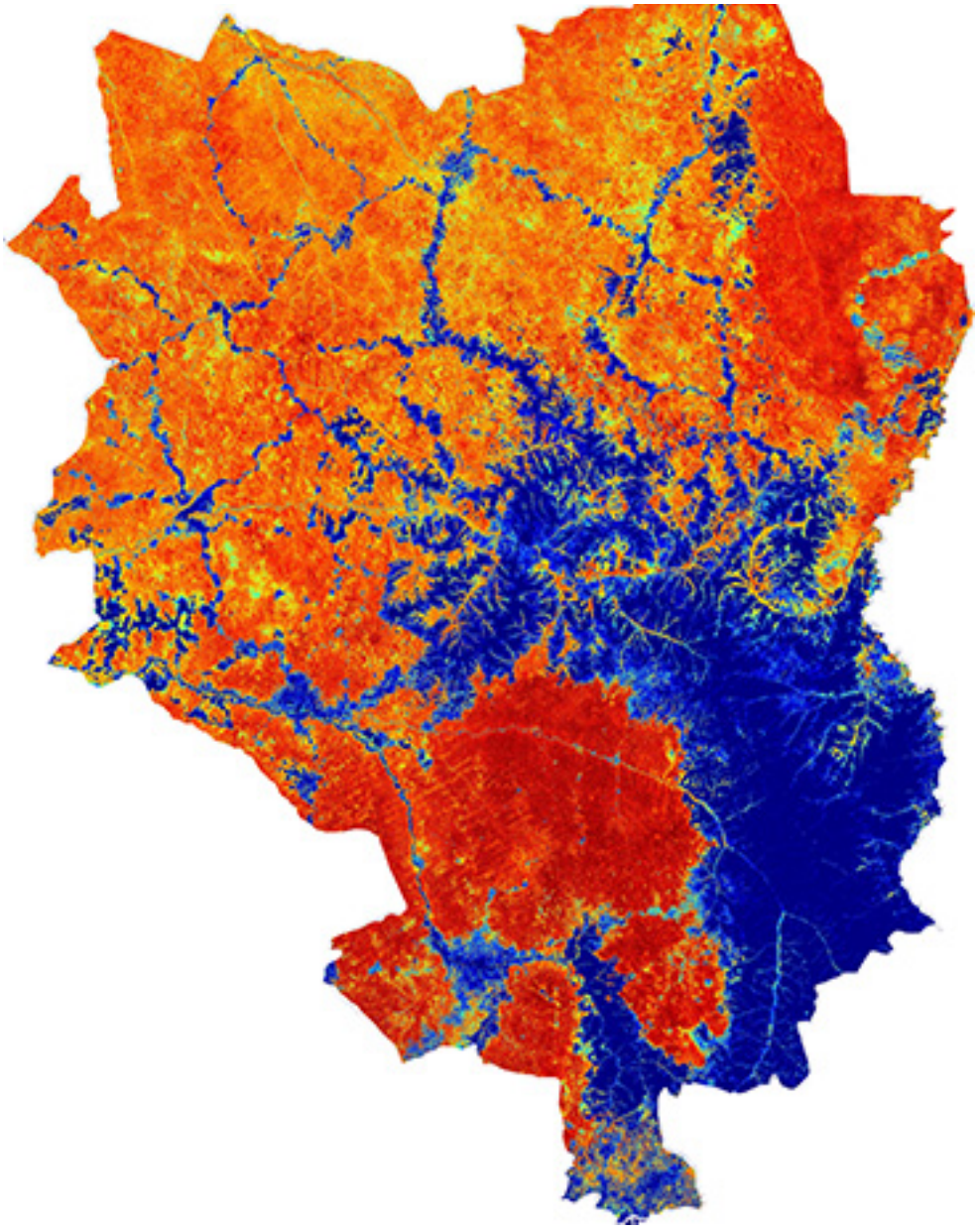

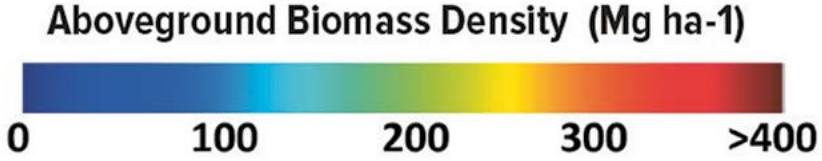

SUD KIVU

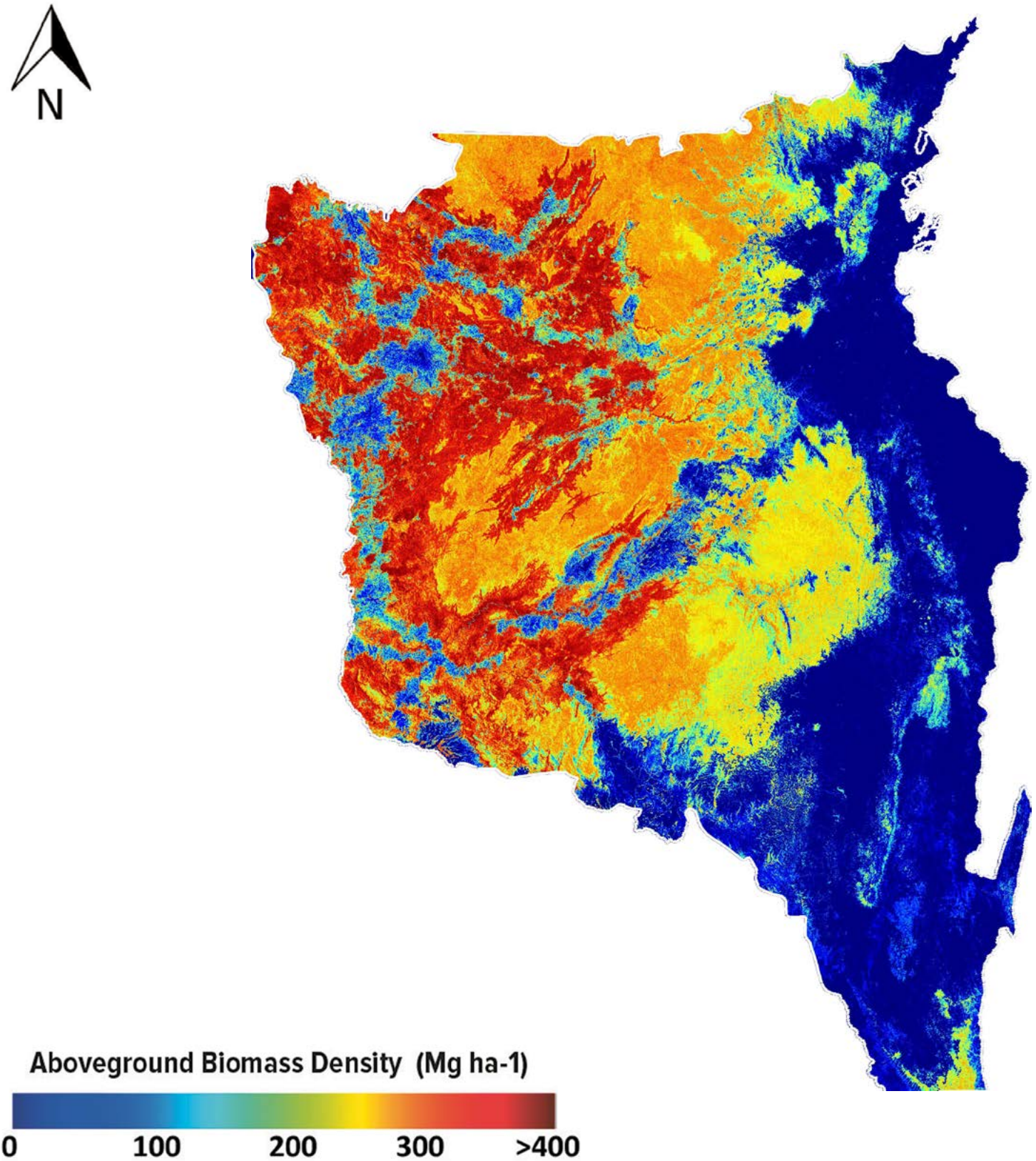

SUD UBANGI

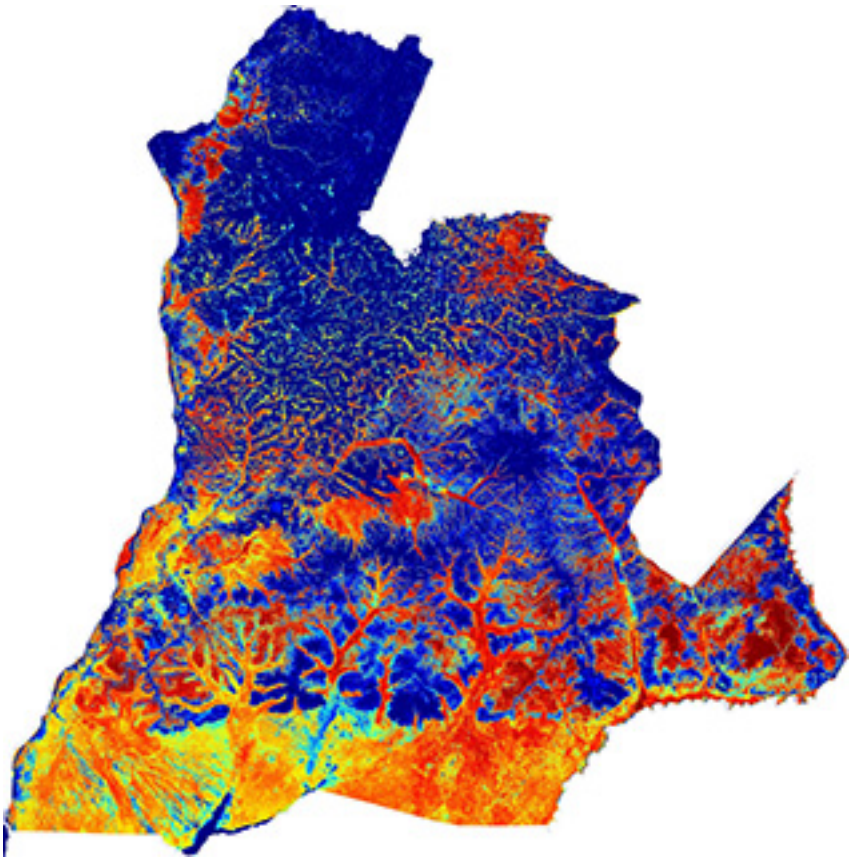

TANGANYKA

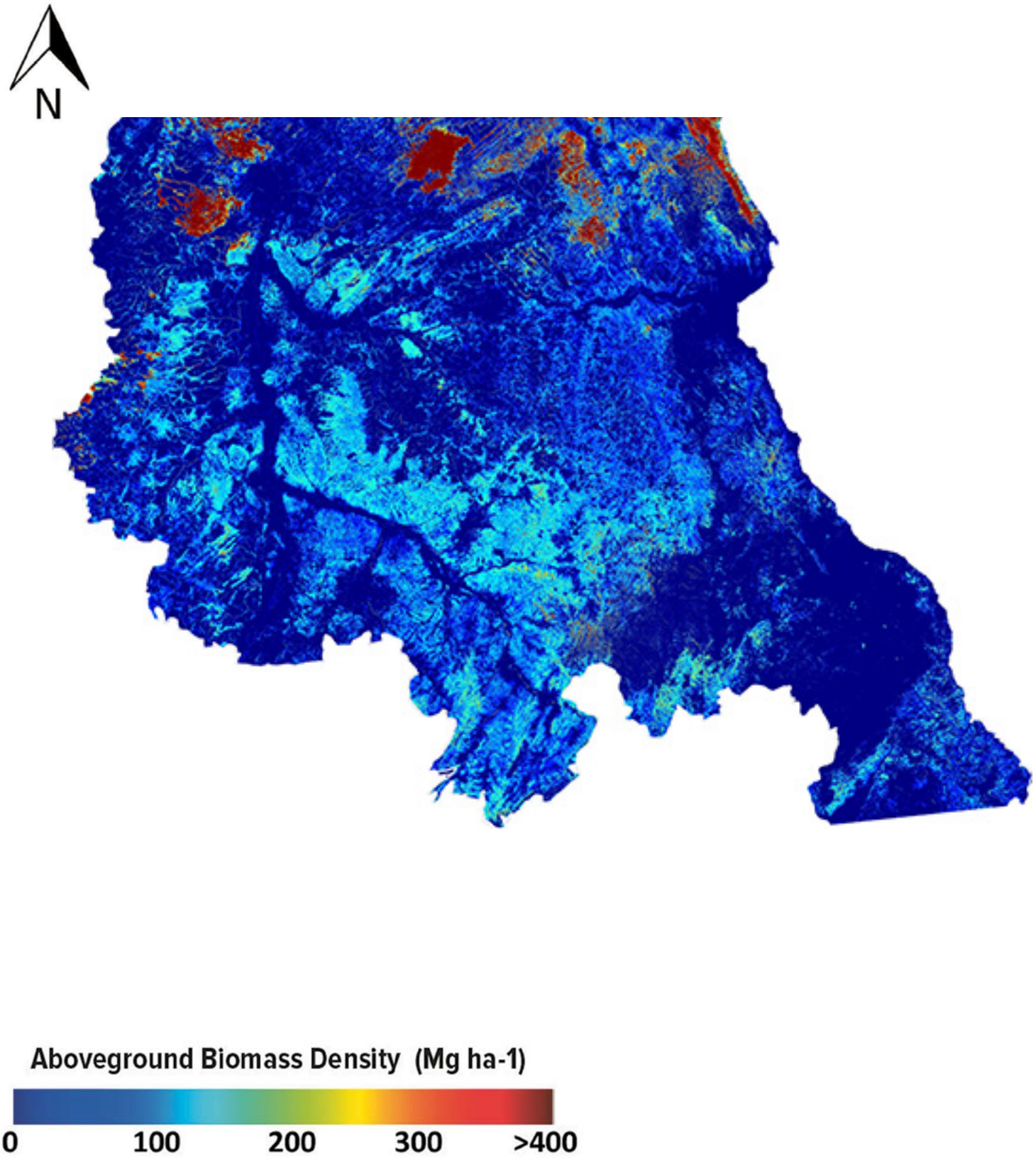

TSHOPO

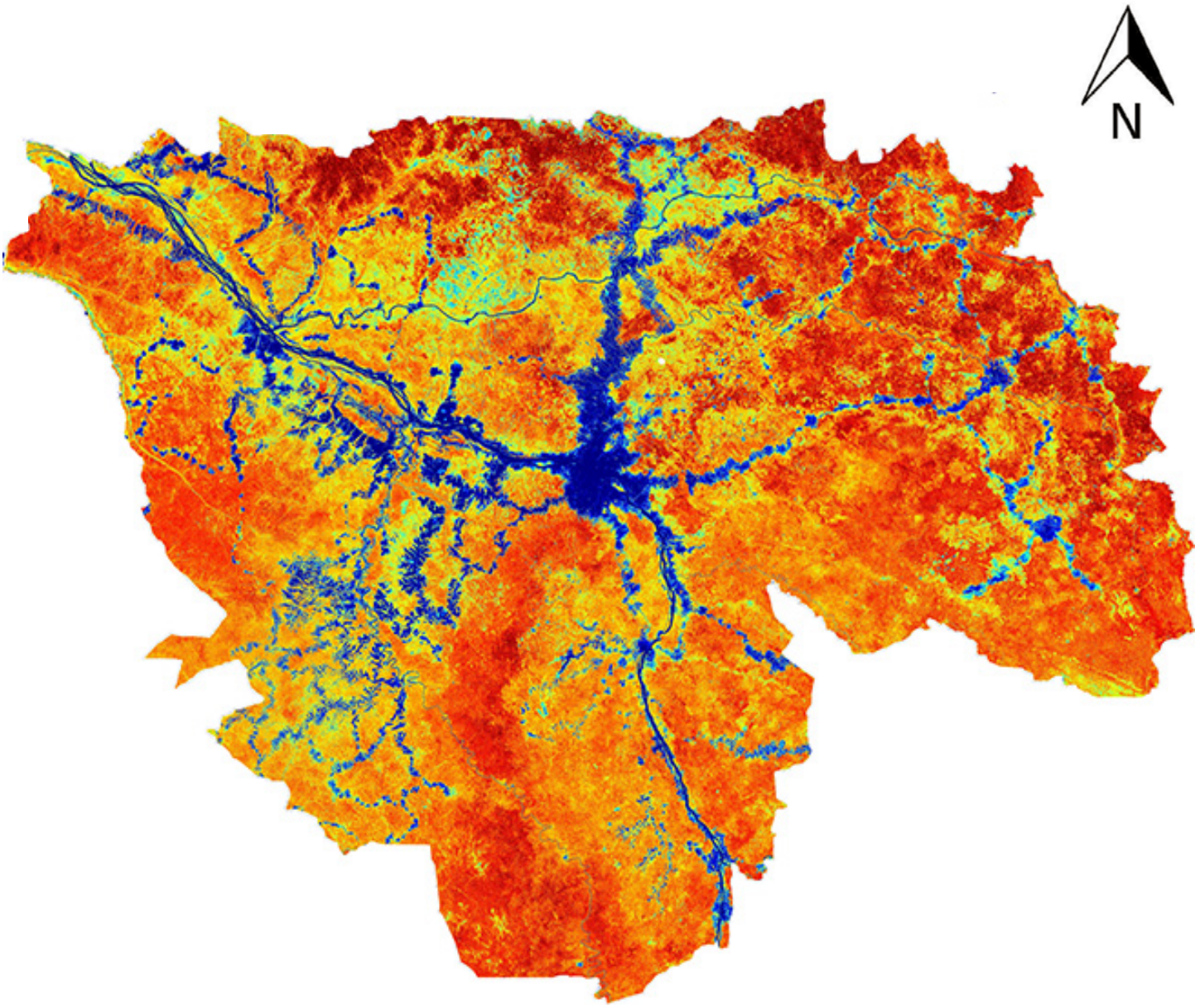

TSHUAPA

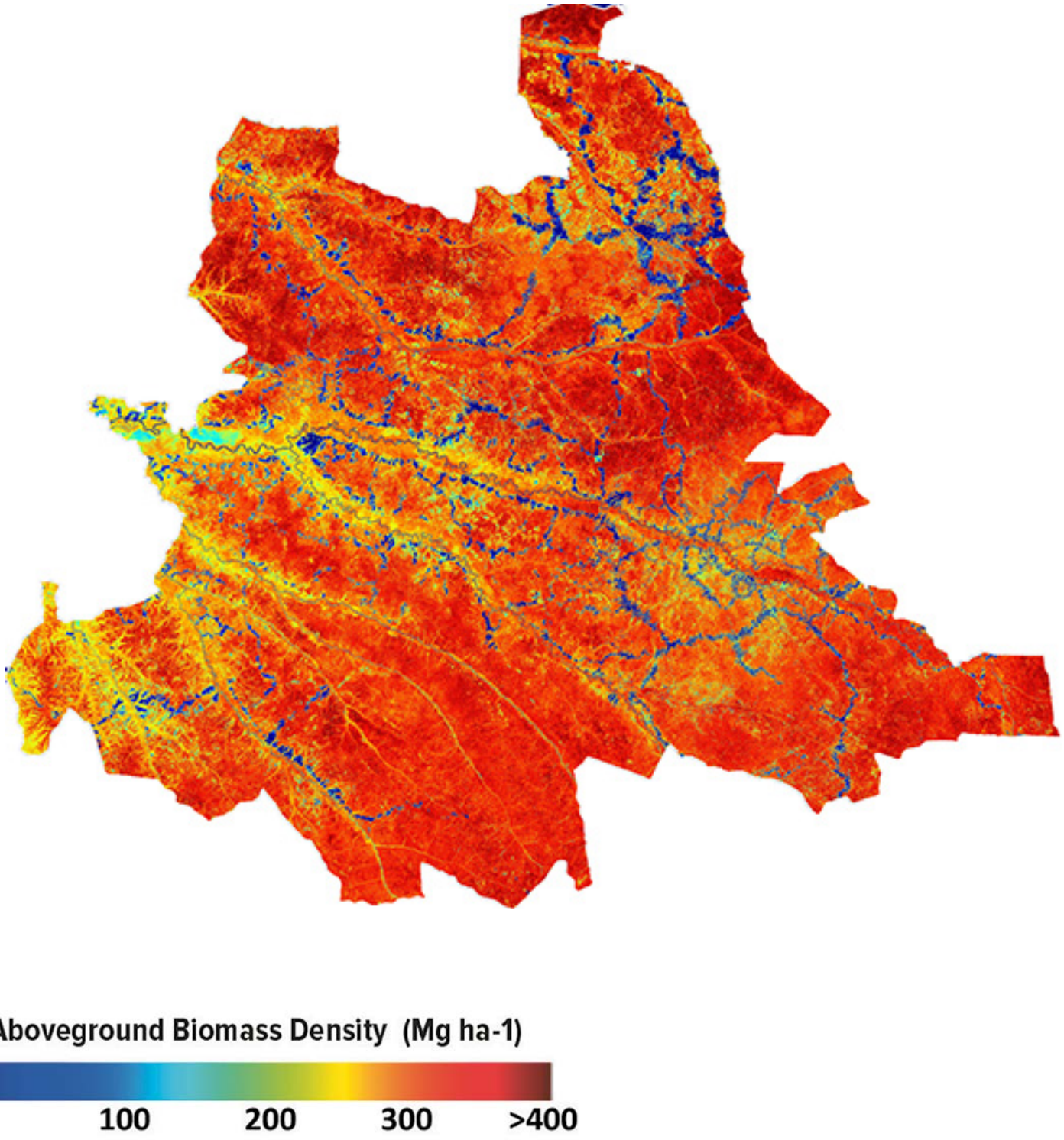

REFERENCES

1. Pan, Y. et al. A Large and Persistent Carbon Sink in the World's Forests. *Science* **333**, 988–993 (2011).
2. Pachauri, R. K. et al. *Climate change 2014: Synthesis Report. Contribution of working groups I, II and III to the fifth assessment report of the intergovernmental panel on climate change.* (IPCC, 2014).
3. Herold, M. & Skutsch, M. Monitoring, reporting and verification for national REDD + programmes: two proposals. Environ. Res. Lett. 6, 14002 (2011).
4. Ene, L. T. *et al*. Large-scale estimation of aboveground biomass in miombo woodlands using airborne laser scanning and national forest inventory data. *Remote Sens. Environ.* **186**, 626–636 (2016).
5. Tomppo, E. *et al*. National forest inventories. *Pathw. Common Report. Eur. Sci. Found.* 541–553 (2010).
6. Saatchi, S. S. *et al*. Seeing the forest beyond the trees. *Glob. Ecol. Biogeogr.* **24**, 606–610 (2015).
7. Mitchard, E. T. *et al*. Uncertainty in the spatial distribution of tropical forest biomass: a comparison of pan-tropical maps. *Carbon Balance Manag*. **8**, 10 (2013).
8. Saatchi, S. S. *et al*. Benchmark map of forest carbon stocks in tropical regions across three continents. *Proc. Natl. Acad. Sci.* **108**, 9899 (2011).
9. Goetz, S. J. *et al*. Mapping and monitoring carbon stocks with satellite observations: a comparison of methods. *Carbon Balance Manag.* **4**, 2 (2009).
10. Hansen, M. C. *et al*. High-Resolution Global Maps of 21st-Century Forest Cover Change. *Science* **342**, 850–853 (2013).
11. Saatchi, S. S., Houghton, R. A., Dos Santos Alvalá, R. C., Soares, J. V. & Yu, Y. Distribution of aboveground live biomass in the Amazon basin. Glob. Change Biol. 13, 816–837 (2007).
12. Baccini, A. *et al*. Estimated carbon dioxide emissions from tropical deforestation improved by carbon-density maps. *Nat. Clim. Change* **2**, 182–185 (2012).
13. Peter Tittmann, Sassan Saatchi & Benktesh Sharma. VCS: Tool for measuring aboveground live forest biomass using remote sensing. (2015). doi:10.13140/RG.2.1.2351.8567
14. Xu, L. *et al*. Satellite observation of tropical forest seasonality: spatial patterns of carbon exchange in Amazonia. *Environ. Res. Lett.* **10**, 84005 (2015).
15. Saarela, S. *et al*. Hierarchical model-based inference for forest inventory utilizing three sources of information. *Ann. For. Sci.* **73**, 895–910 (2016).
16. Ståhl, G. *et al*. Use of models in large-area forest surveys: comparing model-assisted, model-based and hybrid estimation. *For. Ecosyst.* **3**, 5 (2016).
17. Næsset, E., Bollandsås, O. M., Gobakken, T., Gregoire, T. G., & Ståhl, G. (2013). Model assisted estimation of change in forest biomass over an 11 year period in a sample survey supported by airborne LiDAR: A case study with post-stratification to provide "activity data". *Remote Sensing of Environment*, **128**, 299-314.
18. Næsset, E., Ørka, H. O., Solberg, S., Bollandsås, O. M., Hansen, E. H., Mauya, E., ... & Gobakken, T. (2016). Mapping and estimating forest area and aboveground biomass in miombo woodlands in Tanzania using data from airborne laser scanning, TanDEM-X, RapidEye, and global forest maps: a comparison of estimated precision. *Remote Sensing of Environment*, **175**, 282-300.

19. Vancutsem, C., Pekel, J. F., Evrard, C., Malaisse, F., & Defourny, P. (2009). Mapping and characterizing the vegetation types of the Democratic Republic of Congo using SPOT VEGETATION time series. *International Journal of Applied Earth Observation and Geoinformation*, **11**(1), 62-76.
20. Potapov, P. V. *et al*. Quantifying forest cover loss in Democratic Republic of the Congo, 2000–2010, with Landsat ETM + data. *Remote Sens. Environ.* 122, 106–116 (2012).
21. Weisbin, C. R., Lincoln, W., & Saatchi, S. (2014). A Systems Engineering Approach to Estimating Uncertainty in Above-Ground Biomass (AGB) Derived from Remote-Sensing Data. *Systems Engineering*, **17**(3), 361-373.
22. Chave, J., Condit, R., Aguilar, S., Hernandez, A., Lao, S., & Perez, R. (2004). Error propagation and scaling for tropical forest biomass estimates. *Philosophical Transactions of the Royal Society of London B: Biological Sciences*, **359**(1443), 409-420.
23. Meyer, V., Saatchi, S. S., Chave, J., Dalling, J. W., Bohlman, S., Fricker, G. A., ... & Hubbell, S. (2013). Detecting tropical forest biomass dynamics from repeated airborne lidar measurements. *Biogeosciences*, **10**(8), 5421-5438.
24. Chave, J., Réjou-Méchain, M., Búrquez, A., Chidumayo, E., Colgan, M. S., Delitti, W. B., ...& Henry, M. (2014). Improved allometric models to estimate the aboveground biomass of tropical trees. *Global change biology*, 20(10), 3177-3190.
25. Djomo, A. N., Ibrahima, A., Saborowski, J., & Gravenhorst, G. (2010). Allometric equations for biomass estimations in Cameroon and pan moist tropical equations including biomass data from Africa. *Forest Ecology and Management*, **260**(10), 1873-1885.
26. Ngomanda, A., Obiang, N. L. E., Lebamba, J., Mavouroulou, Q. M., Gomat, H., Mankou, G.S., ... & Bobé, K. H. B. (2014). Site-specific versus pantropical allometric equations: Which option to estimate the biomass of a moist central African forest? *Forest Ecology and Management*, **312**, 1-9.
27. Chave, J., Andalo, C., Brown, S., Cairns, M. A., Chambers, J. Q., Eamus, D., ... & Lescure, J.P. (2005). Tree allometry and improved estimation of carbon stocks and balance in tropical forests. *Oecologia*, **145**(1), 87-99.
28. Bastin, J. F., Barbier, N., Couteron, P., Adams, B., Shapiro, A., Bogaert, J., & De Cannière, C. (2014). Aboveground biomass mapping of African forest mosaics using canopy texture analysis: toward a regional approach. *Ecological Applications*, **24**(8), 1984-2001.
29. Mokany, K., Raison, R. J. & Prokushkin, A. S. Critical analysis of root : shoot ratios in terrestrial biomes. Glob. *Change Biol.* **12**, 84–96 (2006).
30. IPCC, 2006. 2006 IPCC Guidelines for National Greenhouse Gas Inventories, Prepared by the National Greenhouse Gas Inventories Programme, Eggleston, HS., Buendia, L., Miwa, K., Ngara, T., Tanabe, K. (eds.), Published: IGES, Japan.
31. WRI. Congo Basin Forest Atlases. *Democratic Republic of Congo | World Resources Institute* (2013). Available at: http://www.wri.org/our-work/project/congo-basin-forests/democratic-republic-congo#project-tabs. (Accessed: 26th August 2016)
32. Shimada, M. et al. New global forest/non-forest maps from ALOS PALSAR data (2007–2010). *Remote Sens. Environ.* **155**, 13–31 (2014).
33. Google Earth Engine. Landsat Algorithms | Google Earth Engine API. *Google Developers* (2016). Available at: https://developers.google.com/earth-engine/landsat. (Accessed: 4th October 2016)
34. Schaaf, C. B. et al. First operational BRDF, albedo nadir reflectance products from MODIS. *Remote Sens. Environ.* **83**, 135–148 (2002).
35. Schaaf, C. B., Liu, J., Gao, F. & Strahler, A. H. in *Land Remote Sensing and Global Environmental Change* (eds. Ramachandran, B., Justice, C. O. & Abrams, M. J.) 549–561 (Springer New York, 2011).
36. Farr, T. G. et al. The Shuttle Radar Topography Mission. *Rev. Geophys.* **45**, RG2004 (2007).

37. Berger, A. L., Pietra, V. J. D. & Pietra, S. A. D. A Maximum Entropy Approach to Natural Language Processing. *Comput Linguist* **22**, 39–71 (1996).
38. Phillips, S. J., Anderson, R. P. & Schapire, R. E. Maximum entropy modeling of species geographic distributions. *Ecol. Model.* **190**, 231–259 (2006).
39. Saatchi, S. S. et al. Benchmark map of forest carbon stocks in tropical regions across three continents. *Proc. Natl. Acad. Sci.* **108**, 9899 (2011).
40. Yu, Y. Global Distribution of Carbon Stock in Live Woody Vegetation. (University of California, Los Angeles, 2013).
41. Mascaro, J. et al. A Tale of Two 'Forests': Random Forest Machine Learning Aids Tropical Forest Carbon Mapping. *PLoS ONE* **9**, e85993 (2014).
42. Zolkos, S. G., Goetz, S. J. & Dubayah, R. A meta-analysis of terrestrial aboveground biomass estimation using lidar remote sensing. *Remote Sens. Environ*. **128**, 289–298 (2013).
43. Schreuder, H. T., Gregoire, T. G. & Wood, G. B. *Sampling Methods for Multiresource Forest Inventory*. (John Wiley & Sons, 1993).
44. Ståhl, G. et al. Model-based inference for biomass estimation in a LiDAR sample survey in Hedmark County, NorwayThis article is one of a selection of papers from Extending Forest Inventory and Monitoring over Space and Time. *Can. J. For. Res.* **41**, 96–107 (2010).
45. Neigh, C. S. R. *et al.* Taking stock of circumboreal forest carbon with ground measurements, airborne and spaceborne LiDAR. *Remote Sens. Environ.* **137**, 274–287 (2013).
46. Xu, L., Saatchi, S. S., Yang, Y., Yu, Y. & White, L. Performance of non-parametric algorithms for spatial mapping of tropical forest structure. *Carbon Balance Manag.* **11**, 18 (2016).
47. Weisbin, C. R., Lincoln, W., & Saatchi, S. (2013). A Systems Engineering Approach to Estimating Uncertainty in Above-Ground Biomass (AGB) Derived from Remote-Sensing Data. *Systems Engineering*
48. Hughes, R. H., Hughes, J. S. & World Wide Fund for Nature. *A directory of African wetlands*. (IUCN, The World Conservation Union, 1992).
49. van der Werf, G. R. *et al*. Global fire emissions and the contribution of deforestation, savanna, forest, agricultural, and peat fires (1997–2009). *Atmos Chem Phys* **10**, 11707–11735 (2010).
50. Clark, D. A. Sources or sinks? The responses of tropical forests to current and future climate and atmospheric composition. *Philos. Trans. R. Soc. Lond. B. Biol. Sci.* **359**, 477–491 (2004).
51. Lloyd, J. & Farquhar, G. D. Effects of rising temperatures and [CO2] on the physiology of tropical forest trees. *Philos. Trans. R. Soc. B Biol. Sci.* **363**, 1811–1817 (2008).
52. Yang, Y. et al. Abiotic Controls on Macroscale Variations of Humid Tropical Forest Height. *Remote Sens.* **8**, 494 (2016).
53. Dargie, G. C. et al. Age, extent and carbon storage of the central Congo Basin peatland complex. *Nature* **advance online publication**, (2017).
54. Wood, T. E., Cavaleri, M. A. & Reed, S. C. Tropical forest carbon balance in a warmer world: a critical review spanning microbial- to ecosystem-scale processes. *Biol. Rev.* **87**, 912–927 (2012).

CARBON MAP OF DRC

HIGH RESOLUTION CARBON DISTRIBUTION IN FORESTS OF DEMOCRATIC REPUBLIC OF CONGO

A Summary Report of UCLA Institute of Environment & Sustainability

UCLA IoES

JPL
Jet Propulsion Laboratory
California Institute of Technology

WWF

Supported by:
Federal Ministry for the Environment, Nature Conservation, Building and Nuclear Safety
based on a decision of the German Bundestag

KFW